TEKST NR 279 1994

Description of a method of measuring the shear modulus of supercooled liquids and a comparison of their thermal and mechanical response functions.

Tage Christensen
IMFUFA, Roskilde University
Postboks 260
DK-4000 Roskilde, Denmark

TEKSTER fra
IMFUFA ROSKILDE UNIVERSITETSCENTER
INSTITUT FOR STUDIET AF MATEMATIK OG FYSIK SAMT DERES FUNKTIONER I UNDERVISNING, FORSKNING OG ANVENDELSER

IMFUFA, Roskilde Universitetscenter, Postboks 260, 4000 Roskilde

Description of a method of measuring the shear modulus of supercooled liquids and a comparison of their thermal and mechanical response functions

by: Tage Christensen

IMFUFA tekst nr. 279/94 90 pages ISSN 0106-6242

Abstract

This dissertation consists of three parts. The main issue is a description of how the frequency dependent shearmodulus of a supercooled liquid can be deduced using a new technique based on a piezoelectric transducer.

The method have been applied to 1,2-butandiol, 1,3-butandiol, 1,2,6-hexantriol, 1,2-propandiol og 2-metyl-2,4-pentandiol. These liquids have been found to obey the temperature/time superposition principle and the frequency dependences of the shear modulus follows a phenomenological extended Maxwell model.

The frequency dependeces of the specific heat have also been studied for the same liquids. This have been done using a method earlier developed by the author.

Both examples of a narrower relaxation spectrum of the specific heat compared to the shear modulus and the opposite have been found. However the relaxation times are in all cases longer for the specific heat than for the shear modulus. That is the liquids are more fluent at the calorimetric glass transition than one would expect.

The dissertation contains also a discussion on how the frequency dependent specific heat and heat conductivity are defined in a relaxing substance.

Description of a method of measuring the shear modulus of supercooled liquids and a comparison of their thermal and mechanical response functions.

Tage Christensen
IMFUFA,Roskilde University Center
Postbox 260
DK-4000 Roskilde
Denmark

Abstract of the ph.d. dissertation entitled

" Description of a method of measuring the shear modulus of supercooled liquids and a comparison of their thermal and mechanical response functions."

By Tage Christensen, IMFUFA, Roskilde University Center, Denmark

This dissertation consists of three parts. The main issue is a description of how the frequency dependent shearmodulus of a supercooled liquid can be deduced using a new technique based on a piezoelectric transducer.

The method have been applied to 1,2-butandiol, 1,3-butandiol, 1,2,6-hexantriol, 1,2-propandiol og 2-metyl-2,4-pentandiol. These liquids have been found to obey the temperature/time superposition principle and the frequency dependences of the shear modulus follows a phenomenological extended Maxwell model.

The frequency dependeces of the specific heat have also been studied for the same liquids. This have been done using a method earlier developed by the author.

Both examples of a narrower relaxation spectrum of the specific heat compared to the shear modulus and the opposite have been found. However the relaxation times are in all cases longer for the specific heat than for the shear modulus. That is the liquids are more fluent at the calorimetric glass transition than one would expect.

The dissertation contains also a discussion on how the frequency dependent specific heat and heat conductivity are defined in a relaxing substance.

Resumé af ph.d afhandlingen med titlen

" Beskrivelse af en metode til bestemmelse af underafkølede væskers shearmodul og en sammenligning af deres termiske og mekaniske responsfunktioner."

Afhandlingen består af tre dele. Hovedvægten er lagt på en beskrivelse af, hvorledes det frekvensafhængige shearmodul af underafkølede væsker kan bestemmes i audio frekvensområdet ved hjælp af en særlig udviklet piezoelektrisk transducer.

Denne metode er blevet anvendt på 1,2-butandiol, 1,3-butandiol, 1,2,6-hexantriol, 1,2-propandiol og 2-metyl-2,4-pentandiol. Væskerne er fundet at adlyde temperatur/tid superpositions princippet, og frekvensafhængigheden af shearmodulet er fundet at følge en fænomenologisk udvidet Maxwell model.

For de samme væsker er den frekvensafhægige varmefylde blevet bestemt ved brug af en metode tidligere udviklet af forfatteren.

Der er både eksempler på at relaksationsspektret er smallere for varmefylden end for shearmodulus og det modsatte. Derimod ses det generelt, at relaksationstiden er længere for varmefylden end for shearmodulet. D.v.s væskerne er mere flydende ved den kalorimetriske glasovergang end man skulle forvente.

Afhandlingen indeholder derudover også en diskussion af definitionen af frekvensafhægig varmefylde og varmeledningsevne for et relakserende medium.

Chapter 1. Introduction.

The thermal and mechanical properties of liquids like the specific heat c_p,the compressibility κ_T, the thermal expansion coefficient α_p ,the shear modulus G etc at temperature T and pressure p are usually considered constant. In fact they are time-dependent (or frequency-dependent). This phenomena is called thermoviscoelasticity. However this only manifests itself on a timescale $\tau_M(T)$ increasing with decreasing temperature T. For liquids amenable to supercooling this phenomena is seen on a timescale of 10^3s at the conventionally defined glass-temperature T_g.

In this thesis two properties, the specific heat $c_p(\omega)$ and the shear modulus $G(\omega)$ of a number of liquids, have been measured and the relaxation times compared. This as a part of a greater programme establishing phenomenological/theoretical connections between all the thermoviscoelastic properties.

The shear modulus was measured by using a new technique based on a piezoelectric transducer. This technique enables the measurement of high moduli (10^7-$5\cdot10^9$ Pa) in the audio frequency range (10-$5\cdot10^4$ Hz). The principle of the method is rather simple: the liquid is mechanically coupled to the piezoelectric transducer and thus the liquid clamps the movement of the transducer more or less depending on its shear modulus. This clamping is seen as a decrease of the electrical capacitance of the transducer. However the analysis and unfolding of data is somewhat involved. Thus the description of this method forms a large part of the thesis.

The specific heat was measured using the same technique as originally applied to glycerol [1] described in detailed elsewhere [2] and only a short review of this method is given here.

This thesis also includes a discussion of how the concepts of the frequency dependent specific heat and heat conductivity can be defined in a macroscopic continuum formulation. This is needed in order to clarify some misunderstandings in the litterature to be discussed.

Chapter 2. The concepts of frequency dependent specific heat and heat conductivity.

2.1 Identification of the proper thermal and mechanical variables.

The purpose of this chapter is to see how the specific heat and heat conductivity can be defined in a relaxing medium. This has been considered also by others [3], but here we emphasize the proper choice of the generalized currents and forces that defines these response functions. By choosing these in a way that their product gives the dissipation of free energy we ensure that the response function they define can be put into the sceme[4] of linear response theory and theorems such as the Fluctuation-Dissipation Theorem [5] applies.

Let a body change its state with the values U of internal energy, S of entropy and V of volume into a state with the corresponding values U_0,S_0,V_0. Then it is a wellknown result[6], that if the body resides in a reservoir of temperature T_0 and pressure p_0, then the maximum work, that can be obtained during the process is

$$R_{max} = U-U_0-T_0(S-S_0)+p(V-V_0) \qquad (2\text{-}1)$$

If one introduces the exergy (availability) A

$$A = U-T_0S+p_0V \qquad (2\text{-}2)$$

then R_{max} is simply the change in exergy *.(2-1) holds for homogeneous changes in the body. When gradients are also present a continuum formulation is needed. The conjugate variables, their products giving the transferred rate of exergy per time per volume, shall now be found.

The 1.law of thermodynamics tells

---

* The exergy A should not be confused with Gibbs free energy $G = U-TS+pV$. During a cyclic proces $\Delta G = 0$, G being a state variable, whereas $-\Delta A$ is equal to the dissipation, the loss of working ability of the surroundings.

$$\frac{\partial}{\partial t}\rho u = -\nabla\cdot(J_Q+J_W) \tag{2-3}$$

where u is the internal energy per volume, ρ the density, J_Q the heat current density and J_W the work current density. The kinetic contribution ρv^2 and the contribution from the gravitational field to the energy is neglected.At temperature T the entropy current associated with the heat current J_Q is $J_S = \frac{1}{T}J_Q$. The 2.law of thermodynamics can be written

$$J_Q = (1-\frac{T_0}{T})J_Q+T_0J_S \tag{2-4}$$

whereby the heat current is split into the available part $(1-\frac{T_0}{T})J_Q$ and unavailable part T_0J_S. $(1-\frac{T_0}{T})$ is also known as the Carnot factor η_C.

$-\nabla\cdot J_W$ is the rate of work done per volume

$$-\nabla\cdot J_W = \sigma_{ij}\dot{e}_{ij} \tag{2-5}$$

where σ_{ij} is the stresstensor and $\dot{e}_{ij}$ is the time derivative of the straintensor e_{ij} (summation over repeated index). Define σ'_{ij} by extracting the reference pressure from σ_{ij},

$$\sigma_{ij} = -p_0\delta_{ij}+\sigma'_{ij} \tag{2-6}$$

Note that σ'_{ij} is not traceless, since there could be variations of pressure p around p_0.(2-4),(2-5) and (2-6) inserted into (2-3) gives then

$$\frac{\partial}{\partial t}\rho u = -\nabla\cdot[(1-\frac{T_0}{T})J_Q]+\sigma'_{ij}\dot{\epsilon}_{ij}-p_0\delta_{ij}\dot{\epsilon}_{ij}-\nabla\cdot(T_0J_S) \qquad (2\text{-}7)$$

or

$$\frac{\partial}{\partial t}\rho u+\nabla\cdot(T_0J_S)+p_0tr(\dot{\epsilon}_{ij}) = -(1-\frac{T_0}{T})\nabla\cdot J_Q-J_Q\cdot\nabla(1-\frac{T_0}{T})+\sigma'_{ij}\dot{\epsilon}_{ij} \qquad (2\text{-}8)$$

Comparison with (2-1) shows that the left-hand side represents the exergy transferred per time per volume.

2.2 Definition of the isobaric specific heat $c_p(\omega)$ and the heat conductivity $\kappa(\omega)$.

Now assume constant pressure $p = p_0$. In (2-8) two pairs of conjugate thermal variables can be identified $(-\nabla\cdot J_Q\ ,\ (1-\frac{T_0}{T}))$ and $(-\nabla(1-\frac{T_0}{T})\ ,\ J_Q)$. For small temperature variations $\delta T = T-T_0$ the Carnotfactor becomes $\frac{\delta T}{T_0}$. In linear response theory there will only be couplings between quantities of the same tensorial order in an isotropic medium (The Curie-Prigogine principle)[7]. Thus one must have

$$-\nabla\frac{\delta T}{T_0} = \int_{-\infty}^{t} Z_\kappa(t-t')dJ_Q(t') \qquad (2\text{-}9)$$

$$-\nabla\cdot J_Q = \int_{-\infty}^{t} Y_{C_p}(t-t')d\frac{\delta T(t')}{T_0} \qquad (2\text{-}10)$$

The isotropy reduces the tensor Z_κ to a scalar .Z_κ and Y_{c_p} are properties of the liquid. They are not dependent on position due to the homogeneity of the liquid on the length scale of interest.

For an ordinary nonrelaxing liquid $Z_\kappa(t)$ becomes simply $\frac{1}{\kappa T_0}$, where κ is the heat conductivity. The continuity equation

$$\frac{\partial}{\partial t}(\rho c_p \delta T) = -\nabla\cdot J_Q \qquad (2\text{-}11)$$

likewise shows that $Y_{c_p}(t)$ is connected to the timedependent heat capacity $c_p(t)$ (a creep function less T_0)

$$T_0\rho c_p(t) = \int_{-\infty}^{t} Y_{c_p}(t')dt' \qquad (2\text{-}12)$$

For a nonrelaxing liquid $Y_{c_p}(t)$ becomes simply $T_0\rho c_p\delta(t-0^+)$, where $\delta(t)$ is the deltafunction*.

The responsefunctions can now be given in the frequency-domain. Let $R(t)$ denote a responsefunction. Then $\tilde{R}(s)$ is defined as $s\int_0^\infty R(t)e^{-st}dt$ and $\hat{R}(\omega)$ is defined as $\tilde{R}(s=-i\omega)$.

The indices κ and c_p is given in order to stress, that $\hat{Z}_\kappa(\omega) = \frac{1}{\hat{Y}_\kappa(\omega)} \neq \frac{1}{\hat{Y}_{c_p}(\omega)}$.

2.3 A generalized diffusion equation.

Taking the divergence of (2-9) and inserting (2-10) one would arrive at the generalization of the heat diffusion equation for a liquid with time dependent specific heat and heat conductivity. It is better however to keep the discussion at the level of the two coupled equations and moreover transform to the frequency domain. For onedimensional problems the solution is facilitated by a transfer matrix [2].

---

* $\delta(t-0^+)$ indicates the limit $\lim_{\epsilon\to 0}\ \delta(t-\epsilon)$, which must be performed after integration of the delta-function

2.4 Accordance with 2.law of thermodynamics.

Now consider a cyclic process for a volume element dV. The total exergy transferred to the element becomes

$$dV\oint(\frac{\partial}{\partial t}\rho u+\nabla\cdot T_0 J_S+p_0 tr\dot{\underline{\underline{\varepsilon}}})dt = dV\oint\nabla\cdot T_0 J_S dt = T_0\Sigma dV \qquad (2\text{-}13)$$

where Σ is the total entropy produced per volume in the element. Thus $T_0\Sigma$ is the dissipation D i.e. the loss of exergy or working ability of the surroundings during the process per volume. The right-hand side of (2-8) on the other hand gives

$$D = Re\{\hat{Y}_{c_p}(\omega)\}(\frac{\delta T}{T_0})^2+Re\{\hat{Z}_\kappa(\omega)\}J_Q\cdot J_Q \qquad (2\text{-}14)$$

This shows that the 2. law of thermodynamics will be fulfilled if and only if

$$Re\,\hat{Y}_{c_p}(\omega)\ \geq 0 \qquad and \qquad Re\,\hat{Z}_\kappa(\omega)\ \geq\ 0 \qquad (2\text{-}15)$$

since geometries and boundary conditions with $J_Q \approx 0$ suitable for measuring the specific heat or with $\frac{\delta T}{T_0} \approx 0$ suitable for measuring the heat conductivity can be devised. From this discussion three points are inferred:

1) Since $\hat{Y}_{c_p}(\omega) = -i\omega\rho c_p(\omega)$, $c_p(\omega)$ has the ordinary significance of a generalized susceptibility, its imaginary part $Imc_p(\omega) = \frac{1}{\omega\rho}Re\,\hat{Y}_{c_p}(\omega)$ according to (2-14) being proportional to the mean dissipation pr time. This conclusion is opposed to Donth [8], saying that $Imc_p(\omega)$ cannot describe dissipation because the energy connected to $c_p(\omega)$

is heat itself. However dissipation is only synonymous with heat production under isothermal conditions. Therefore Donths argument is wrong. The puzzling thing is that during the cyclic process the total amount of heat, put into the system is zero. However when $Im\, c_p(\omega) \neq 0$, the time lag between temperature and enthalpy implies, that in mean the temperature is higher , when heat is put into the liquid than it is, when heat is withdrawn. Thereby exergy is dissipated, or equivalently entropy created. This is in accordance with the statement of N.O. Birge and S.R. Nagel [9]. However in their experiment both terms in (2-14) gives contribution and integrated up in space in fact must give $(\frac{\delta T}{T_0})^2 Re\{\sqrt{-i\omega\rho c_p(\omega)\kappa(\omega)}\}$ per area of the plate. Here δT is the temperature amplitude at the plate at which the thermal waves are excited.

2) Formula (2-14) also shows that opposed to some authors [10] the frequency dependence of the heat conductivity cannot be ruled out on thermodynamic grounds. From a microscopic point of view on the other hand it is difficult to see how a frequency dependence of κ near the glass transition should come about, since heat is transported by vibrations which are not affected by the glass transition. A mechanism, which could introduce frequency dependence would be diffusion of molecules with internal thermal relaxation, but this is ruled out due to the low diffusion constant near the glass transition.

3) There have been a discussion [11] [12] [13] on whether a frequency and wavevector dependent heat conductivity $\lambda(k,s)$ should be more fundamental than the quantities $c_p(\omega)$ and $\kappa(\omega)$. From a macroscopic point of view one can clearly distinguish between $c_p(\omega)$ and $\kappa(\omega)$. They are - as defined by the equations (2-9), (2-10) - independent measurable quantities. Moreover it is difficult to understand, how the wavevector comes in as long as we do not consider microscopic distances. Long range correlations are not to be expected for the glass transition as for a continous (2.order) phase transition.

Chapter 3. The specific heat $c_p(\omega)$.

3.1 Methods of measuring $c_p(\omega)$.

The specific heat c_p of a substance can be determined by measuring the temperature response following an oscillatoric heat input. This technique is known as the AC-temperature technique[14] [15] and can be traced back to Ångstrøm[16]. Likewise with an appropriate geometry the heat conductivity can be found.

The method takes advantage of the possibility of using a correlation technique in order to see a tiny temperature amplitude and phase on a noisy background [17]. The requirement of a little amplitude arises in temperature ranges, were the temperature dependence of c_p is large e.g. at phase transition. The correlation between imposed AC-heatcurrent and AC-temperature may be executed by a lock-in amplifier at high frequencies ($\omega \gtrsim 1$ Hz) or by a computer ($\omega \lesssim 100$ Hz) at low frequencies.

Earlier the method had been used in determination of frequency independent heat capacities only. Recently the use of the AC-temperature technique has been extended [9] [1] to the study of the frequency dependence of the specific heat in supercooled liquids at the glass transition.

The frequency dependent specific heat $c_p(\omega)$ is the Laplace-Stielties transformed of the time dependent specific heat $c_p(t)$, which in turn is nothing but the relaxing enthalpy H(t) following a little temperature step divided by this step. Earlier there have been studies of the enthalpy relaxation in glasses [18] [19] [20] although usually in a nonlinear regime. Thus the new methods do not introduce any physical entity not considered before. However $c_p(\omega)$ can be determined more accurately because of the correlation technique. Besides the temperature amplitude can be kept small to ensure linear response.

Independently two differing methods have been developed in order to measure $c_p(\omega)$. In short they can be distinguished as follows. Consider a sample of density ρ, specific heat c_p, heat conductivity κ and a characteristic size L. Let $D = \frac{\kappa}{\rho c_p}$ denote the heat

diffusivity. At a cyclic frequency ω the damping length of a thermal wave will be $\lambda = \sqrt{\frac{D}{\omega}}$, the diffusion length.

The one method [9 21 22] uses a geometry which assures $\lambda < L$ and measures the ratio $Y = \frac{J_0}{T_0}$ between the heat current $J_0 e^{-i\omega t}$ and the temperature $T_0 e^{-i\omega t}$ at the end face of a semiinfinite medium. This ratio can be classified as an admittance and for this geometry $Y = \sqrt{-i\omega\rho c_p(\omega)\kappa}$. Assuming κ is frequency independent one can calculate relative variations of $c_p(\omega)$.

The other method [1] described in detail elsewhere[2] uses a geometry and frequency so that $\lambda > L$, and measures $c_p(\omega)$ without involving κ. Only a short summary of this method will be given here.

The calorimeter consists of to concentric cylinders e = 0.3 mm apart with a mean diameter of 12 mm and the height of 8 mm. The space in between the cylinders is the space to be filled with the sample liquid. It has a volume of approximately 0.1 cm^3. the cylinder walls have a thickness of 0.06 mm , and they are both wound with a 0.05 mm electrical wire on the sides not facing the liquid chamber. The characteristic diffusion time τ_D, given a typical liquid heat diffusivity D of 0.1 mm^2/s, is $\tau_D = \frac{e^2}{D}$ = 1 s .An electrical voltage $V(t) = V_0\cos(\frac{\omega}{2}t)$ is applied to the one wire, and given an electrical resistance R of the wire, a heat current

$$P(t) = P_0 + P_0\cos(2\omega t) \qquad (3\text{-}1)$$

is generated. Here $P_0 = \frac{V_0^2}{2R}$. The DC heat current P_0 is carried off by a thermal conductance Λ

(nonadiabatic calorimetry) to the cryostat, giving raise to a temperature offset $T_{off} = \frac{P_0}{\Lambda}$

of the calorimeter relative to the cryostat. The timevarying temperature of the calorimeter is measured through the electrical resistance of the other wire. For small oscillations it will be harmonic too,

$$T(t) = T_0 + T_a \cos(\omega t) + T_b \sin(\omega t) \tag{3-2}$$

. T_a and T_b is computed as the size of these two Fourier components in the measured temperature variations.Defining the measured thermal impedance

$$Z = \frac{T_a + iT_b}{P_0} \tag{3-3}$$

, a model of the experiment, valid for $\omega\tau_D \ll 1$, gives

$$\frac{1}{Z} = \Lambda - i\omega C_0 - i\omega C(\omega) \tag{3-4}$$

C_0 being the heat capacitance of the empty calorimeter and i the imaginary unit. Determination of Λ and C_0 (calibration) is done by measuring Z with an empty calorimeter $(C(\omega) = 0)$. Then (3-4) gives $C(\omega)$, when Z has been measured with a filled calorimeter.

3.2 The specific heat of 1,2-butanediol; 1,3-butanediol; 1,2,6-hexanetriol 1,2-propanediol ; 2-methyl-2,4- pentanediol.

The results of the measurements is presented in the curves of App. 3.1 .For each liquid is shown

1) The real part of the measured total capacity C_t $(= Re\{\frac{1}{-i\omega Z}\})$ versus temperature for different frequencies.

2) The real part of the measured admittance Y $(= Re\{\frac{1}{Z}\})$ versus temperature for different frequencies.

3) The real part of the heat capacitance of the liquid with the liquid curve $C(\omega=0,T)$ and the glassy curve $C(\omega=\infty,T)$.

4) The Nyquist plot of the normalized heat capacity. The measured points joins a common curve indicating the principle of time-temperature equivalence to be valid. A model of the form

$$C(s) = \frac{1+qs^{1-\alpha}}{1+s+qs^{1-\alpha}} \quad , s = -i\omega\tau(T) \tag{3-5}$$

discussed in [2] is fitted to data by varying q and α.

5) The mastercurves ($Re\ C$, log ω) and ($Im\ C$, log ω) of the fit of 4). The time-displaced data also shown.

6) The model-relaxation time $\tau(T)$ found by the logarithmic displacement of data needed to fit mastercurves in 5). $\tau(T)$ is fitted with

$$\tau(T) = \exp(\frac{A}{T} - \frac{A}{T_0}) \tag{3-6}$$

Table 3.1 gives the results of the fitting constants

Table 3.1

Parameters of fit to the Specific Heat $c_p(\omega)$

	q	α	A	T
			10^4 K	K
1,2-butanediol	1.1	.50	2.43	182.3
1,3-butanediol	1.5	.54	2.15	180.4
1,2,6-hexanetriol	1.7	.22	2.96	206.5
1,2-propanediol	.75	.48	2.19	174.1
2-metyl-2,4-pentanediol	1.0	.50	2.91	191.4

Fig. 3.2.1 shows the dependence of the relaxation times on temperature for the 5 liquids

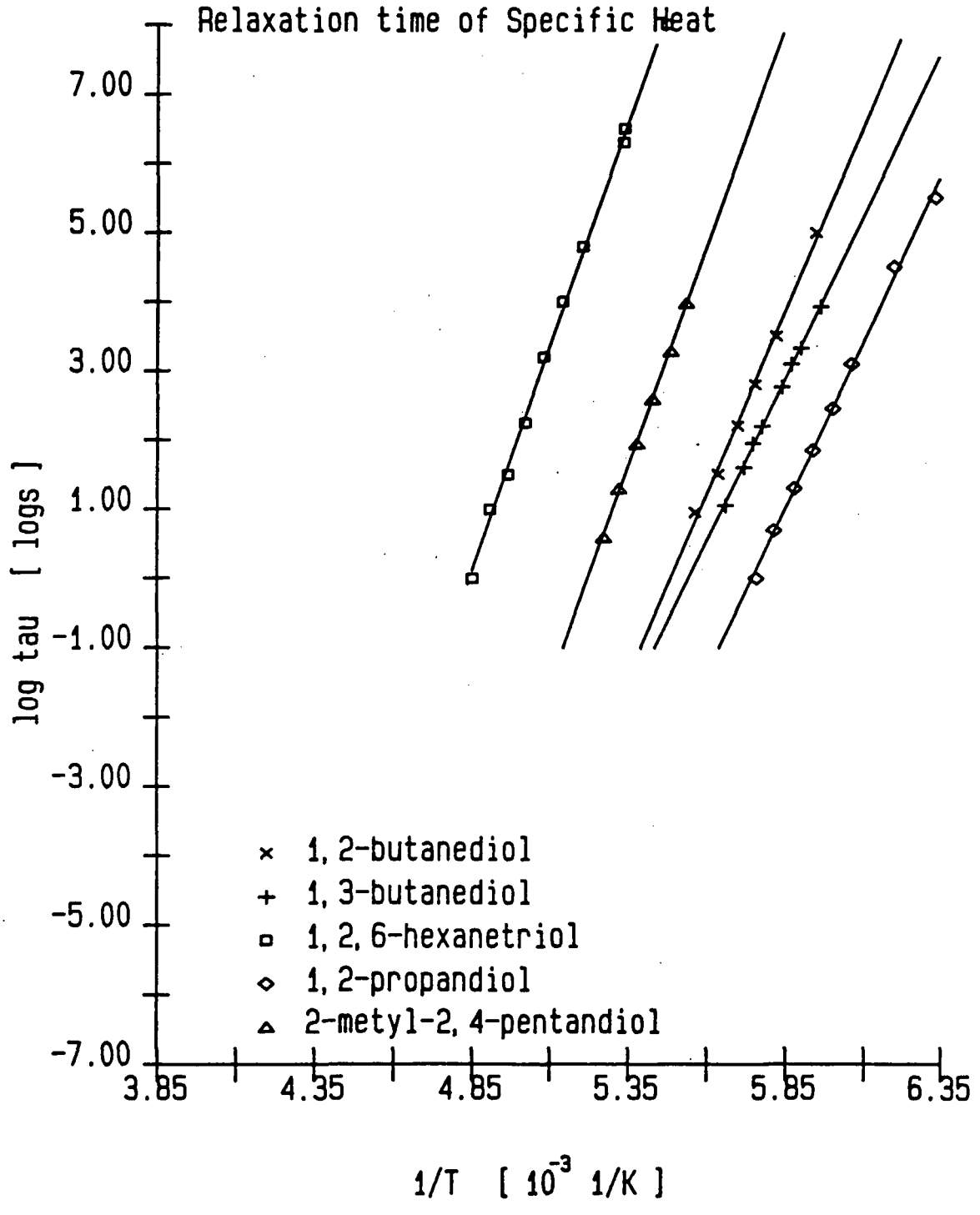
Relaxation time of Specific Heat
7.00
5.00
3.00
1.00
-1.00
-3.00
-5.00
-7.00
log tau [logs]
3.85
4.35
4.85
5.35
5.85
6.35
1/T [10^-3 1/K]
1, 2-butanediol
1, 3-butanediol
1, 2, 6-hexanetriol
1, 2-propandiol
2-metyl-2, 4-pentandiol

Chapter 4. The shearmodulus $G(\omega)$.

4.1 Theory of the Piezoelectric Shearmodulus Gauge,PSG.

In order to measure the shear modulus of a viscoelastic substance at high modulus and low frequencies (audio range) a novel technique have been developed at IMFUFA, Roskilde University Center. It is based on a transducer, the socalled Piezoelctric Shearmodulus Gauge (PSG). Contrary to the methods of resonance or reflection of waves [23] the PSG measures $G_s(\omega)$ at low frequencies, where the wavelength is much longer than the size of the sample. Using the piezoelectric effect the transducer couples a mechanical signal to an electrical signal. Thus the mechanical properties of liquids can be measured with an electrical impedance bridge (HP4192A).

In the following a description of how $G_s(\omega)$ can be deduced from the measured electrical capacitance $C_m(\omega)$ will be given.

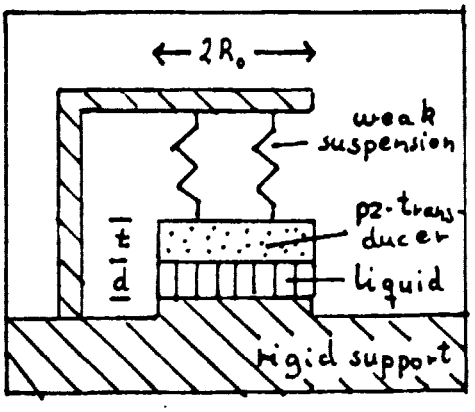

fig. 1a

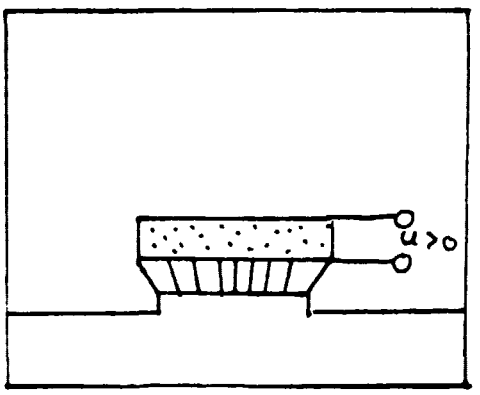

fig. 1b

Consider the following model system. A liquid layer of thickness d is placed between a completely rigid surface on one side and a piezoelectric disc (pz- disc) of radius R_0 and thickness t on the other, fig. 1a. The pz-disc has been poled axially and has rotational symmetry. It is coated with electrodes on top and bottom.

The pz-disc contracts (or expands) radially on application of an electric voltage and the liquid is given a shear strain. Dependent on the shearmodulus the liquid pulls more or less at the disc. This can be seen in the electrical capacitance of the disc. Notice that the strain field in the liquid will not be homogeneous.

Further details on the transducer will not be given here , but as will be shown the measurements are in good agreement with the model system.

Place a cartesian coordinate system with base vectors (e_x,e_y,e_z) at the center of the pz-disc, e_z in the axial direction. The equations are set up in cylinder coordinates (r,ϕ,z). These refers in the neighbourhood of $r = r\cos(\phi)e_x+r\sin(\phi)e_y+ze_z$ to the radial e_r, the azimuthal e_ϕ and axial e_z unit vectors. A material point lays at r before the displacement and r' after the displacement. The displacement field is $u(r) = r'-r = u_re_r+u_\phi e_\phi+u_ze_z$. The strain tensor becomes [24]

$$\epsilon_{rr} = \frac{\partial u_r}{\partial r} \qquad \epsilon_{\phi\phi} = \frac{1}{r}\frac{\partial u_\phi}{\partial \phi}+\frac{u_r}{r} \qquad \epsilon_{zz} = \frac{\partial u_z}{\partial z}$$

$$\epsilon_{\phi z} = \frac{1}{2}\left(\frac{1}{r}\frac{\partial u_z}{\partial \phi}+\frac{\partial u_\phi}{\partial z}\right) \qquad \epsilon_{rz} = \frac{1}{2}\left(\frac{\partial u_r}{\partial z}+\frac{\partial u_z}{\partial r}\right) \qquad \text{(4-1)}$$

$$\epsilon_{r\phi} = \frac{1}{2}\left(\frac{\partial u_\phi}{\partial r}-\frac{u_\phi}{r}+\frac{1}{r}\frac{\partial u_r}{\partial \phi}\right)$$

The cylindrical symmetry gives $u_\phi = 0$. Furthermore u_z is neglected, since the thickness of the disc is much lesser than radius. (t = .5mm , R_0 = 10mm). The only remaining nonzero components thus becomes

$$\epsilon_{rr} = \frac{\partial u_r}{\partial r} \quad , \quad \epsilon_{\phi\phi} = \frac{u_r}{r} \tag{4-2}$$

The offdiagonal elements of the stress tensor $\underline{\sigma}$ are zero being proportional to the offdiagonal elements of $\underline{\epsilon}$. Neglecting inertial effects σ_{zz} is also zero, because the pz-disc is free to move in axial direction.

The external electrical field of the piezoelectric ceramic is directed along the axial direction . This is also the pole axis and therefore the field of $\boldsymbol{E}$ and $\boldsymbol{D}$ must have the same directions inside the ceramic. The constitutive matrix connecting the inputvariables σ_{rr} , $\sigma_{\phi\phi}$, E_z with the outputvariables ϵ_{rr} , $\epsilon_{\phi\phi}$, D_z is symmetric (reciprocity/Onsager relations).Furthermore the axial symmetry means that there is no difference between the directions of $\boldsymbol{e}_r$ and $\boldsymbol{e}_\phi$. So one has [25]

$$\begin{pmatrix} \epsilon_{rr} \\ \epsilon_{\phi\phi} \\ D_z \end{pmatrix} = \begin{pmatrix} s_{11} & s_{12} & d_{31} \\ s_{12} & s_{11} & d_{31} \\ d_{31} & d_{31} & \epsilon_{33}^T \end{pmatrix} \begin{pmatrix} \sigma_{rr} \\ \sigma_{\phi\phi} \\ E_z \end{pmatrix} \tag{4-3}$$

If instead ϵ_{rr} , $\epsilon_{\phi\phi}$ and E_z are considered as inputvariables then

$$\begin{pmatrix} \sigma_{rr} \\ \sigma_{\phi\phi} \\ D_z \end{pmatrix} = \begin{pmatrix} c_{11} & c_{12} & -e_{31} \\ c_{12} & c_{11} & -e_{31} \\ e_{31} & e_{31} & \epsilon_{33}^S \end{pmatrix} \begin{pmatrix} \epsilon_{rr} \\ \epsilon_{\phi\phi} \\ E_z \end{pmatrix} \tag{4-4}$$

Denoting Poissons cross-contraction ratio by $p \equiv -\frac{s_{12}}{s_{11}}$ and the planar coupling factor [25]

by $k_p \equiv \left(\frac{2d_{13}^2}{\epsilon_{33}^T(s_{11}+s_{12})}\right)^{\frac{1}{2}}$ one has

$$c_{11} = \frac{1}{s_{11}+ps_{12}} \qquad c_{12} = \frac{p}{s_{11}+ps_{12}}$$
$$e_{31} = \frac{d_{13}}{s_{11}+s_{12}} \qquad \epsilon_{33}^{S} = \epsilon_{33}^{T}(1-k_p^2) \tag{4-5}$$

Let Q be the charge and U the potential difference of the electrodes of the pz-disc. The capacitance $C_m = Q/U$ is the measured quantity. Now $U = E_z t$ and

$$Q = \int_0^{R_0} 2\pi r D_z(r) dr \tag{4-6}$$

The free capacitance C_f defined by $\sigma_{rr} = \sigma_{\phi\phi} = 0$ becomes

$$C_f = \pi \epsilon_{33}^{T} \frac{R_0^2}{t} \tag{4-7}$$

and the clamped capacitance C_{cl} defined by $\epsilon_{rr} = \epsilon_{\phi\phi} = 0$ becomes

$$C_{cl} = \pi \epsilon_{33}^{S} \frac{R_0^2}{t} \tag{4-8}$$

Thus

$$\frac{C_{cl}}{C_f} = 1-k_p^2 \tag{4-9}$$

The coupling factor k_p is a dimensionless measure of the strength of the piezoelectric effect *. k_p ranges from zero to one. A value close to one means a strong coupling between the mechanical and electrical port. Typical values of k_p are 0.1 for quartz, .4 for barium titanate ceramic and .6 for lead zirconium titanate ceramic. The latter is the kind used here.

From (4-6) , (4-4) and (4-2) one deduce

$$Q = \int_0^{R_0} 2\pi r\{e_{31}(\epsilon_{rr}+\epsilon_{\phi\phi})+\epsilon_{33}^S E_z\}dr$$

$$= 2\pi\int_0^{R_0}\{e_{31}\frac{\partial}{\partial r}(ru_r)+r\epsilon_{33}^S E_z\}dr \qquad (4\text{-}10)$$

$$= 2\pi\{e_{31}R_0u_r(R_0)+\frac{1}{2}\epsilon_{33}R_0^2E_z\}$$

and thereby the measured capacitance

$$C_m = \frac{2\pi e_{31}R_0}{E_z t}u_r(R_0)+C_{cl} \qquad (4\text{-}11)$$

Introducing the dimensionless quantity

$$F \equiv \frac{C_m-C_{cl}}{C_f-C_{cl}} = (\frac{C_m}{C_{cl}}-1)\frac{1-k_p^2}{k_p^2} \qquad (4\text{-}12)$$

one finds

---

* In the computer programme the variable $kob = \frac{C_f-C_{cl}}{C_{cl}} = \frac{k_p^2}{1-k_p^2}$ is used instead of k_p

$$F = \frac{1}{E_z R_0 d_{31}} u_r(R_0) \qquad (4\text{-}13)$$

F is by (4-12) directly given by the measurable quantity C_m. It is left to find the displacement $u_r(R_0)$ of the edge of the pz-disc as a function of the shear rigidity G of the liquid and to invert this function.

The radial equation of motion becomes (fig.2)

$$(r+dr)d\phi t\sigma_{r+dr,r+dr} - rd\phi t\sigma_{rr} - drt2\frac{d\phi}{2}\sigma_{\phi\phi} \qquad (4\text{-}14)$$

$$-\sigma_v r dr d\phi = \rho t dr r d\phi \ddot{u}_r$$

Here the tangential stress $-\sigma_v$ on the surface element $drrd\phi$ being due to the liquid gives rise to the force $-\sigma_v drrd\phi$ *. ρ is the density of the piezoelectric ceramic.

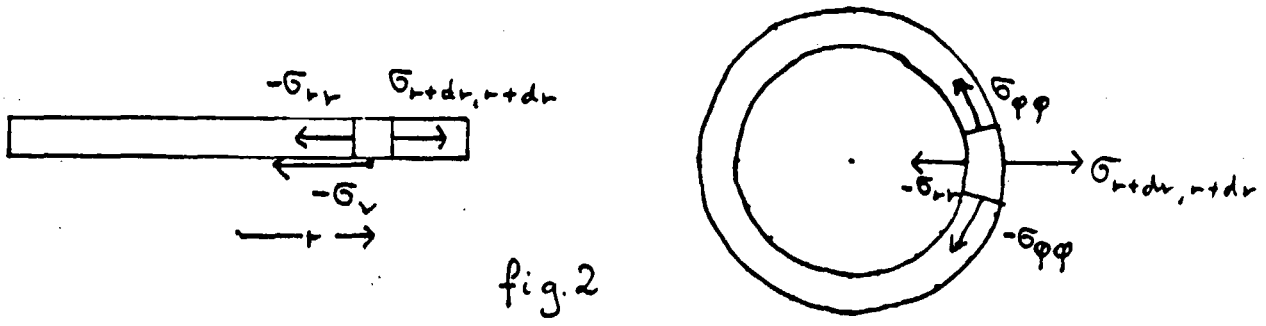

fig. 2

(4-14) becomes

---

* Obviously $-\sigma_v$ has a torque about the azimuthal axis. This is compensated by torques of gradients of σ_{rz} emerging as the disc bends. This bending is neglected. Otherwise the two constitutive equations $\epsilon_{rz} = s_{44}\sigma_{rz} + d_{15}E_r$, $D_r = d_{15}\sigma_{rz} + \epsilon_{11}^T E_r$ and the axial equation of motion should be taken into account

$$\frac{\partial}{\partial r}(r\sigma_{rr}) - \sigma_{\phi\phi} - \sigma_v \frac{r}{t} = \rho r \ddot{u}_r \qquad (4\text{-}15)$$

In the following harmonic time variation of E_z and u_r at cyclic frequency ω is assumed and the factor $e^{-i\omega t}$ is eliminated. An essential assumption is that the deformation in the liquid is pure shear and that only the component $\epsilon_{rz}^{liquid}(r)$ is nonzero. Again this approximation holds because $d \ll R_0$. Then (fig.3)

$$\sigma_v = 2G(\omega)\epsilon_{rz}^{liquid} = G(\omega)\frac{u_r(r)}{d} \qquad (4\text{-}16)$$

where $G(\omega)$ is the shearmodulus of the liquid.

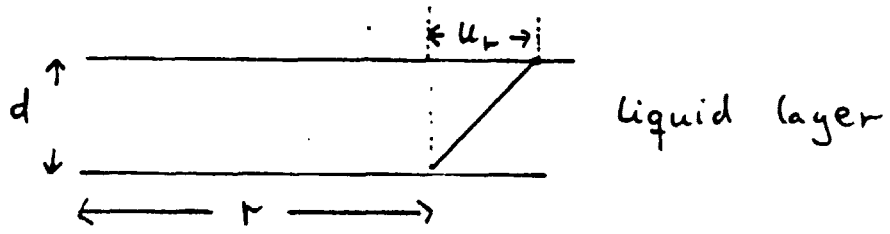

fig. 3

Using (4-2) , (4-4) and (4-16) the tensions of equation (4-15) can be expressed by the displacement u_r,

$$r^2 u_r'' + r u_r' + \{(\frac{\omega^2 \rho}{c_{11}} - \frac{G(\omega)}{c_{11} dt}) r^2 - 1\} u_r = 0 \qquad (4\text{-}17)$$

The boundary conditions of this differential equation is zero deformation at the center,

$$u_r(0) = 0 \qquad (4\text{-}18)$$

and zero stress at the edge,

$$\sigma_{rr}(R_0) = 0 \qquad (4\text{-}19)$$

or using (4-4) , (4-5) and (4-2)

$$u_r'(R_0) + \frac{p}{R_0} u_r(R_0) = (1+p) d_{31} E_z \qquad (4\text{-}20)$$

The problem becomes dimensionless by the definition

$$x \equiv r/R_0 \quad , \quad e(x) \equiv \frac{1}{(1+p) d_{13} E_z R_0} u_r(R_0 x) \qquad (4\text{-}21)$$

Define the characteristic

$$\textit{modulus} \qquad G_K \equiv \frac{c_{11} dt}{R_0^2} \qquad (4\text{-}22)$$

$$\textit{inertance} \qquad M_K \equiv \rho\, dt \qquad (4\text{-}23)$$

and

$$\textit{frequency} \qquad 2\pi f_K \equiv \omega_K \equiv \sqrt{\frac{G_K}{M_K}} = \sqrt{\frac{c_{11}}{\rho R_0^2}} \tag{4-24}$$

together with

$$V \equiv \frac{G(\omega)}{G_k} \quad , \quad S \equiv (\frac{\omega}{\omega_K})^2 \quad , \quad k^2 \equiv S-V \tag{4-25}$$

Then (4-17) becomes a Bessel differential equation

$$x^2e''+xe'+(k^2x^2-1)e = 0 \tag{4-26}$$

with boundary conditions

$$e(0) = 0 \tag{4-27}$$

$$e'(1)+pe(1) = 1 \tag{4-28}$$

The dimensionless measure (4-13) of the measured electrical capacitance becomes

$$F(\omega) = (1+p)e(1) \tag{4-29}$$

$e(1)$ is by (4-26) a function of k and thereby ω. The solution of (4-26) is given by 1.order Bessel functions

$$e(x) = AJ_1(kx)+BY_1(kx) \tag{4-30}$$

(4-27) yields $B = 0$, while (4-28) leads to

$$A = (kJ_1(k)+pJ_1(k))^{-1} = (kJ_0(k)+(p-1)J_1(k))^{-1} \tag{4-31}$$

Thus the measured electrical capacity C_m becomes

where

and

$$C_m(\omega) = C_{cl}(F(S(\omega),V(\omega))\frac{k_p^2}{1-k_p^2}+1) \tag{4-32}$$

$$F(S,V) = (1+p)\frac{J_1(k)}{kJ_0(k)+(p-1)J_1(k)} \tag{4-33}$$

$$k = \sqrt{S-V} = \sqrt{(\frac{\omega}{\omega_K})^2-\frac{G(\omega)}{G_K}} \tag{4-34}$$

The resonances occur for those $k = k_n$, $n = 1,2...$, which satisfy

$$0 = k_nJ_0(k_n)+(p-1)J_1(k_n) \tag{4-35}$$

Thus the resonances depends on Poissons ratio p. A numerical solution of (4-35) gives approximately

$$k_1(p) = 0.621p+1.861 \qquad 0.2 < p < 0.4 \tag{4-36}$$

$$k_2(p) = 0.192p+5.332 \qquad 0.2 < p < 0.4 \tag{4-37}$$

and so

$$p(k_2/k_1) = -1.417k_2/k_1+4.032 \qquad 2.5 < k_2/k_1 < 2.75 \tag{4-38}$$

$f_i \equiv f_K k_i$ are the measured dimensional resonance frequencies of an empty transducer ($G(\omega) = 0$). Since $f_2/f_1 = k_2/k_1$, (4-38) makes it possible to determine Poissons ratio directly from the observed 1. and 2. resonance frequencies without knowing the characteristic frequency f_K. p is found to be 0.31 within a variation of 3% in the temperature interval 180 K - 250 K. This variation is neglected in the following. Thus

$$k_1 = 2.054 \qquad k_2 = 5.391 \qquad for \quad p = 0.31 \tag{4-39}$$

The zeros of F occur for those $k = j_n$, $n = 1,2...$,which satisfy

$$0 = J_1(j_n) \tag{4-40}$$

The first two are $j_1 = 3.8317$, $j_2 = 7.0156$. Hence it is possible to determine C_{cl} as the measured capacitance at the first antiresonance frequency

$$f_{al} = \frac{j_1}{k_1} f_1 = 1.865 f_1 \quad , \quad C_{cl} = C_m(f_a) \tag{4-41}$$

Fig. 4 shows a fit to C_m of the empty transducer at 250 K obtained by suitable scaling. The fitting parameters f_K (or rather $f_1 = f_K k_1$) and k_p was varied to give the best proportionality between C_m and $F\frac{k_p^2}{1-k_p^2}+1$ at all frequencies as shown in fig.5. Thereby C_{cl} is automatically given as the proportionality constant. At this temperature it was found $f_1 = 107.1\ kHz$, $k_p = 0.55$ and $C_{cl} = 7.53\ nF$. Typical values of the other characteristic entities can then be given.Since $\rho = 7.65 \cdot 10^3\ kgm^{-3}$, $d = \frac{1}{6} \cdot 10^{-3}\ m$ and $t = \frac{1}{2} \cdot 10^{-3}\ m$ one has $M_K = \rho dt = 6.4 \cdot 10^{-4} kgm^{-1}$ and hence $G_K = M_K(\frac{2\pi f_1}{k_1})^2 = 6 \cdot 10^7\ Pa$.

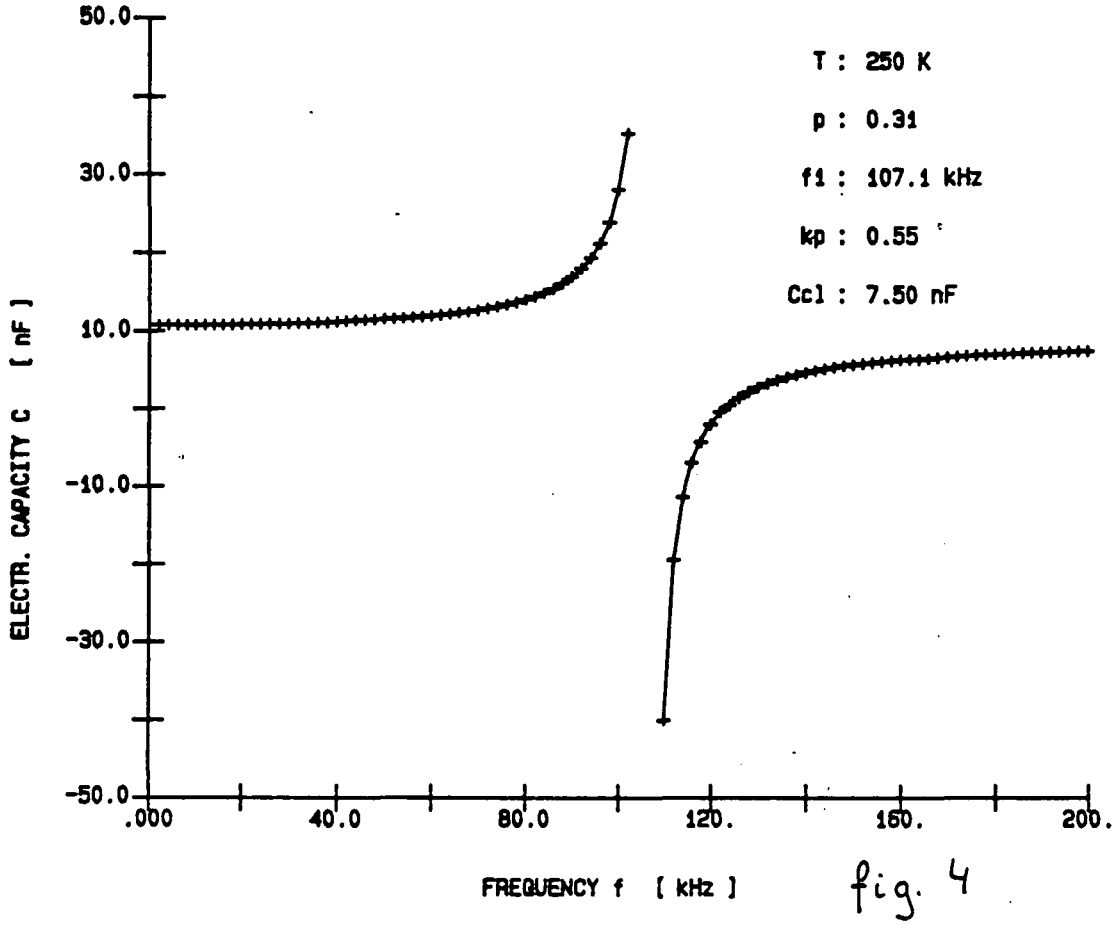
T : 250 K
p : 0.31
f1 : 107.1 kHz
kp : 0.55
Cc1 : 7.50 nF
50.0
30.0
10.0
-10.0
-30.0
-50.0
ELECTR. CAPACITY C [nF]
.000
40.0
80.0
120.
160.
200.
FREQUENCY f [kHz]

fig. 4

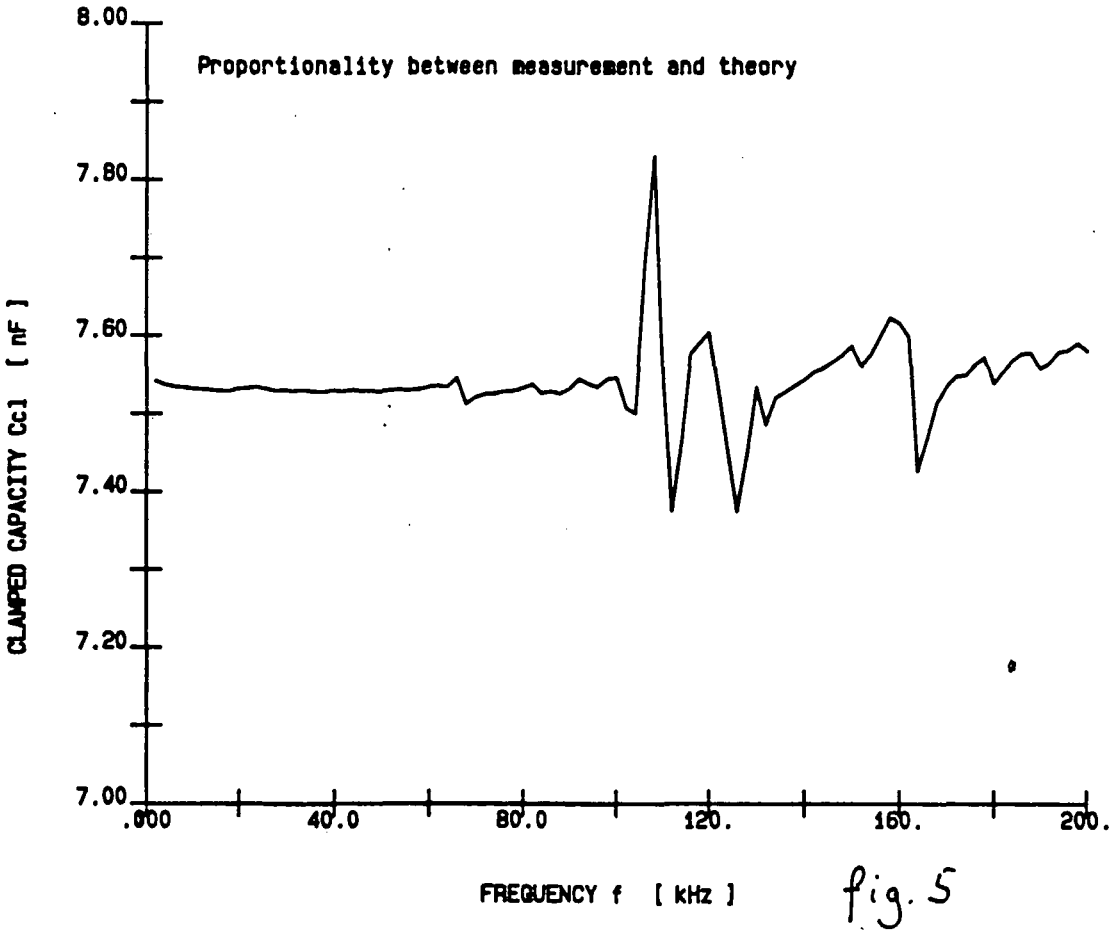
Proportionality between measurement and theory
8.00
7.80
7.60
7.40
7.20
7.00
CLAMPED CAPACITY Cc1 [nF]
.000
40.0
80.0
120.
160.
200.
FREQUENCY f [kHz]

fig. 5

4.1.2 A resonance method.

The transducer can in principle be used in a very simple way to determine shearmodulus $G(f_i)$ of a substance in temperature ranges, where G shows no dispersion and is real at the resonance frequencies. Denoting $f_i(0)$ and $f_i(G)$ the i'th resonance frequency of the empty and filled transducer respectively. Then according to (4-34)

$$k_i^2 = \frac{f_i(0)}{f_K} = (\frac{f_i(G)}{f_K})^2 - \frac{G(f_i)}{G_K} \qquad (4\text{-}42)$$

or

$$G(f_i) = k_i^2 G_K((\frac{f_i(G)}{f_i(0)})^2 - 1) \qquad (4\text{-}43)$$

$$= (2\pi)^2 M_K(f_i^2(G) - f_i^2(0)$$

Thus G is determined by the movement of the resonances. In practice however thickness and floppy modes not considered in the present treatment can trouble this method. Indeed the interest here is the case of G showing dispersion and the complete solution (4-32) - (4-34) has to be used.

4.1.3 The partially filled transducer.

A complication arises when the liquid does not fill out the cell completely. This is inevitable since the cell is filled at T = 300 K and the measurement perhaps done at 200 K. With a typical expansion coefficient of $4 \cdot 10^{-4}\ K^{-1}$, $\frac{\Delta R_l}{R_l}$ becomes 3% . This is of importance since the greatest shear deformation is at the edge. Thus an enlarged model with the liquid filling up the cell to radius R_l is considered. Put $x_l = R_l/R_0$. (4-26) is replaced by

$$\begin{aligned} x^2 e_1'' + x e_1' + [(k_1 x)^2 - 1] e_1 &= 0 \quad , \quad k_1^2 = \frac{M_K \omega^2 - G}{G_K} \\ x^2 e_2'' + x e_2' + [(k_2 x)^2 - 1] e_2 &= 0 \quad , \quad k_2^2 = \frac{M_K \omega^2}{G_K} \end{aligned} \tag{4-44}$$

The boundary conditions are as before plus continuity of displacement and stress at x_l,

$$\begin{aligned} e_1(0) &= 0 \quad , \quad e_1(x_l) = e_2(x_l) \\ e_1'(x_l) + \frac{p}{x_l} e_1(x_l) &= e_2'(x_l) + \frac{p}{x_l} e_2(x_l) \\ e_2'(1) + p e_2(1) &= 1 \end{aligned} \tag{4-45}$$

Introduce

$$\begin{aligned} P &= k_2 J_o(k_2) + (p-1) J_1(k_2) \\ Q &= k_2 Y_0(k_2) + (p-1) Y_1(k_2) \\ R &= k_1 x_l J_0(k_1 x_l) J_1(k_2 x_l) - k_2 x_l J_0(k_2 x_l) J_1(k_1 x_l) \\ T &= k_1 x_l J_0(k_1 x_l) Y_1(k_2 x_l) - k_2 x_l Y_0(k_2 x_l) J_1(k_1 x_l) \end{aligned} \tag{4-46}$$

$$\begin{aligned} \Delta &= PT - RQ \\ C &= T/\Delta \end{aligned}$$

$$D = -R/\Delta$$

Then

$$e_2(1) = CJ_1(k_2)+DY_1(k_2) \tag{4-47}$$

$e_2(1)$ is by C , D and k_2 a function of V , S and x_l .

F defined by (4-12) becomes now a function of x_l also . It is still given by (4-13), that is (4-33) is replaced by

$$F(S,V,x_l) = (1+p)e_2(1) \tag{4-48}$$

while (4-32) , (4-34) still hold.

4.1.4 The weak dispersion of the dielectric constants of the piezoceramics.

Another problem also must be taken into account.In fig.6 is shown again the ratio between C_m and $F\frac{k_p^2}{1-k_p^2}+1$ but in a logarithmic plot over a wider frequency span. Below the resonances, C_{cl} is seen to have a weak dispersion. This reflects dispersion of the dielectric constant $\epsilon_{33}^S \propto C_{cl}$. Similarly $C_f \propto \epsilon_{33}^T$ will show dispersion, but it is assumed in the following that C_f/C_{cl} and thereby the coupling factor k_p is not frequency dependent.

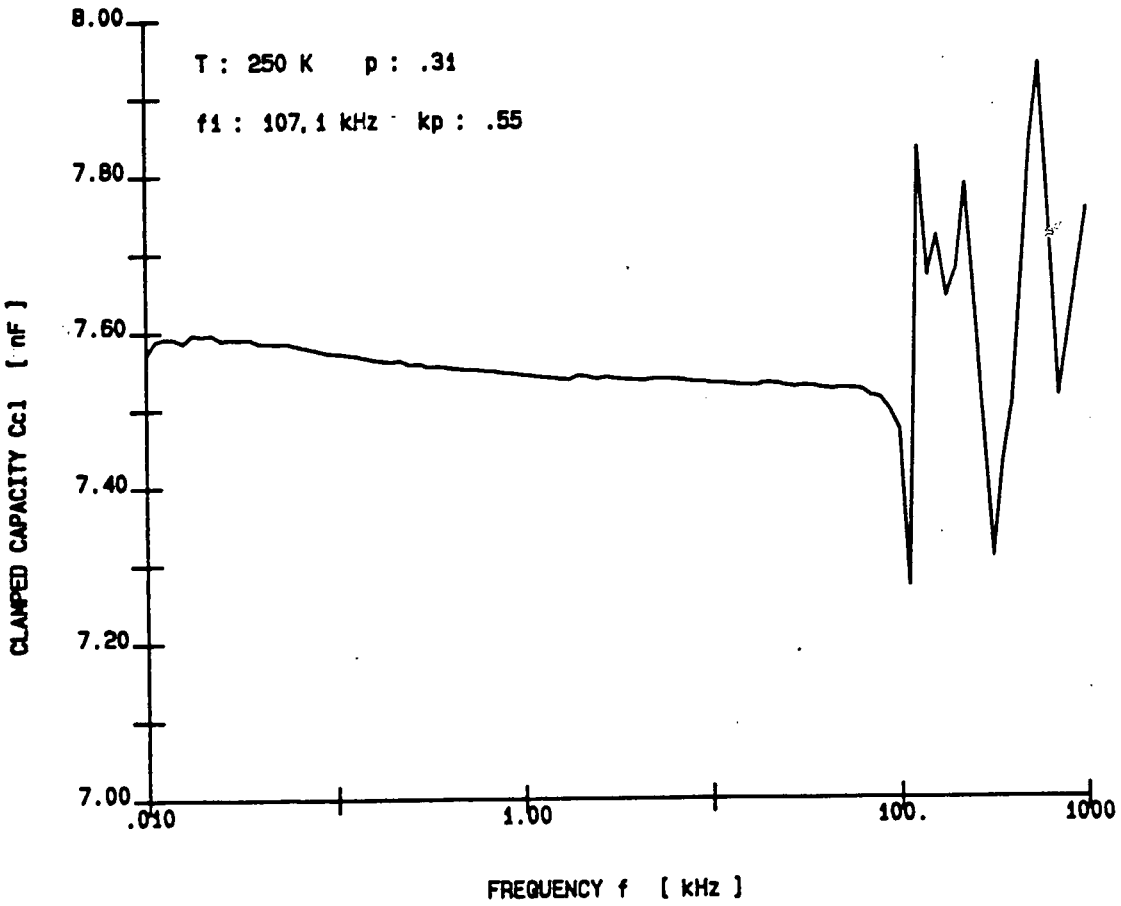

Fig. 6

Then the frequency dependence can be eliminated in the analysis by considering the ratio of a referencespectrum $C_r(\omega)$ of an empty transducer and a spectrum $C_m(\omega)$ of a filled cell. Introduce

$$\Phi(S,V,x_l) = \frac{C_m - C_{cl}}{C_r - C_{cl}} = \frac{F(S,V,x_l)}{F(S,0,1)} \tag{4-49}$$

$$= \frac{C_m}{C_r}\left(1 + \frac{1-k_p^2}{k_p^2}\frac{1}{F(0,S,1)}\right) - \frac{1-k_p^2}{k_p^2}\frac{1}{F(0,S,1)}$$

$F(S,V,x_l)$ and $F(S,0,1)$ and thus $\Phi(S,V,x_l)$ are known analytically. C_m and C_v can be measured and thus Φ determined experimentally. Left is only an inversion to give $V = G(\omega)/G_K$. This is done by approximating Φ with an algebraic expression. Since $\Phi \to 1$ *for* $V \to 0$ and $\Phi \to 0$ *for* $V \to \infty$ a broken rational function with the denominater of 1 degree higher the numerator is chosen,

$$\Phi(S,V,x_l) = \frac{1 + a(S,\epsilon)V}{1 + b(S,\epsilon)V + c(S,\epsilon)V^2} \tag{4-50}$$

where $\epsilon = 1 - x_l$ and

$$a(s,\epsilon) = \frac{1}{a_1(\epsilon)\left(1 - s\frac{1}{a_2(\epsilon)}\right)} \tag{4-51}$$

$$a_1(x) = 25.82(1 - 0.407\epsilon - 22.27\epsilon^2)$$

$$a_2(x) = 13.25(1 + 0.2\epsilon + 11\epsilon^2)$$

$$b(s,\epsilon) = \frac{1}{(4.54 + 14.7\epsilon)\left(1 - \frac{s}{4.22}\right)} \tag{4-52}$$

$$c(s,\epsilon) = \frac{1}{(740. + 18500.\epsilon)(1 - 0.287s + 0.118s^2)} \tag{4-53}$$

This expression approximates Φ within 5% for $0.95 < x_l < 1.0$ and $0.0 < s < 4.0$, that is up to the first resonance of the free transducer.

Inversion of (4-50) yields

$$V(S,x_l) = \frac{a-b\Phi+\sqrt{(a-b\Phi)^2-4\Phi c(\Phi-1)}}{2\Phi c} \qquad (4\text{-}54)$$

Fig. 7 and 8 illustrate the accuracy of the algebraic fit to Φ . These Nyquist plots show the imaginary versus real part of the modulus of a hypothetical Maxwell liquid

$$G_M(\omega) = G_\infty \frac{-i\omega\tau}{1-i\omega\tau} \qquad (4\text{-}55)$$

with $G/G_\infty = 10$ and radius $x_l = 1.00$ respectively 0.95. The solid line is the Maxwell model G_M. The crosses are $V(\Phi)$ calculated from (4-54) but with Φ calculated from G_M by the analytical formulas (4-48),(4-47),(4-46).

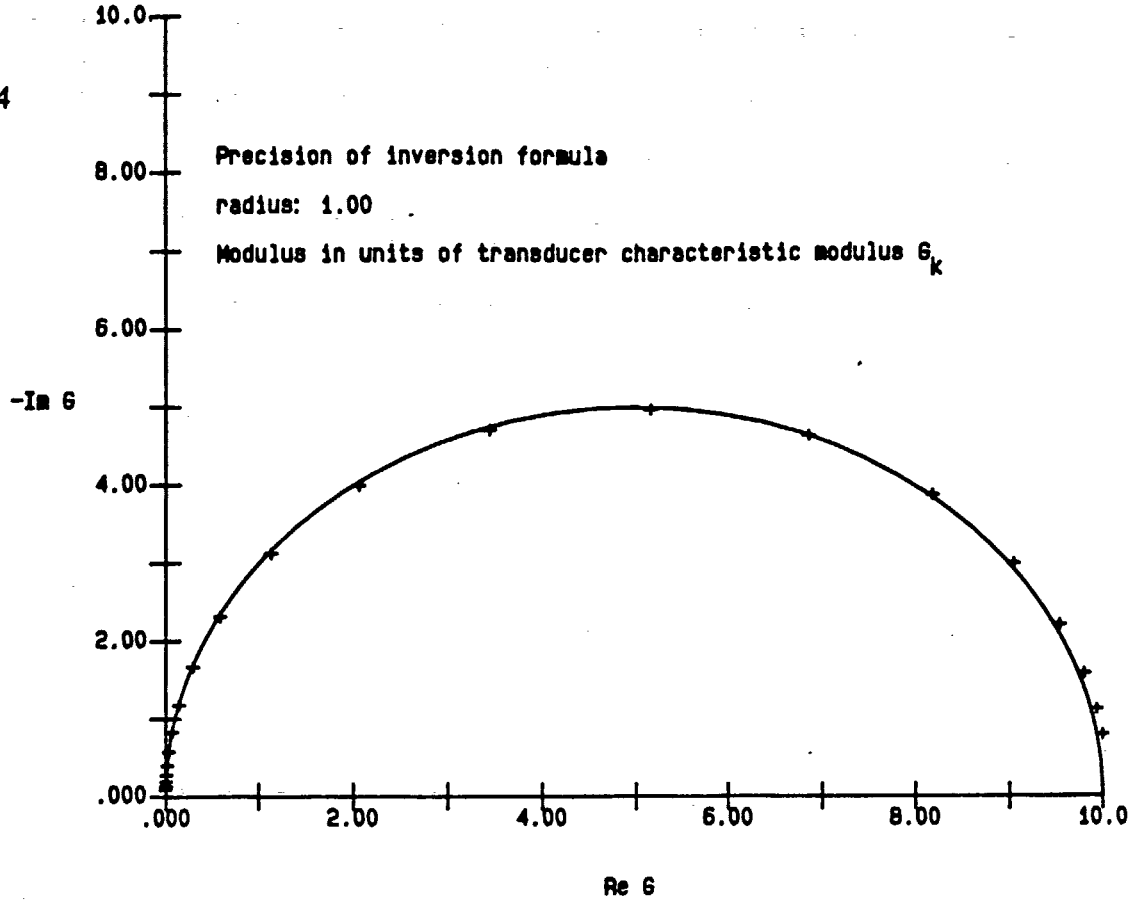
Precision of inversion formula
radius: 1.00
Modulus in units of transducer characteristic modulus G_k
-Im G
Re G
10.0
8.00
6.00
4.00
2.00
.000
.000
2.00
4.00
6.00
8.00
10.0

Fig 7

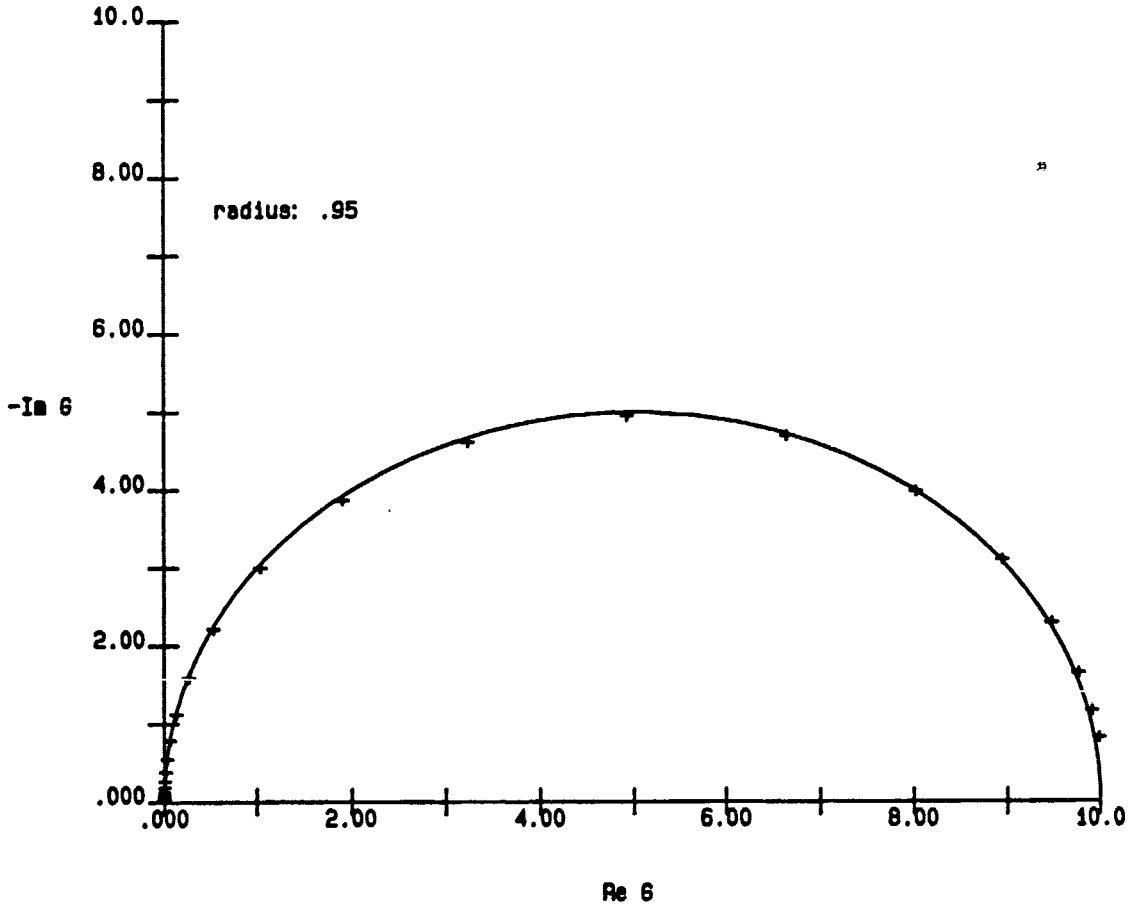
radius: .95
-Im G
Re G
10.0
8.00
6.00
4.00
2.00
.000
.000
2.00
4.00
6.00
8.00
10.0

Fig 8

In order to further increase the accuracy in calculating V one can now resort to a Newton algorithm with the V calculated by (4-54) as a trial function V_t. It follows from (4-32) that

$$F(S,V,x_l) = \frac{C_m}{C_r}(F(S,0,1)+\frac{1-k_p^2}{k_p^2})-\frac{1-k_p^2}{k_p^2} \tag{4-56}$$

Denote the value of F calculated by this formula using the measured $C_m(\omega)$ and $C_r(\omega)$ by F_m (the measured F) and the exact V corresponding to this value by V_0. Thus $F_m = F(S,V_0,x_l)$. Since V_0 is near V_t one has

$$F_m-F_t \approx(\frac{\partial F}{\partial V}_{V_t})(V_0-V_t) \approx(\frac{\Delta F}{\Delta V}_{V_t})(V_0-V_t) \tag{4-57}$$

V is complex. A complex derivative is independent of the direction of the differention. Let $\Delta V = V_t\delta$, where δ is a small real positive number, that is differentiate in the direction of V_t. Then

$$F_m-F(V_t) \approx \frac{F(V_t(1+\delta))-F(V_t))}{V_t\delta}(V_0-V_t) \tag{4-58}$$

or

$$V_0 \approx V_t(1+\delta\frac{F_m-F(V_t)}{F(V_t(1+\delta))-F(V_t)}) \tag{4-59}$$

If one uses the V_0 calculated by (4-59) as a new trial function the process can be iterated since the successive V_t will have V_0 as a fix point. However (4-54) is so close to the exact value that in practise one iteration suffices.

4.2 shearmodulus $G(\omega)$ of 1,2-butanediol; 1,3- butanediol; 1,2,6-hexanetriol 1,2-propanediol ; 2- methyl-2,4-pentanediol.

Shearmodulus of 6 different liquids have been measured. The experimental procedures were identical, and the liquid 2-methyl-2,4-pentanediol is taken as an example.
Preliminary the empty transducer was calibrated. The properties of the piezoelectric ceramic is temperature and timedependent (annealing effects), and so an identical time schedule was followed in calibration and measurement.
The transducer is placed in a cryostat. First the temperature was lowered from about 300 K to 250.0 K and the ceramic annealed for 200 minutes. Then one spectrum $C_r(\omega)$ was taken and another 15 minutes later. The temperature was now lowered in steps of 4 K every 30 minutes and for each temperature step two spectra was taken, respectively 15 and 30 minutes after the step until the temperature was 170 K.
By fitting the theoretical spectrum to the measured the scaling factors f_1 (resonance frequency), k_p (coupling factor) and C_{cl} (clamped capacity) was found at some temperatures as described page 26 and their temperature dependences interpolated at both annealing times.
After the calibration , the spectrum $C_m(\omega)$ of the frequency dependence of the electrical capacitance of the filled transducer was taken following the same time schedule. In fig. 4.2.1 is shown the real part of C_m versus frequency $f = \frac{\omega}{2\pi}$ at some of these temperatures. The curves are twofold due to the annealing of the ceramic. That this is so, and not an annealing effect of the liquid, becomes clear, when the modulus is calculated by (4-49) and (4-54) using the different reference spectra of the two annealing times.

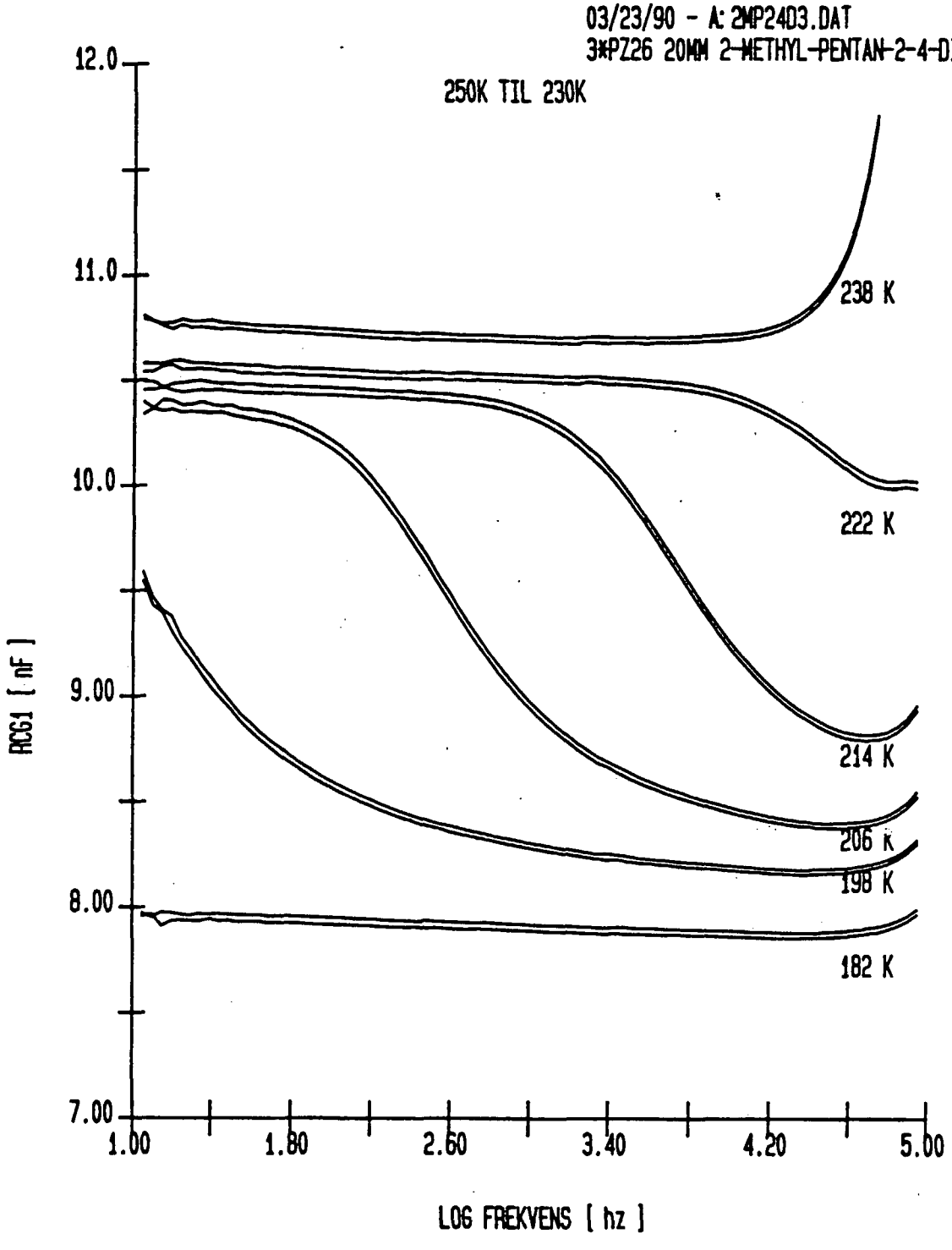
03/23/90 - A: 2MP2403.DAT
3*PZ26 20MM 2-METHYL-PENTAN-2-4-DIOL
250K TIL 230K
238 K
222 K
214 K
206 K
198 K
182 K
RCG1 [nF]
12.0
11.0
10.0
9.00
8.00
7.00
1.00
1.80
2.60
3.40
4.20
5.00
LOG FREKVENS [hz]

Fig 4.2.1

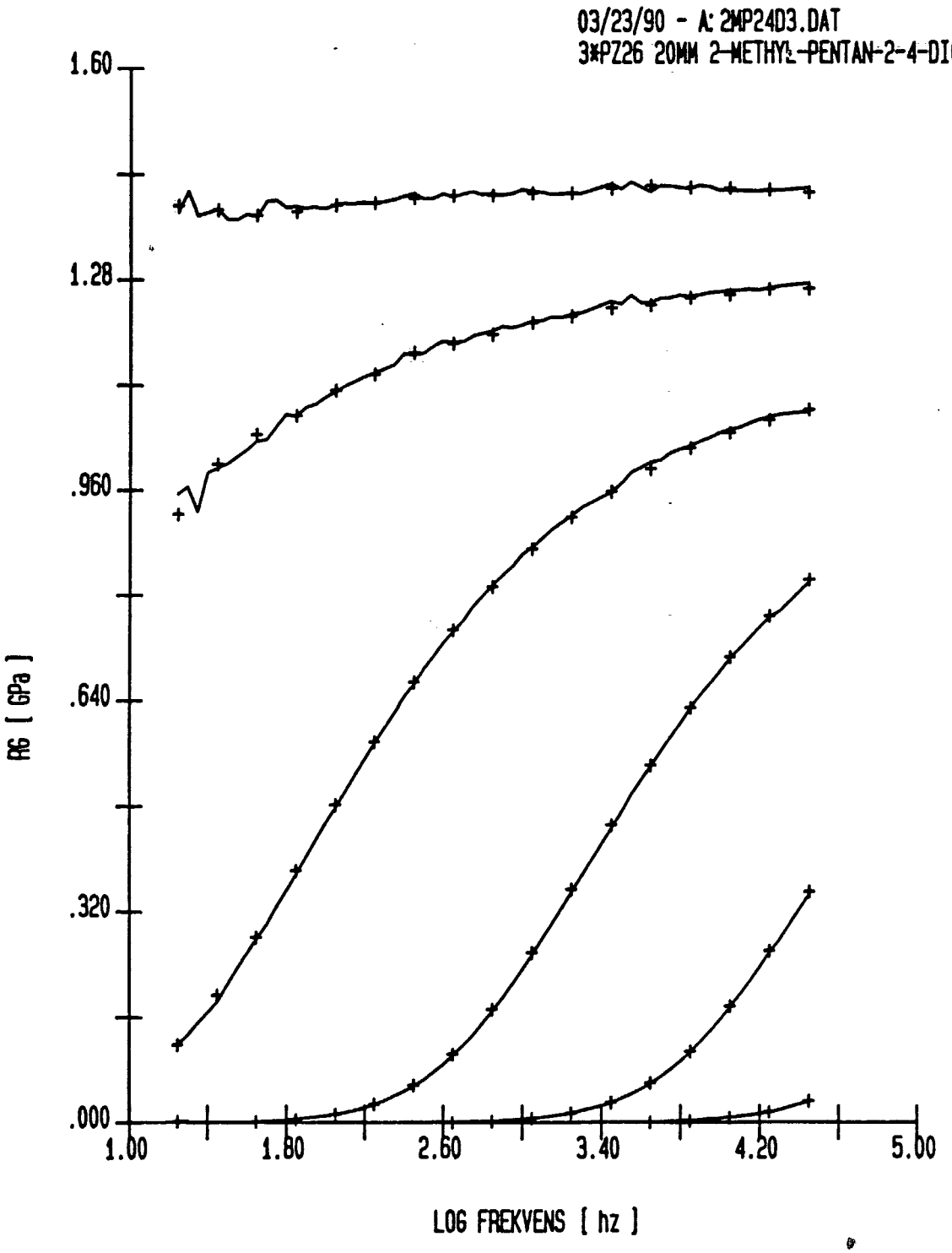
03/23/90 - A:2MP24D3.DAT
3*PZ26 20MM 2-METHYL-PENTAN-2-4-DIOL
1.60
1.28
.960
.640
.320
.000
RG [GPa]
1.00
1.80
2.60
3.40
4.20
5.00
LOG FREKVENS [hz]

Fig 4.2.2

The real part of the modulus versus frequency is shown fig. 4.2.2, the solid line is the results at first annealing time (20 points/decade) and the crosses the results at second annealing time (for clarity 4 points/decade picked out). In the modulus no difference is seen between measurements at different annealing times. The liquids were all assumed to have a thermal expansion of $4*10^{-4}$ K, in order to calculate the radius of the liquid at different temperatures *.

It has turned out that the data of the liquids consider here can be represented by a simple extension of the Maxwell model. Recapitulate this, the simplest model of a viscoelastic liquid. The response of the liquid to a shear stress is represented as the connection of a dashpot and a spring giving the creep function

$$J(\omega) = J_\infty + \frac{1}{-i\omega\eta} = J_\infty(1+(-i\omega\tau_M)^{-1}) \qquad \tau_M = \frac{\eta}{G_\infty} \tag{4-60}$$

or the modulus

$$G(\omega) = \frac{1}{J(\omega)} = G_\infty \frac{-i\omega\tau_M}{1-i\omega\tau_M} \quad , \quad G_\infty = \frac{1}{J_\infty} \tag{4-61}$$

The plot of Re G versus Im G gives the characteristic half circle fig 4.1.7. This model fails for most liquids but the liquids considered here are astonishing well represented by adding a term to the Maxwell model

$$J(\omega) = J_\infty(1+(-i\omega\tau)^{-1}+q(-i\omega\tau)^{-\alpha}) \tag{4-62}$$

$G(\omega)$ changes with temperature, but it is possible to keep q and α of the fit constant, only varying $\tau(T)$ and $G_\infty(T)$. That is the so-called principle of temperature-time equivalence holds.

*Trials with different expansion coefficients of the same order has shown that $G(\omega)$ only becomes scaled with a constant factor, so it is not critical not knowing exact value of the expansion coefficient for the determination of q, α and $\tau(T)$ in the following.

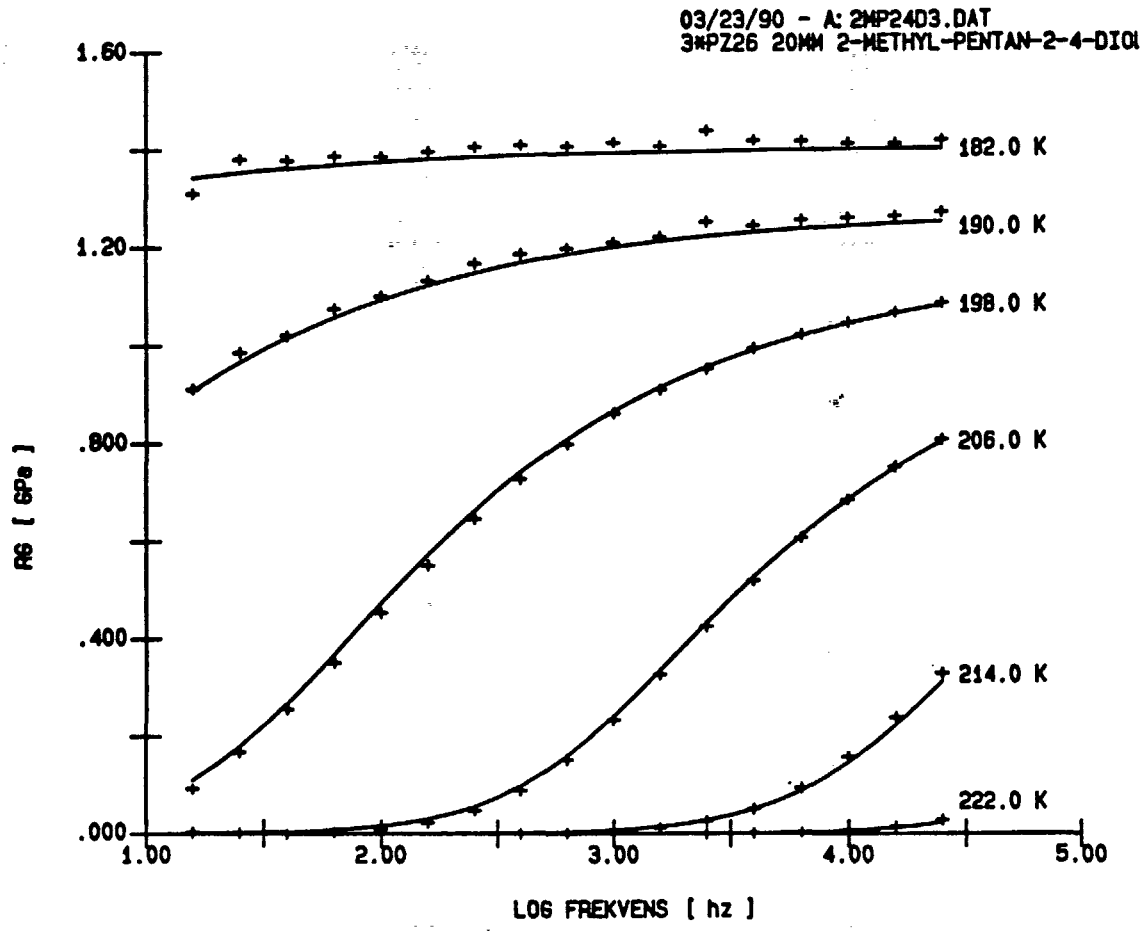

Fig 4.2.3

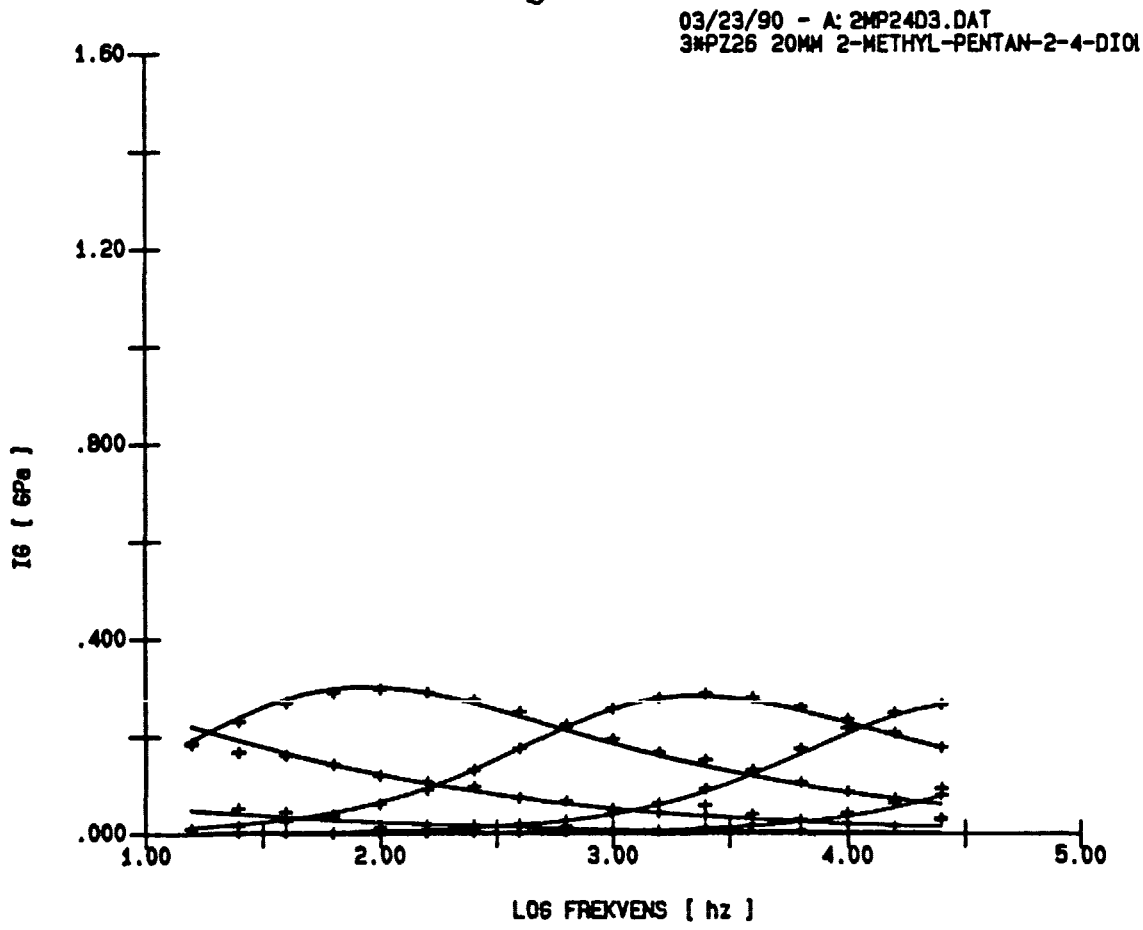

Fig 4.2.4

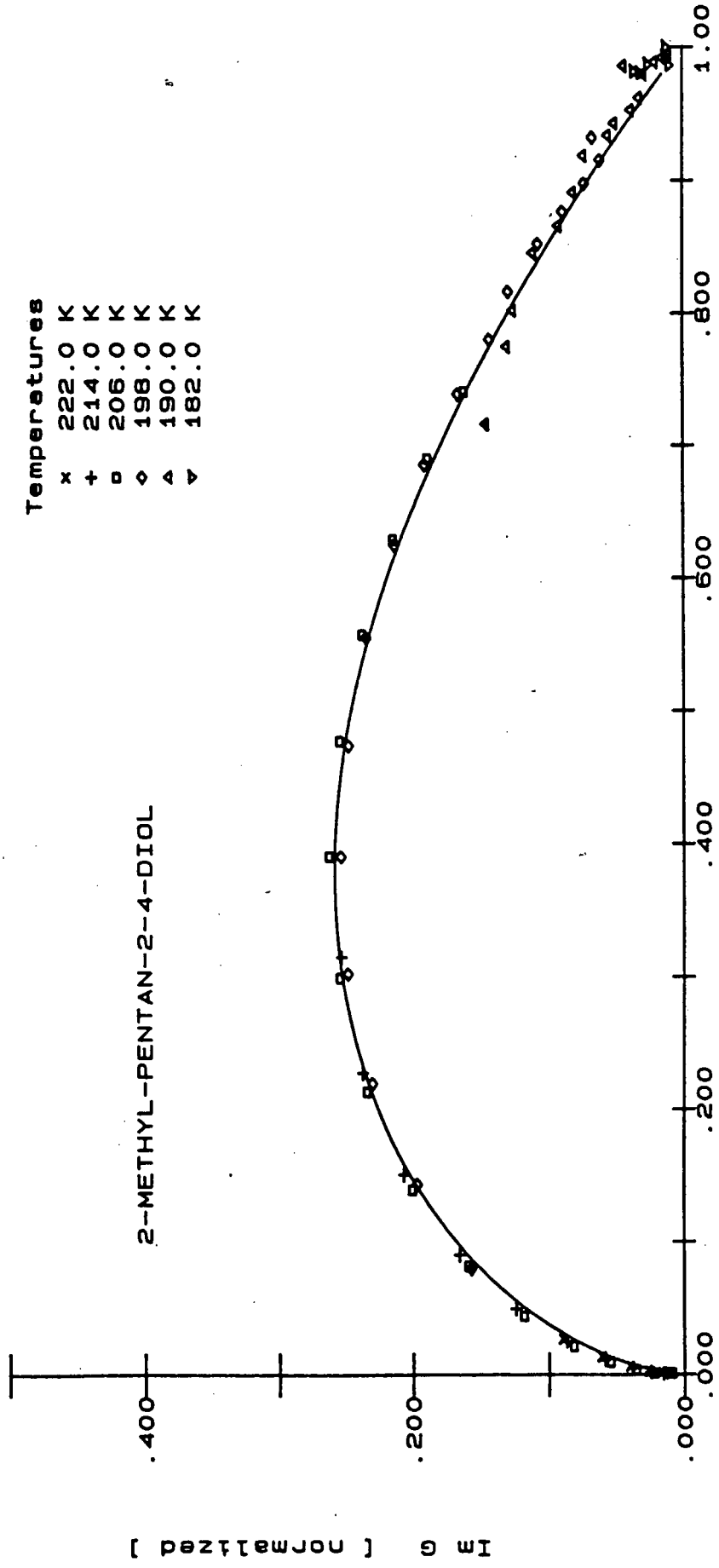
Temperatures
x 222.0 K
+ 214.0 K
□ 206.0 K
◇ 198.0 K
△ 190.0 K
▽ 182.0 K
2-METHYL-PENTAN-2-4-DIOL
Im G [normalized]
Re G [normalized]
.000
.200
.400
.600
.800
1.00

Fig 4.2.5

Fig. 4.2.3. and 4.2.4 shows such a fit (the solid line) to the measured $G(\omega,T)$ (the crosses) with α = .42 , q = 1.25 ,

$$G(\omega,T) = G_\infty(T)\frac{-i\omega\tau(T)}{1-i\omega\tau(T)+q(-i\omega\tau(T))^{1-\alpha}} \qquad (4\text{-}63)$$

Fig 4.2.5 shows the normalized plot $Re\{\frac{G}{G_\infty(T)}\}$ versus $Im\{\frac{G}{G_\infty(T)}\}$. The standard deviation of one point respective to the fitted curve is even at the lowest temperatures lesser than 2%.

The measured modulus of the other liquids can be fitted equally well and the results on q and α is showed in table 4.1

Fig. 4.2.6 shows the temperature dependence of the relaxation time of the model (4-63) .This could be fitted for all the liquids by

$$\tau(T) = \exp(A_3(\frac{1}{T^3}-\frac{1}{T_0^3})) \qquad (4\text{-}64)$$

where the constants A_3 and T_0 is given in table 4.1.

Table 4.1

Parameters of fit to Shear Modulus

	q	alfa	A_3 10^8 K^3	T_0 K
1,2-butanediol	1.63	.42	1.76	177.2
1,3-butanediol	1.53	.425	1.73	176.5
1,2,6-hexanetriol	2.1	.42	2.74	201.3
1,2-propanediol	1.8	.48	1.44	169.8
2-metyl-2,4-pentanediol	1.25	.42	2.27	186.4

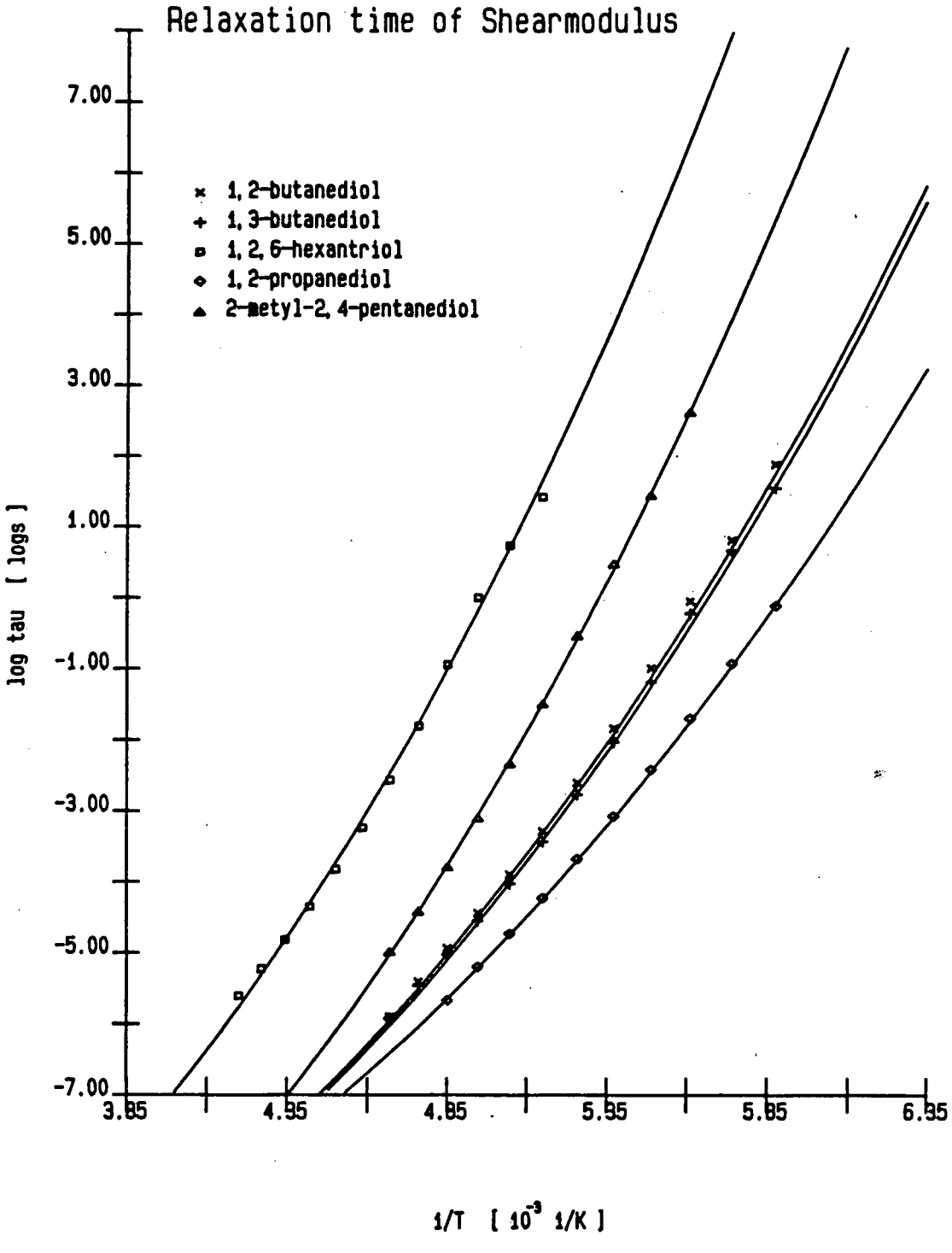
Relaxation time of Shearmodulus
1, 2-butanediol
1, 3-butanediol
1, 2, 6-hexantriol
1, 2-propanediol
2-metyl-2, 4-pentanediol
7.00
5.00
3.00
1.00
-1.00
-3.00
-5.00
-7.00
log tau [logs]
3.85
4.35
4.85
5.35
5.85
6.35
1/T [10^-3 1/K]

fig 4.2.6

Chapter 5. Comparison of relaxation times.

The specific heat $c_p(\omega)$ and shearmodulus $G(\omega)$ of five liquids have been found.

It is already clear from table 3.1 and 4.1, that the relaxation times are not equal for the two kinds of experiments. T_0 of both fits (3-6) and (4-64) is the temperature, where τ is 1 s, and this temperature is systematically higher for $c_p(\omega)$ than for $G(\omega)$.

This fact becomes more clear in the figures 5.1-5.3. The relaxation time of the specific heat is seen to be 1-1.5 decade longer than that of the shear modulus.

The two cryostats used in the measurements were calibrated using a pt100 platinum resistor and they have the same temperature within 0.1 K. Therefore a temperature difference cannot explain the difference.

Moreover, the experiments reported here are supported by other experiments. The solid lines of fig 5.1 and 5.2 are relaxation times deduced from enthalpy relaxation [20] and the solid line of fig 5.3 the relaxation time by an alternative measurement of $c_p(\omega)$ [26] The dashed lines of fig 5.1 and 5.2 are the relaxation times of shearmodulus measured in the Mhz-range [27].

A theory of the glass transition of these liquids should connect the thermal and mechanical properties, but will have to explain the differences in the relaxation times of the shear modulus and the specific heat. Regarding the shape of the relaxation functions a theory must tell how they should be compared. It seems naturel however that the exponent α describing the high frequency behaviour in both cases, should be the same. In terms of a distribution of relaxation times a small α reflects a broad distribution. In comparing table 3.1 and 4.1 one finds that the spectrum of the specific heat is equal to or perhaps a little narrower than that of the shearmodulus.1,2,6-hexantriol is an exception to this. Here α of $c_p(\omega)$ is significant smaller than that of $G(\omega)$.

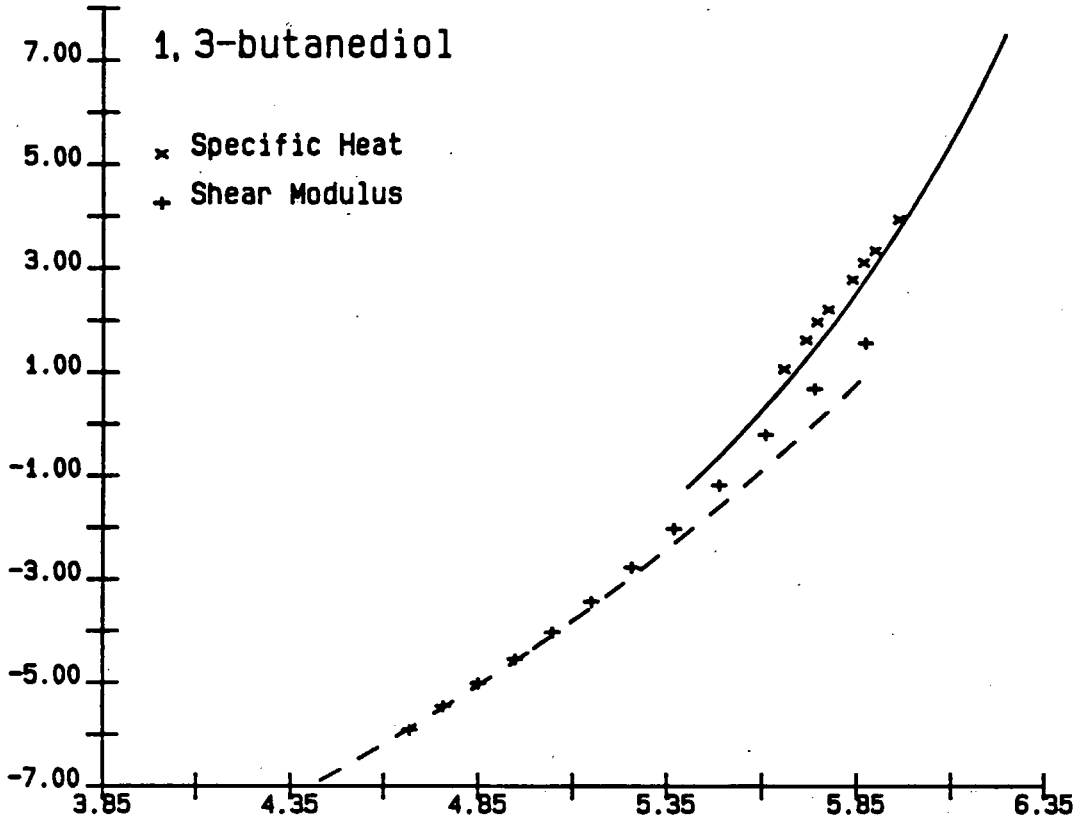
1, 3-butanediol
× Specific Heat
+ Shear Modulus
7.00
5.00
3.00
1.00
-1.00
-3.00
-5.00
-7.00
3.85
4.35
4.85
5.35
5.85
6.35

fig 5.1

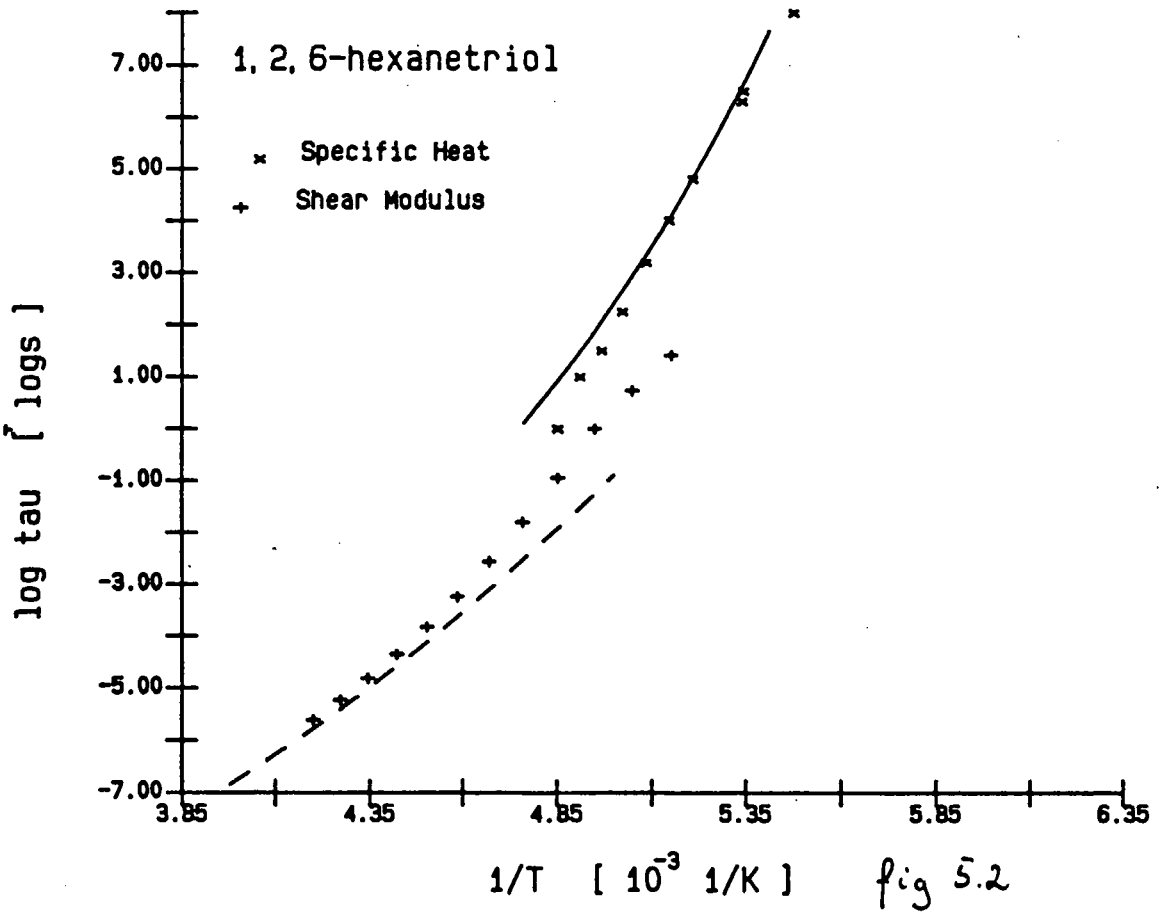
1, 2, 6-hexanetriol
× Specific Heat
+ Shear Modulus
log tau [logs]
7.00
5.00
3.00
1.00
-1.00
-3.00
-5.00
-7.00
3.85
4.35
4.85
5.35
5.85
6.35
1/T [10⁻³ 1/K]

fig 5.2

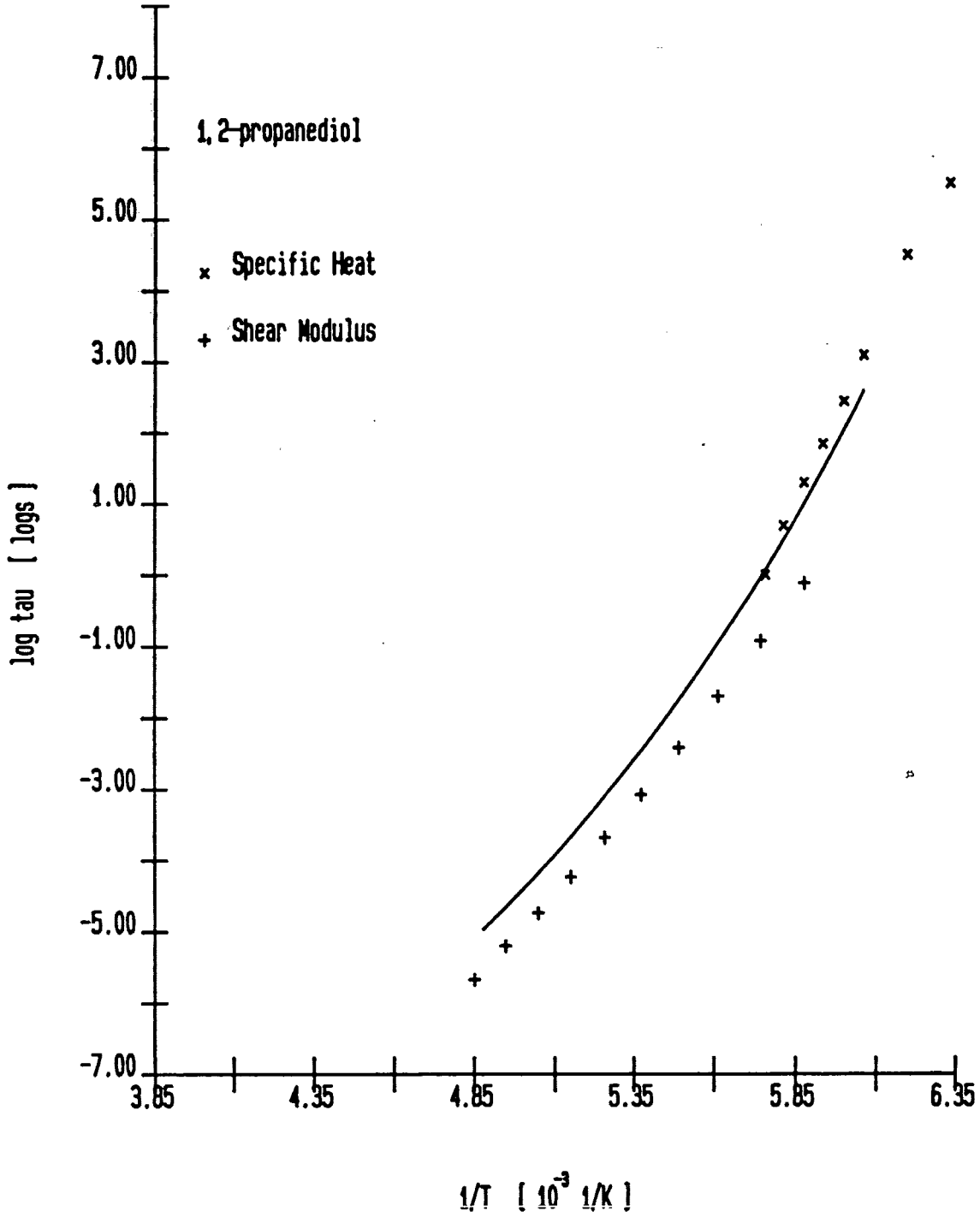
1,2-propanediol
Specific Heat
Shear Modulus
log tau [logs]
7.00
5.00
3.00
1.00
-1.00
-3.00
-5.00
-7.00
3.85
4.35
4.85
5.35
5.85
6.35
1/T [10^-3 1/K]

fig 5.3

1.Christensen T., J. d. Physique C8, 635 (1985)

2.Christensen T., IMFUFA tekst 184 , RUC 1989, " En metode til bestemmelse af den frekvensafhaengige varmefylde af en underafkoelet vaeske ved glasovergangen" ,(speciale KU 1986).
(dissertation for the cand.scient degree in physics, " A method for the determination of the frequency dependent specific heat of a supercooled liquid at the glass transition"). In Danish.

3.Jäckle J., Physica A162, 377 (1990)

4.Christiansen P.V.,IMFUFA tekst 22 (1979) and 238 (1993), "Semiotik og systemegenskaber".In Danish

5.Kubo R., Toda M., Hashitsume N., Statistical Physics II, Springer 1978

6.Landau L.D., Lifshitz E.M., Statistical Physics 2.ed p.57ff, Pergamon Press (1969)

7.De Groot S.R.,Mazur P., Nonequlibrium Thermodynamics, North Holland 1962

8.Donth E.J.,Glasubergang, Akademie Verlag, Berlin 1981

9.Birge N.O., Nagel S.R., Phys. Rev. Lett. 54, 2674 (1985)

10.Christensen R.M., Theory of Viscoelasticity, Academic Press 1971

11.Birge N.O. Phys.Rev.B34 ,1631 (1986)

12.Oxtoby D.W., J.Chem.Phys 85, 1549 (1986)

13.Zwanzig R.,J.Chem.Phys. 88, 5831 (1988)

14. Gmelin E., Thermochimica Acta 29, 1 (1979)

15.Lakshimukamar S. T., Gopal E. S. R., J Indian Inst.Sci.63A, 277 (1989)

16.Ångstrøm A. J. ,Phil.Mag. 25, 130 (1863)

17.Sullivan P.F.,Seidel G., Phys.Rev. 173, 679 (1968)

18.Moynihan C.T. et al., Ann N.Y. Acad. Sci. 279, 15 (1976)

19.Davies R.O., Jones G.O.,Adv. Phys. 2, 370 (1953)

20.Fransson Åke, Thermophysical Properties of Glasses, 1987 Umeå University,Sweden

21.Birge N.O. Phys.Rev.B34 ,1631 (1986)

22.Birge N.O. , Nagel S.R. , Rev.Sci.Instrum. 58 , 1464 (1987)

23.Harrison G., The Dynamic Properties of Supercooled Liquids, Academic Press 1976

24. Landau L.D., Lifshitz E.M. Theory of elasticity, Pergamon Press 1970

25. Jaffe B., Cook W., Jaffe H, Piezoelectric Ceramics, Academic Press, 1971

26.Birge N.O., Phys.Rev.B34 ,1631 (1986)

27.Meister R., Marhoeffer C.J., Sciamanda R, Cotter L., Litovitz T., J.Appl.Phys31, 854 (1960) .

Appendix 3.1. Experimental data for $c_p(\omega)$.

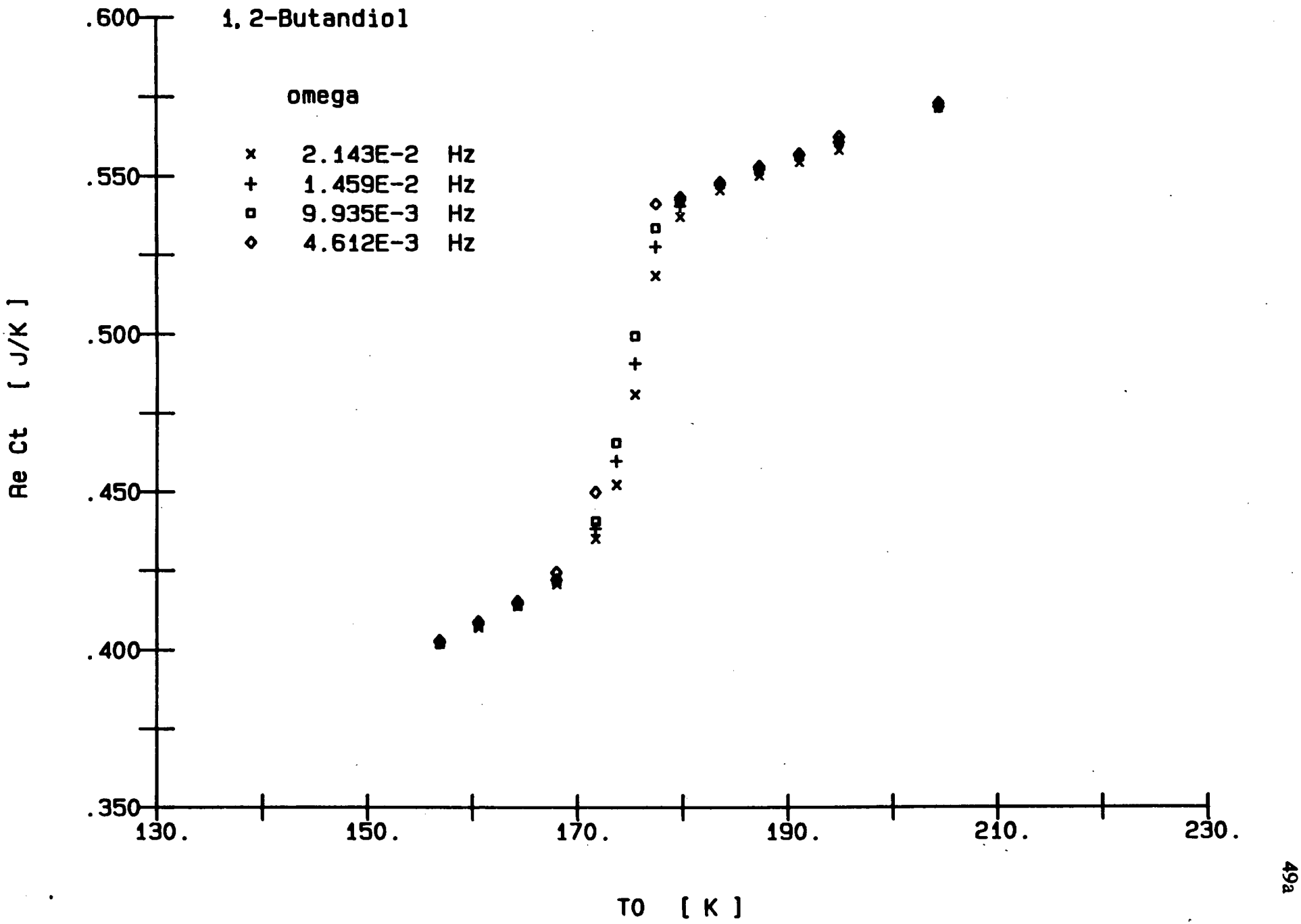
1,2-Butandiol
omega
2.143E-2 Hz
1.459E-2 Hz
9.935E-3 Hz
4.612E-3 Hz
.600
.550
.500
.450
.400
.350
Re Ct [J/K]
130.
150.
170.
190.
210.
230.
TO [K]

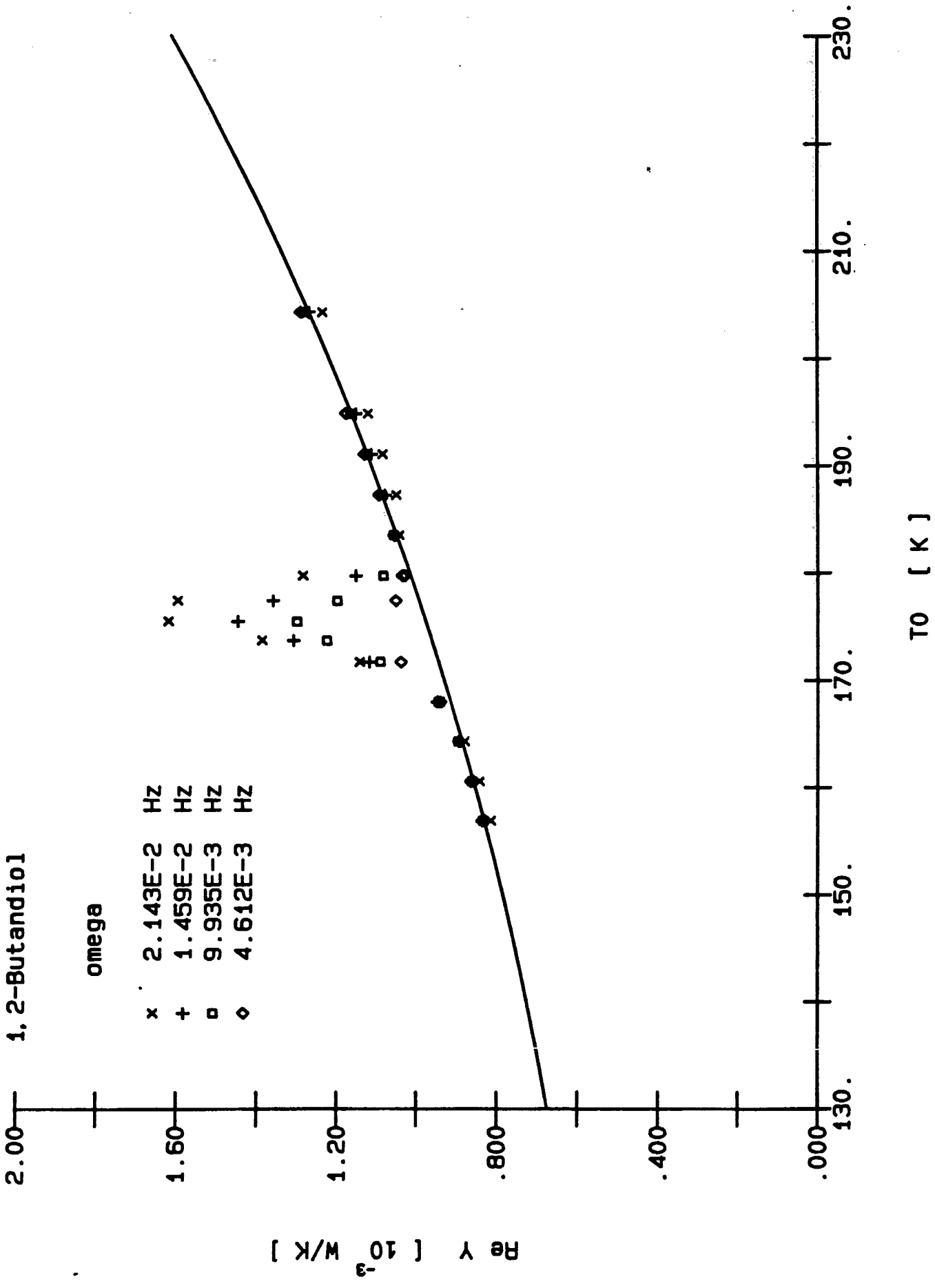
1,2-Butandiol
omega
2.143E-2 Hz
1.459E-2 Hz
9.935E-3 Hz
4.612E-3 Hz
Re γ [10⁻³ W/K]
2.00
1.60
1.20
.800
.400
.000
130.
150.
170.
190.
210.
230.
T0 [K]

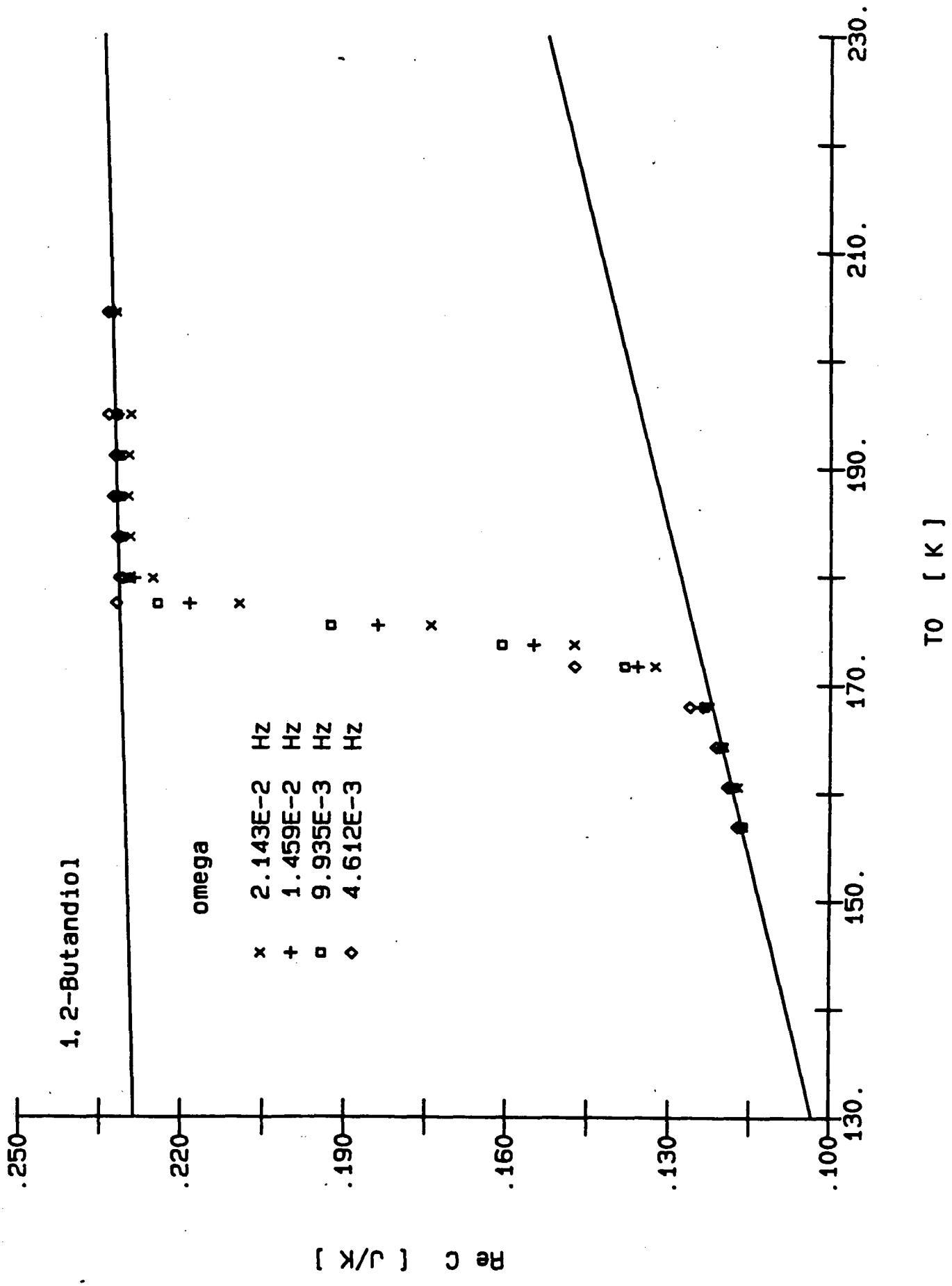
1,2-Butandiol
omega
x 2.143E-2 Hz
+ 1.459E-2 Hz
▫ 9.935E-3 Hz
◇ 4.612E-3 Hz
Re C [J/K]
.250
.220
.190
.160
.130
.100
130.
150.
170.
190.
210.
230.
TO [K]

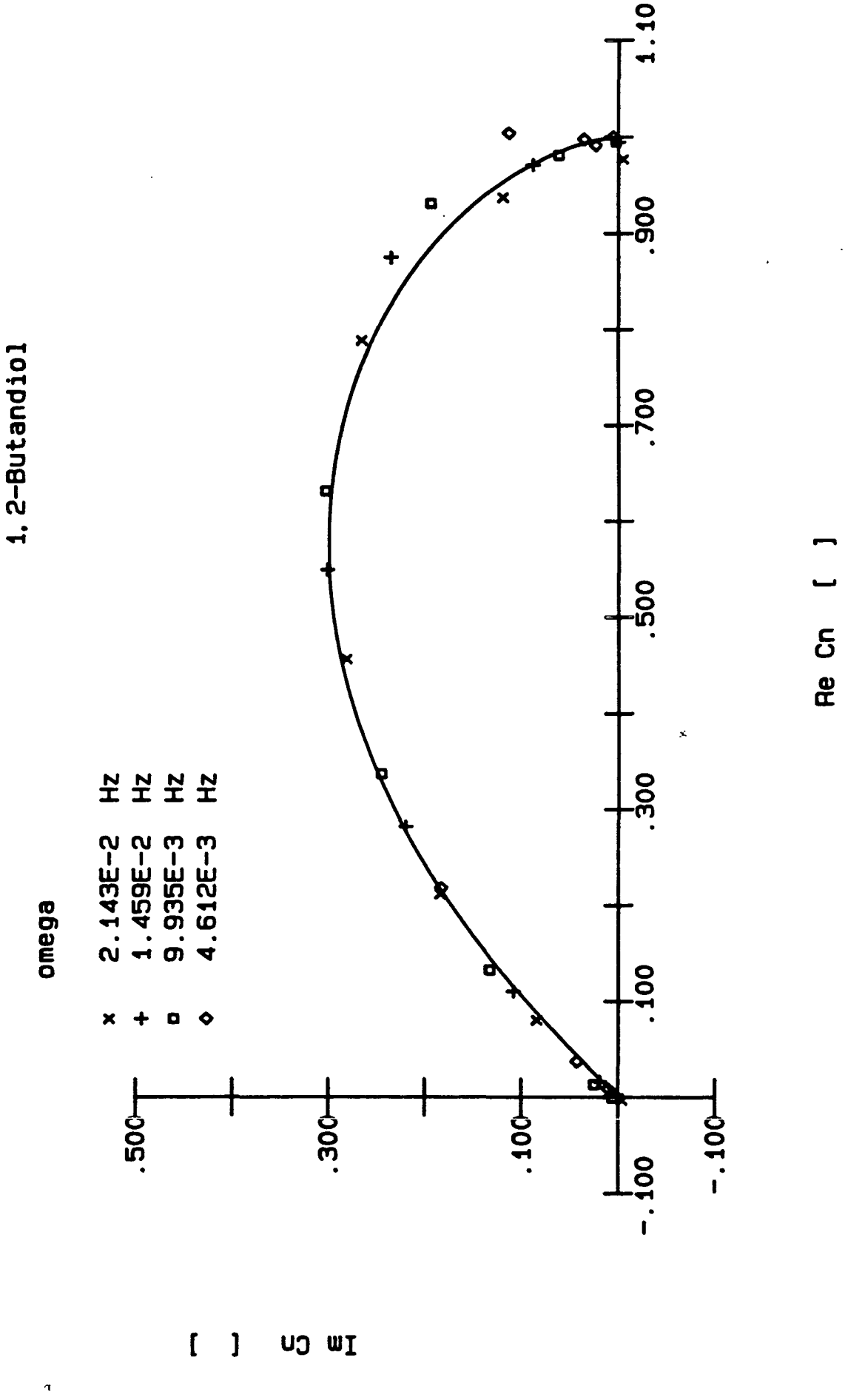
1,2-Butandiol
omega
x 2.143E-2 Hz
+ 1.459E-2 Hz
□ 9.935E-3 Hz
◇ 4.612E-3 Hz
.500
.300
.100
-.100
-.100
.100
.300
.500
.700
.900
1.10
Im Cn [ ]
Re Cn [ ]

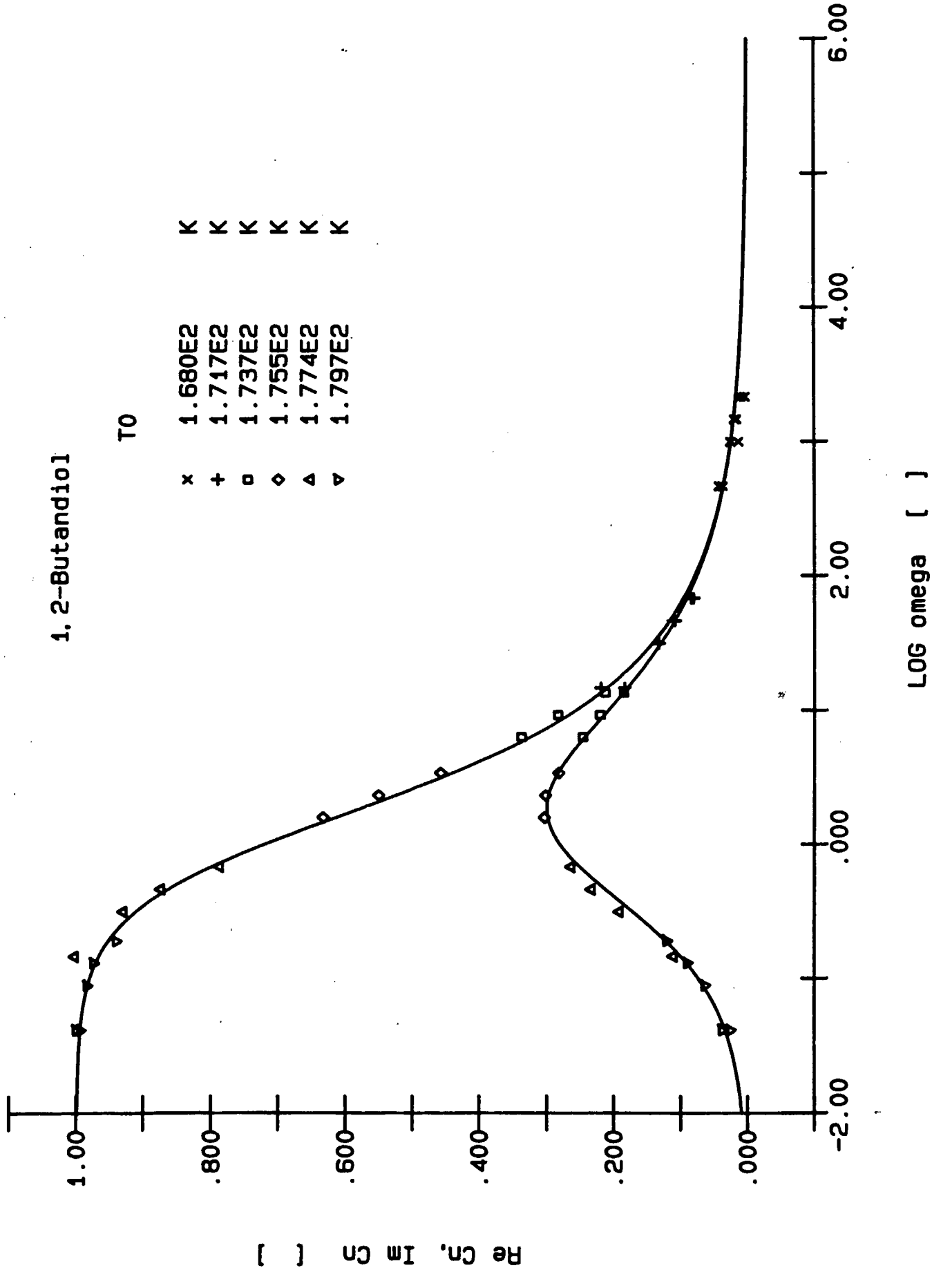
1,2-Butandiol
T0
x 1.680E2 K
+ 1.717E2 K
▫ 1.737E2 K
◇ 1.755E2 K
△ 1.774E2 K
▽ 1.797E2 K
1.00
.800
.600
.400
.200
.000
-2.00
.000
2.00
4.00
6.00
Re Cn, Im Cn [ ]
LOG omega [ ]

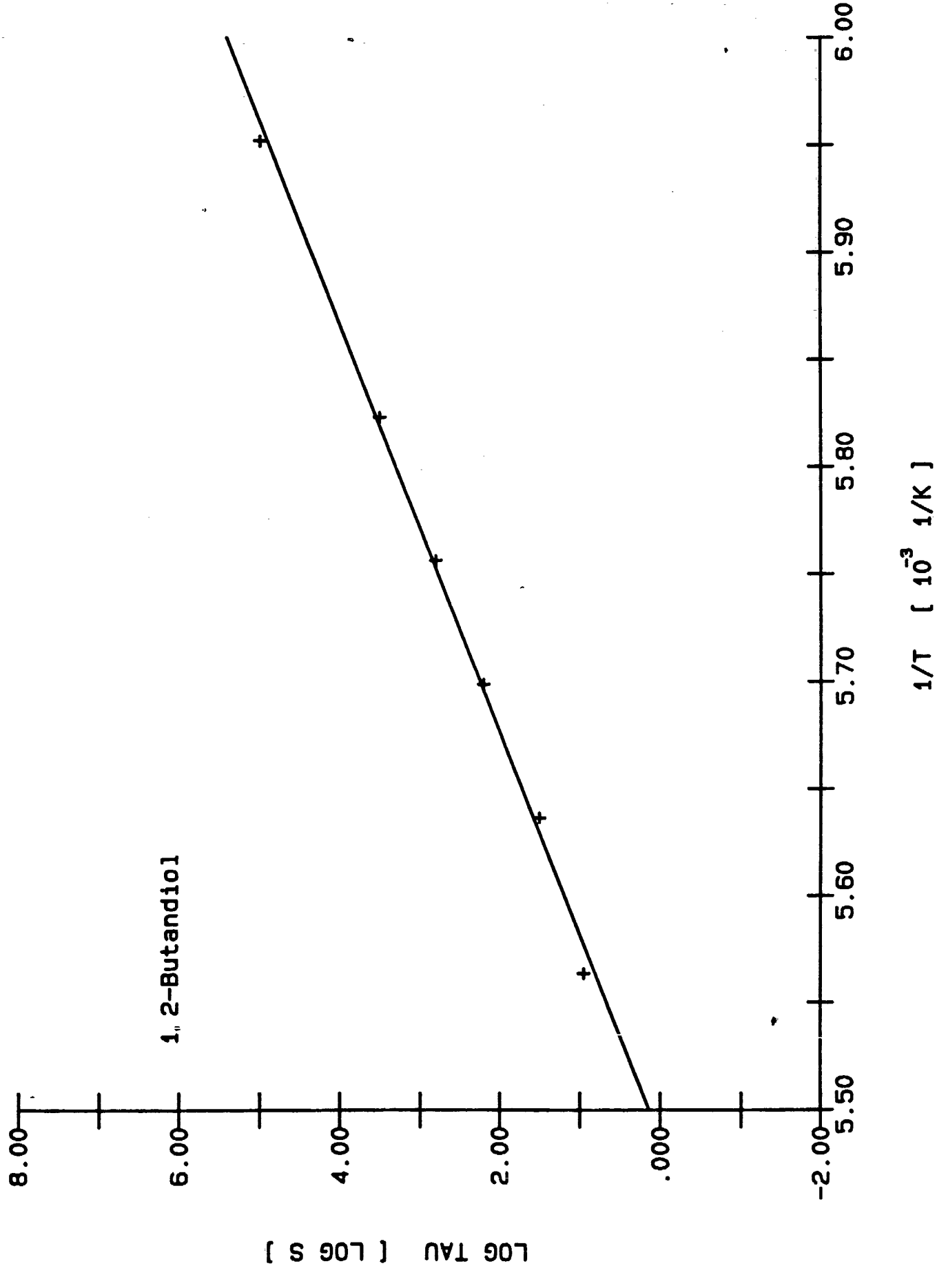
1,2-Butandiol
LOG TAU [LOG S]
8.00
6.00
4.00
2.00
.000
-2.00
5.50
5.60
5.70
5.80
5.90
6.00
1/T [10^-3 1/K]

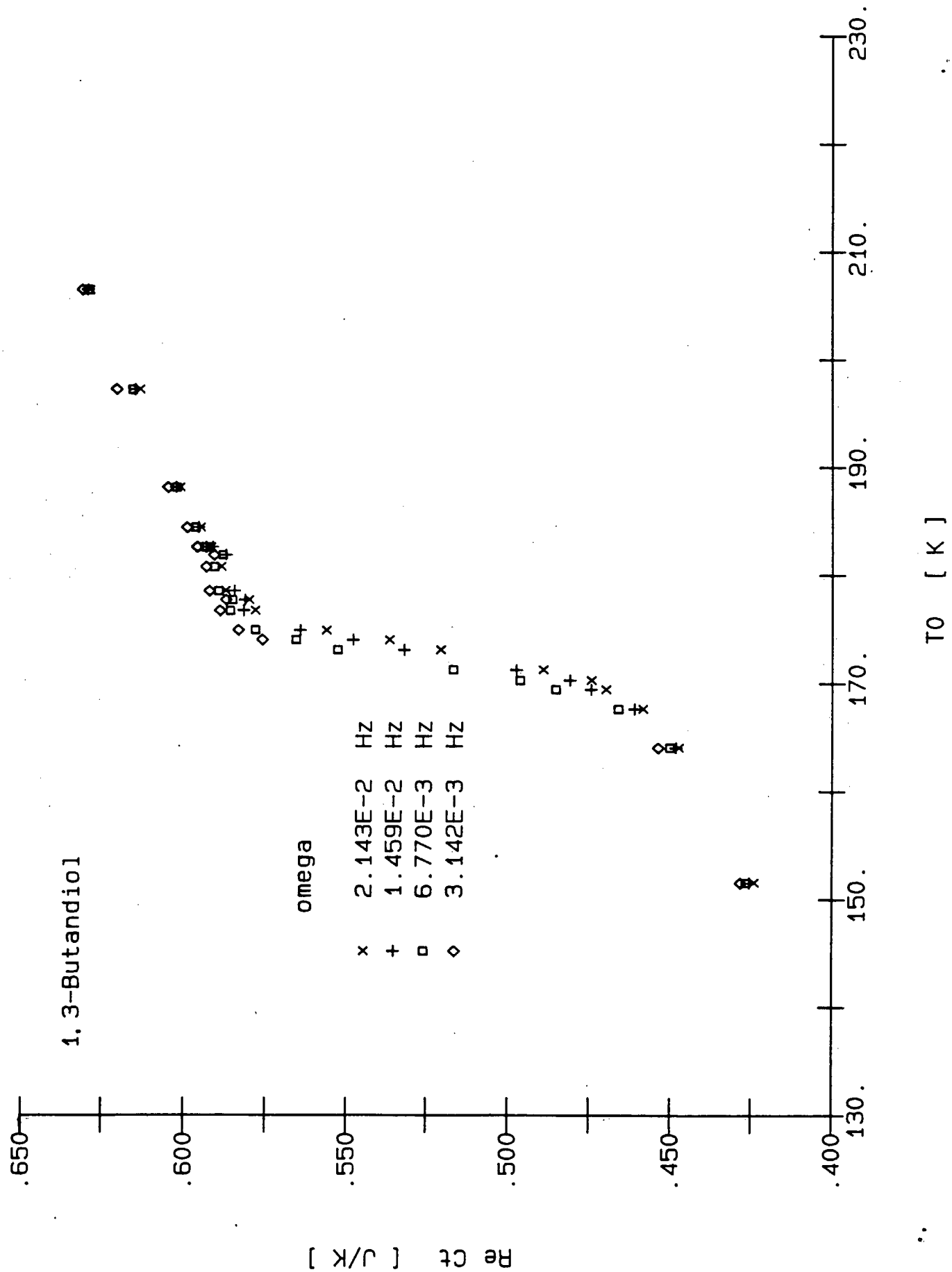
1,3-Butandiol
omega
2.143E-2 Hz
1.459E-2 Hz
6.770E-3 Hz
3.142E-3 Hz
Re Ct [J/K]
.650
.600
.550
.500
.450
.400
130.
150.
170.
190.
210.
230.
TO [K]

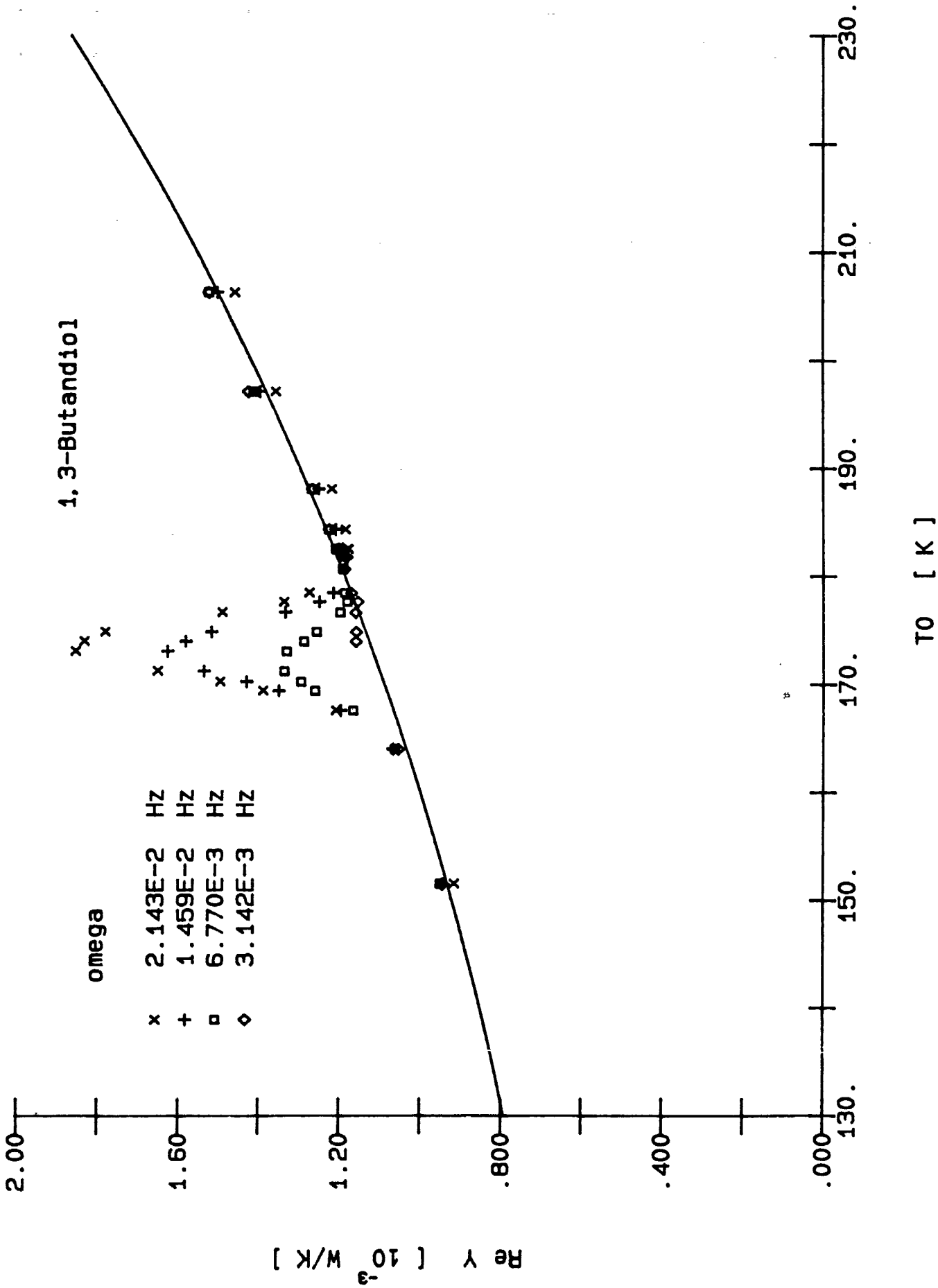
1,3-Butandiol
omega
2.143E-2 Hz
1.459E-2 Hz
6.770E-3 Hz
3.142E-3 Hz
Re γ [10⁻³ W/K]
2.00
1.60
1.20
.800
.400
.000
130.
150.
170.
190.
210.
230.
TO [K]

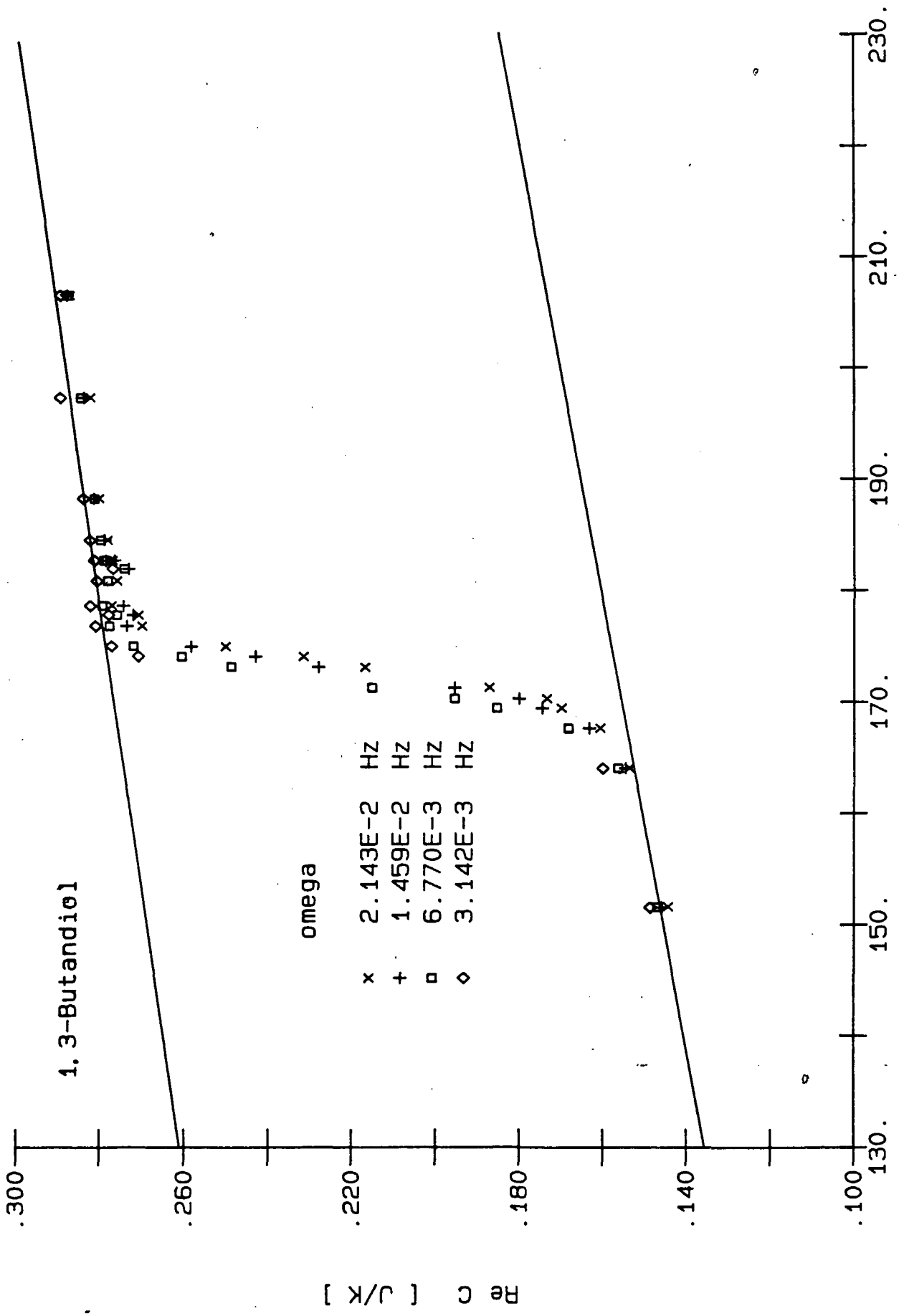
1,3-Butandiol
omega
× 2.143E-2 Hz
+ 1.459E-2 Hz
□ 6.770E-3 Hz
◇ 3.142E-3 Hz
Re C [J/K]
.300
.260
.220
.180
.140
.100
130.
150.
170.
190.
210.
230.
TO [K]

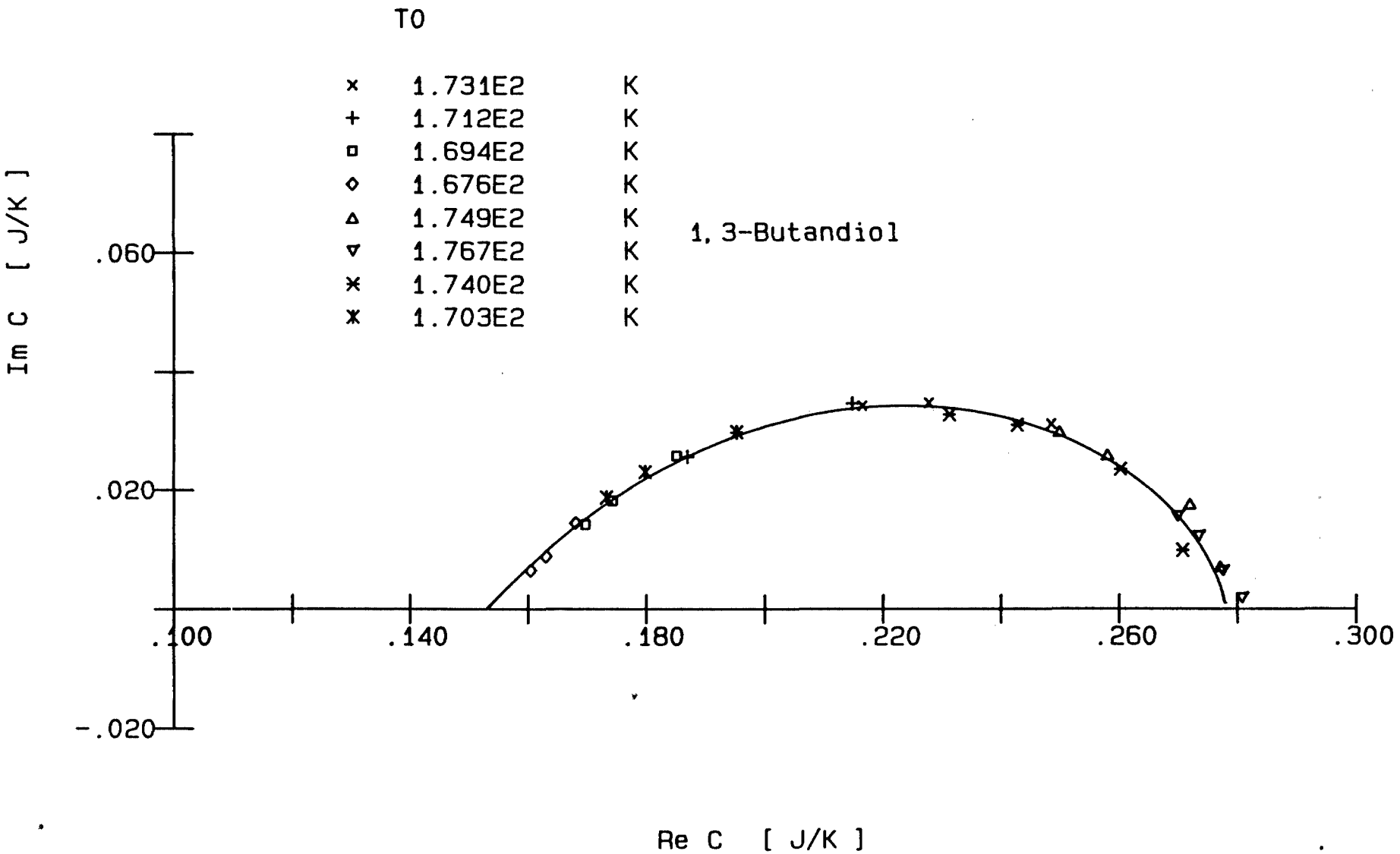
T0
× 1.731E2 K
+ 1.712E2 K
▫ 1.694E2 K
◇ 1.676E2 K
△ 1.749E2 K
▽ 1.767E2 K
✳ 1.740E2 K
✳ 1.703E2 K
1, 3-Butandiol
Im C [J/K]
.060
.020
-.020
.100
.140
.180
.220
.260
.300
Re C [J/K]

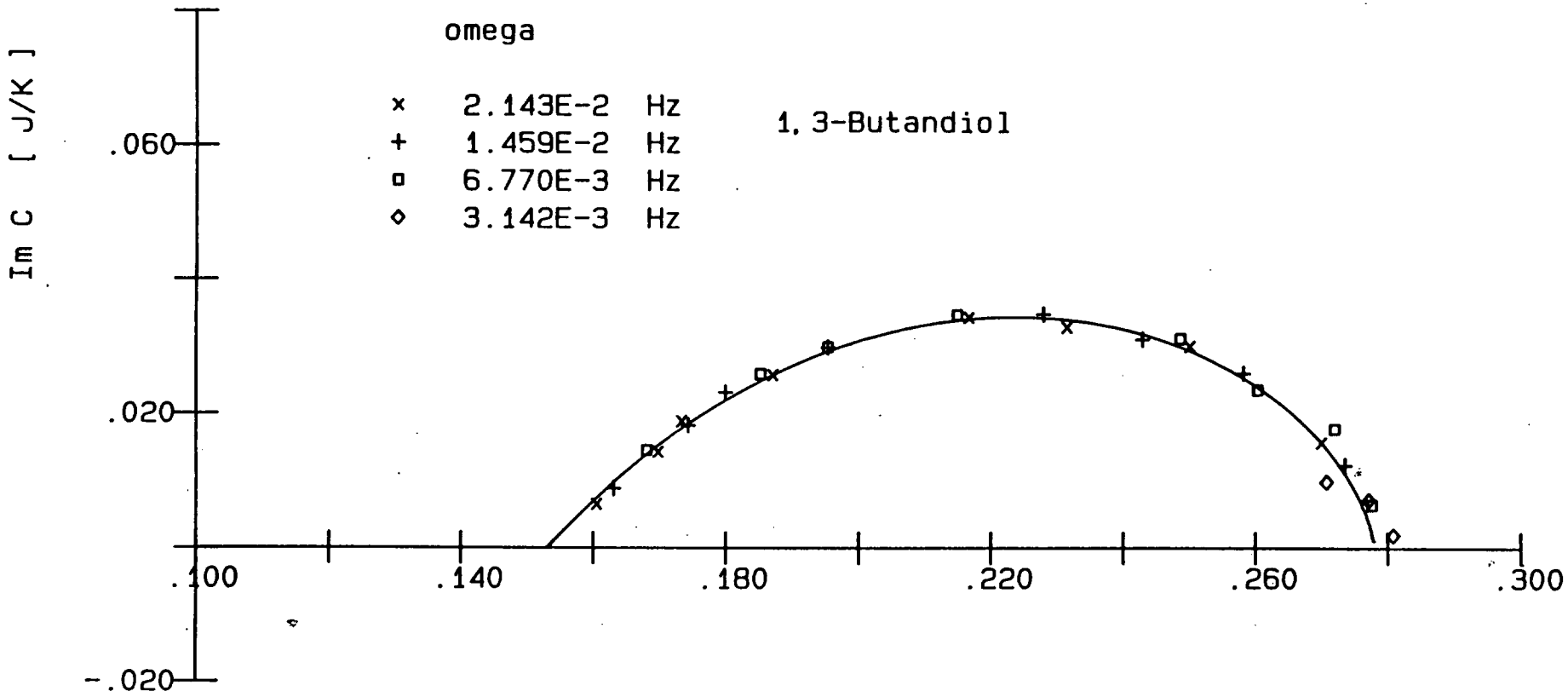
omega
× 2.143E-2 Hz
+ 1.459E-2 Hz
▫ 6.770E-3 Hz
◇ 3.142E-3 Hz
1,3-Butandiol
Im C [J/K]
.060
.020
-.020
.100
.140
.180
.220
.260
.300
Re C [J/K]

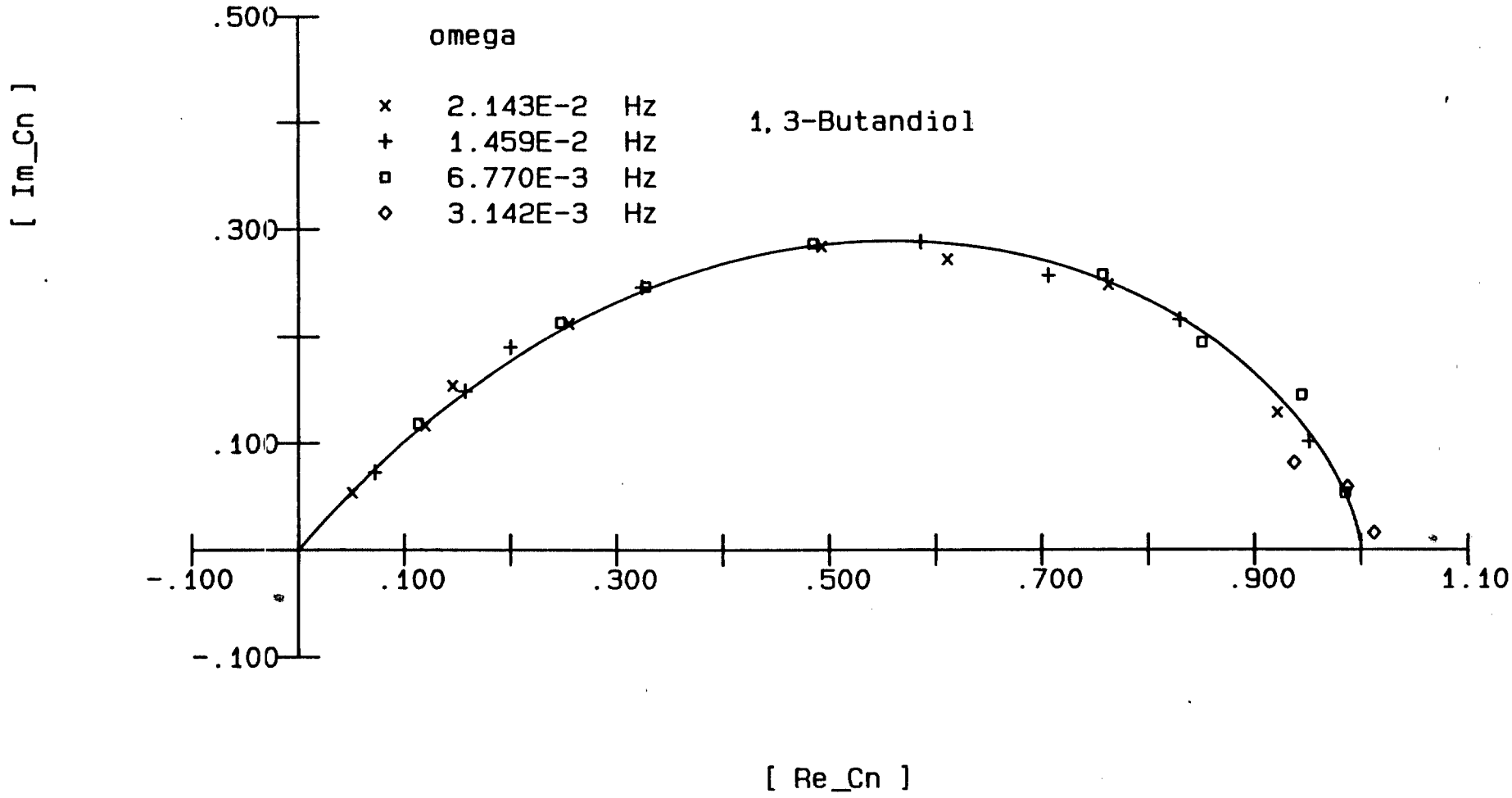
omega
× 2.143E-2 Hz
+ 1.459E-2 Hz
▫ 6.770E-3 Hz
◇ 3.142E-3 Hz
1,3-Butandiol
.500
.300
.100
-.100
-.100
.100
.300
.500
.700
.900
1.10
[Im_Cn]
[Re_Cn]

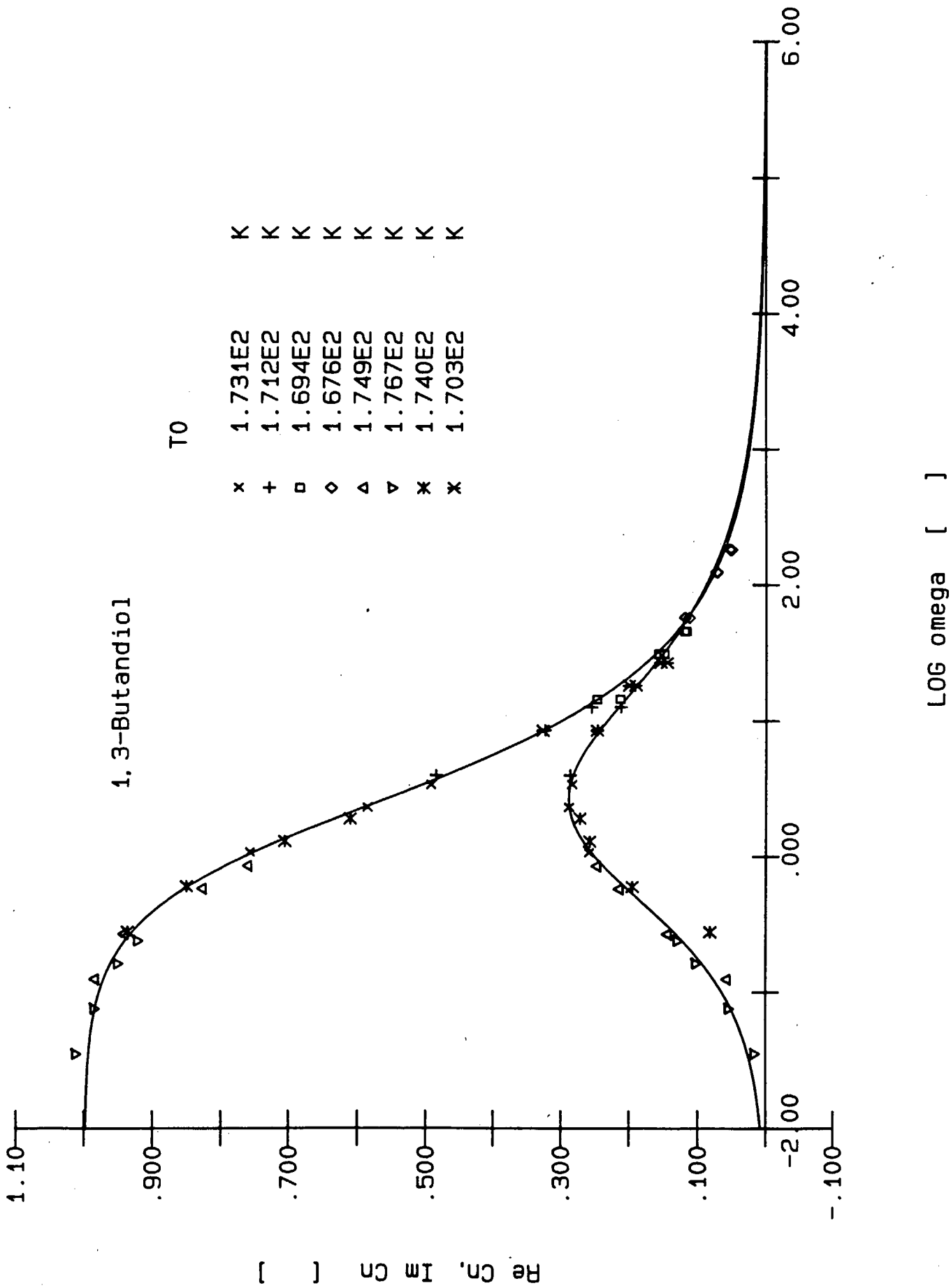
1,3-Butandiol
T0
x 1.731E2 K
+ 1.712E2 K
□ 1.694E2 K
◇ 1.676E2 K
△ 1.749E2 K
▽ 1.767E2 K
✱ 1.740E2 K
✱ 1.703E2 K
1.10
.900
.700
.500
.300
.100
-.100
-2.00
.000
2.00
4.00
6.00
Re Cn, Im Cn [ ]
LOG omega [ ]

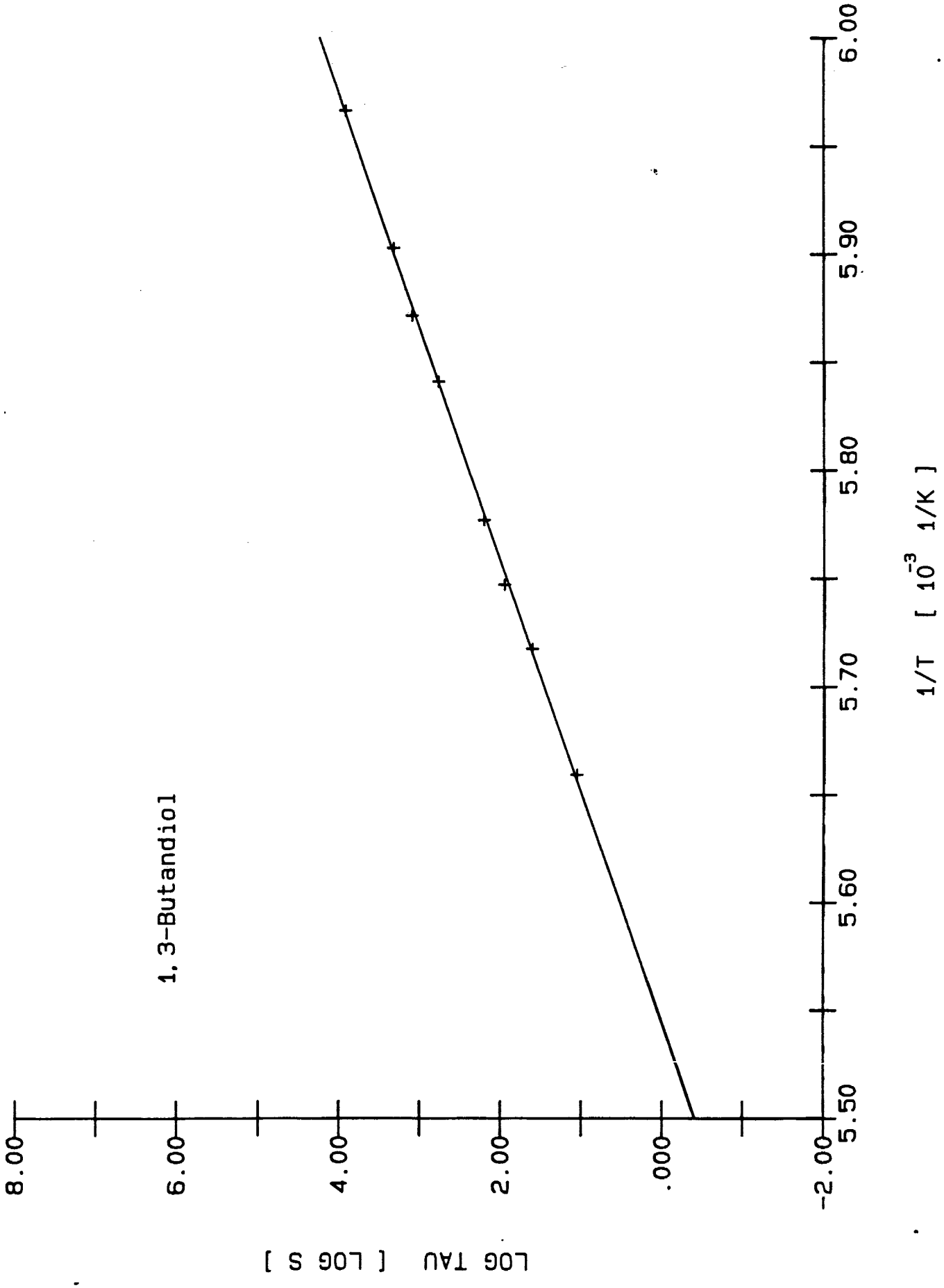
1,3-Butandiol
LOG TAU [LOG S]
8.00
6.00
4.00
2.00
.000
-2.00
5.50
5.60
5.70
5.80
5.90
6.00
1/T [10^-3 1/K]

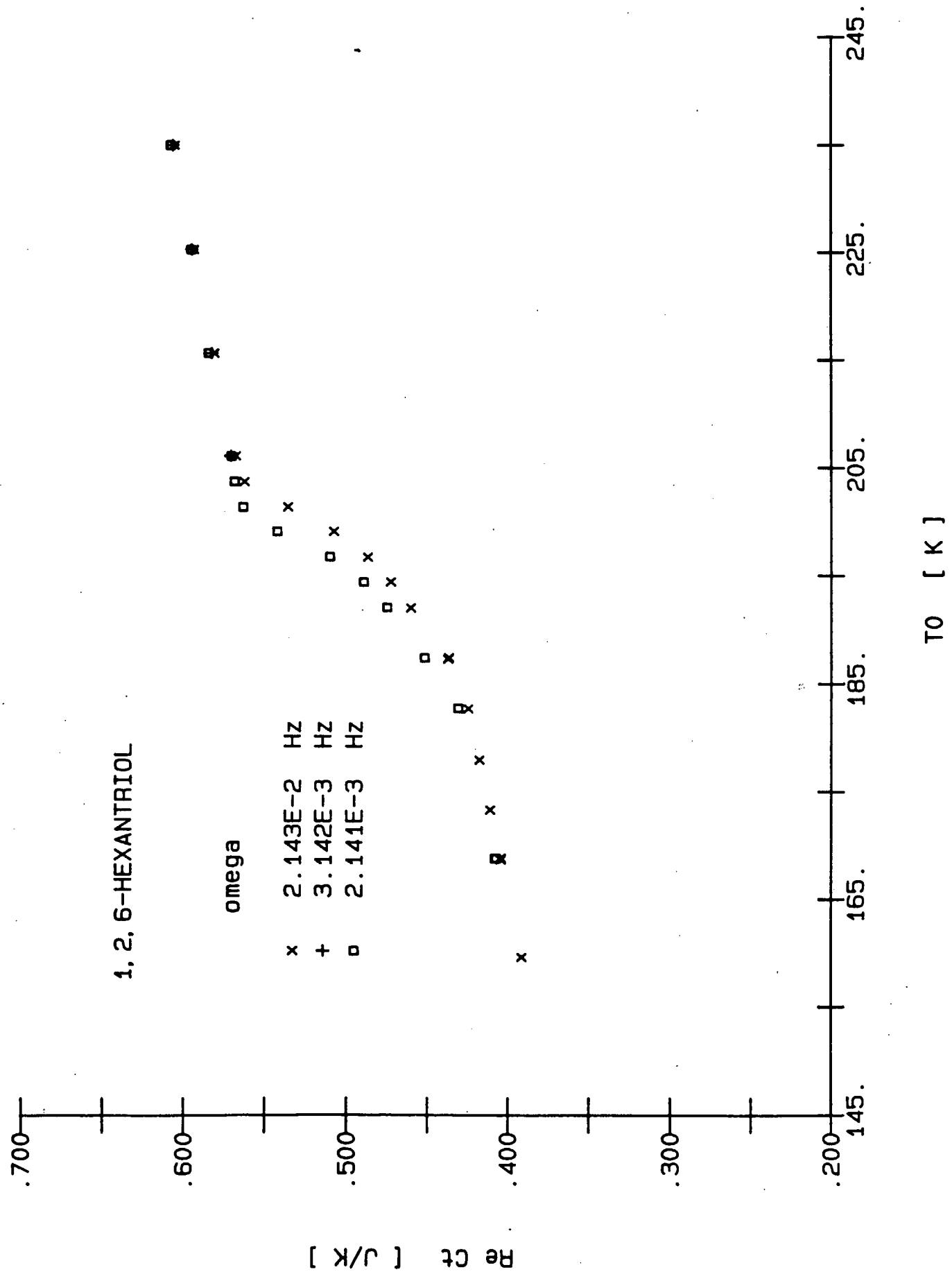
1, 2, 6-HEXANTRIOL
omega
× 2.143E-2 Hz
+ 3.142E-3 Hz
□ 2.141E-3 Hz
Re Ct [J/K]
.700
.600
.500
.400
.300
.200
145.
165.
185.
205.
225.
245.
TO [K]

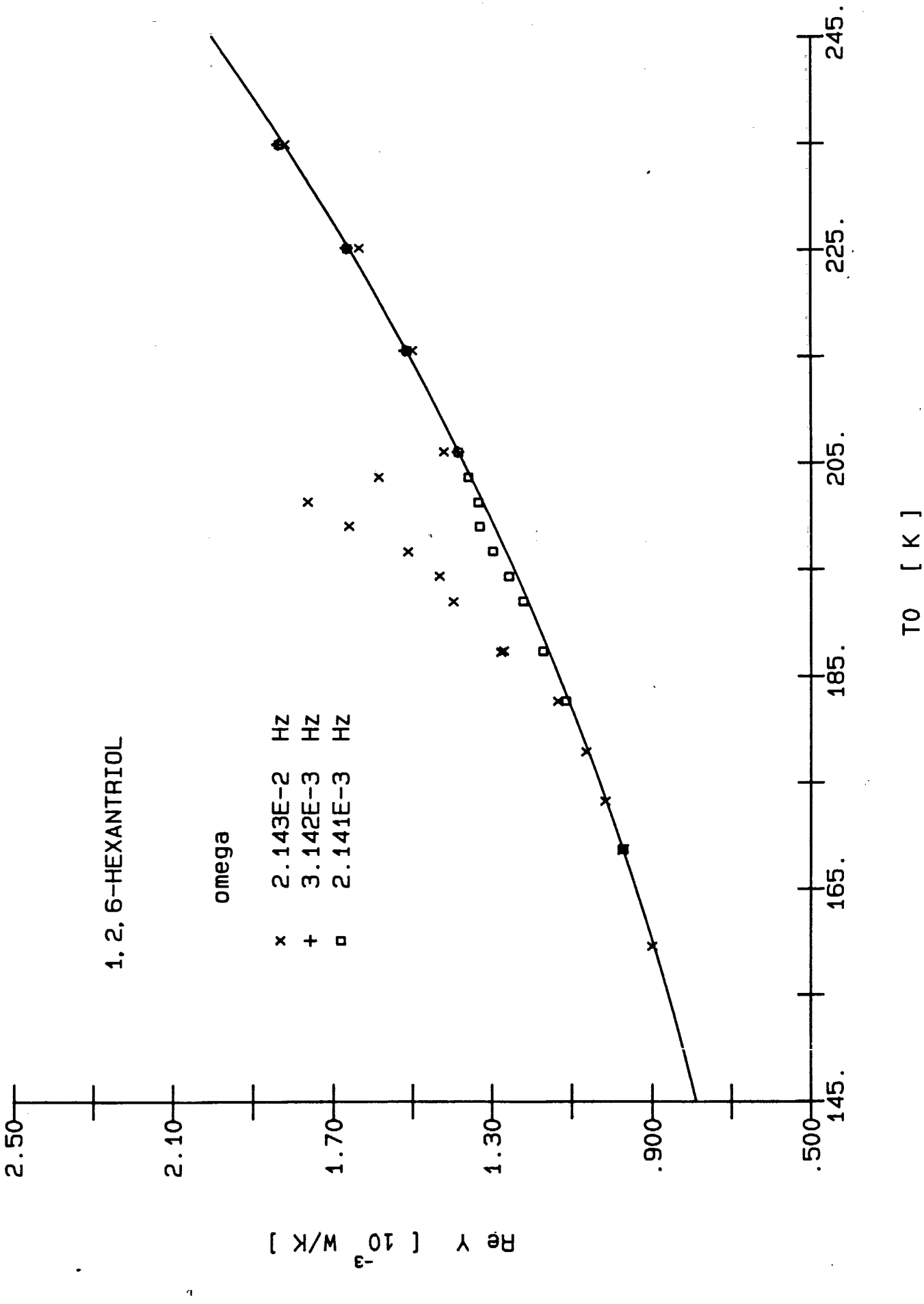
1, 2, 6-HEXANTRIOL
omega
x 2.143E-2 Hz
+ 3.142E-3 Hz
□ 2.141E-3 Hz
Re Y [10⁻³ W/K]
2.50
2.10
1.70
1.30
.900
.500
145.
165.
185.
205.
225.
245.
TO [K]

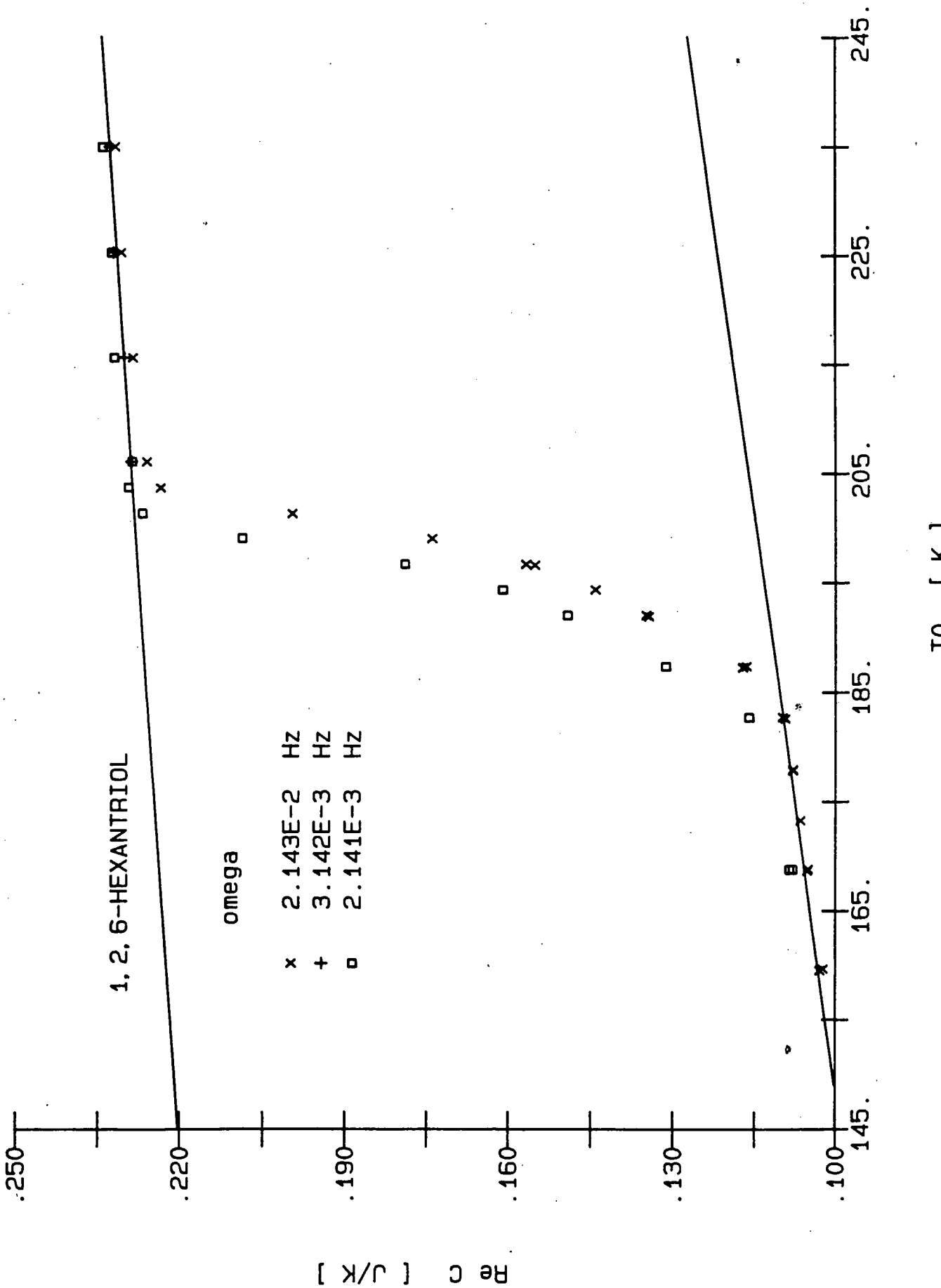
1, 2, 6-HEXANTRIOL
omega
× 2.143E-2 Hz
+ 3.142E-3 Hz
□ 2.141E-3 Hz
Re C [J/K]
TO [K]
.250
.220
.190
.160
.130
.100
145.
165.
185.
205.
225.
245.

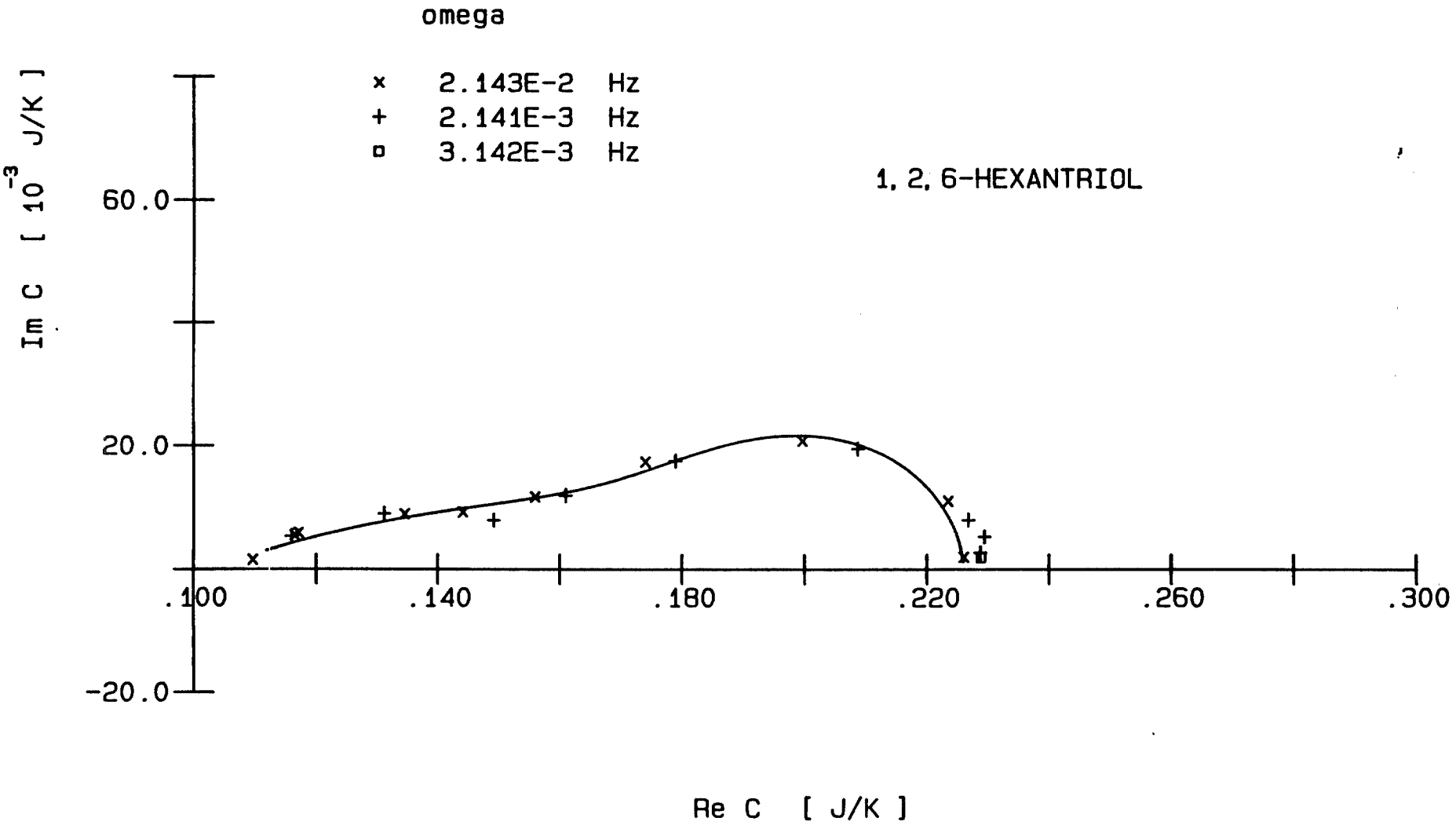
omega
x 2.143E-2 Hz
+ 2.141E-3 Hz
□ 3.142E-3 Hz
1, 2, 6-HEXANTRIOL
Im C [10^-3 J/K]
60.0
20.0
-20.0
.100
.140
.180
.220
.260
.300
Re C [J/K]

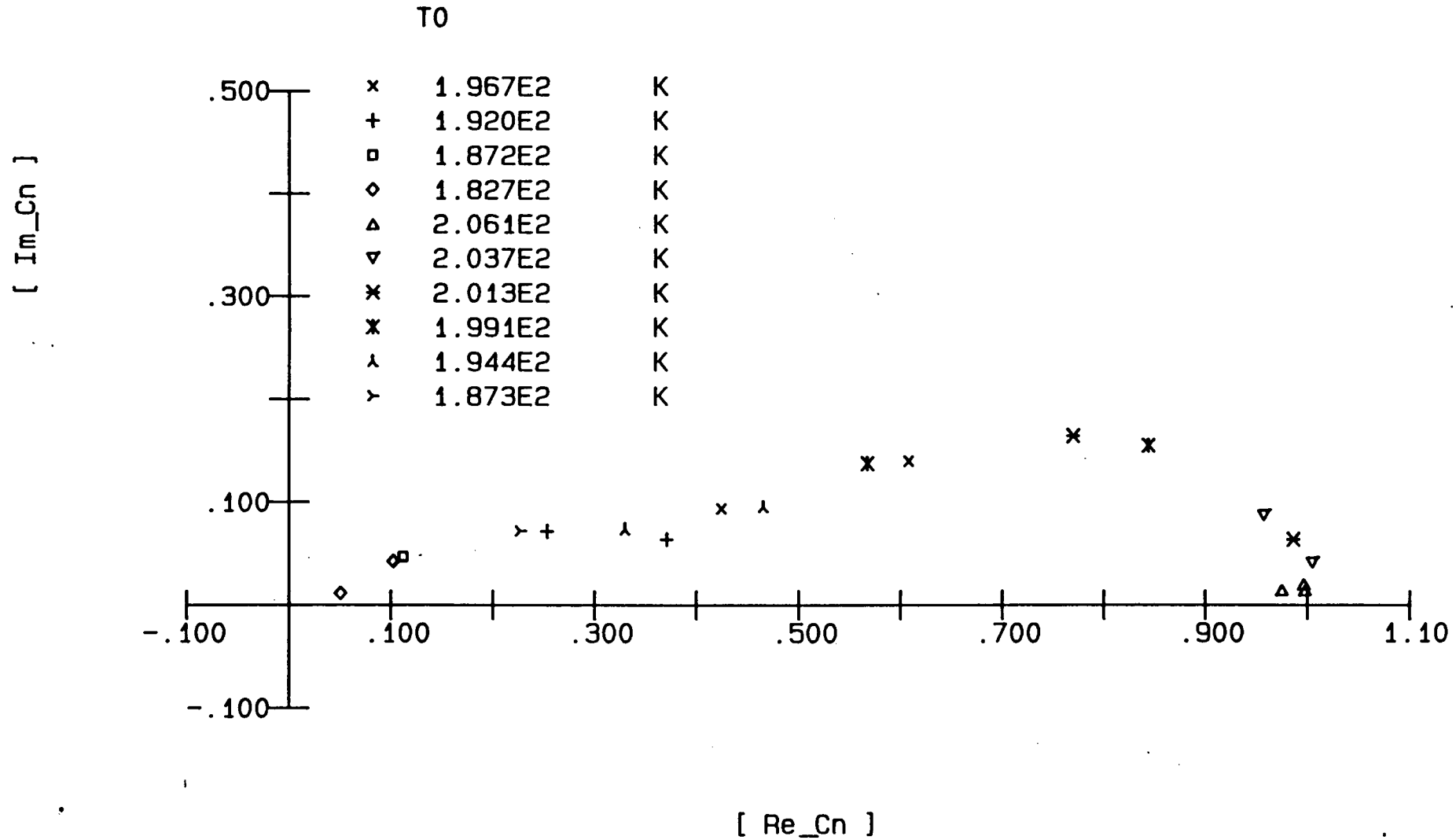
T0
1.967E2 K
1.920E2 K
1.872E2 K
1.827E2 K
2.061E2 K
2.037E2 K
2.013E2 K
1.991E2 K
1.944E2 K
1.873E2 K
.500
.300
.100
-.100
-.100
.100
.300
.500
.700
.900
1.10
[Im_Cn]
[Re_Cn]

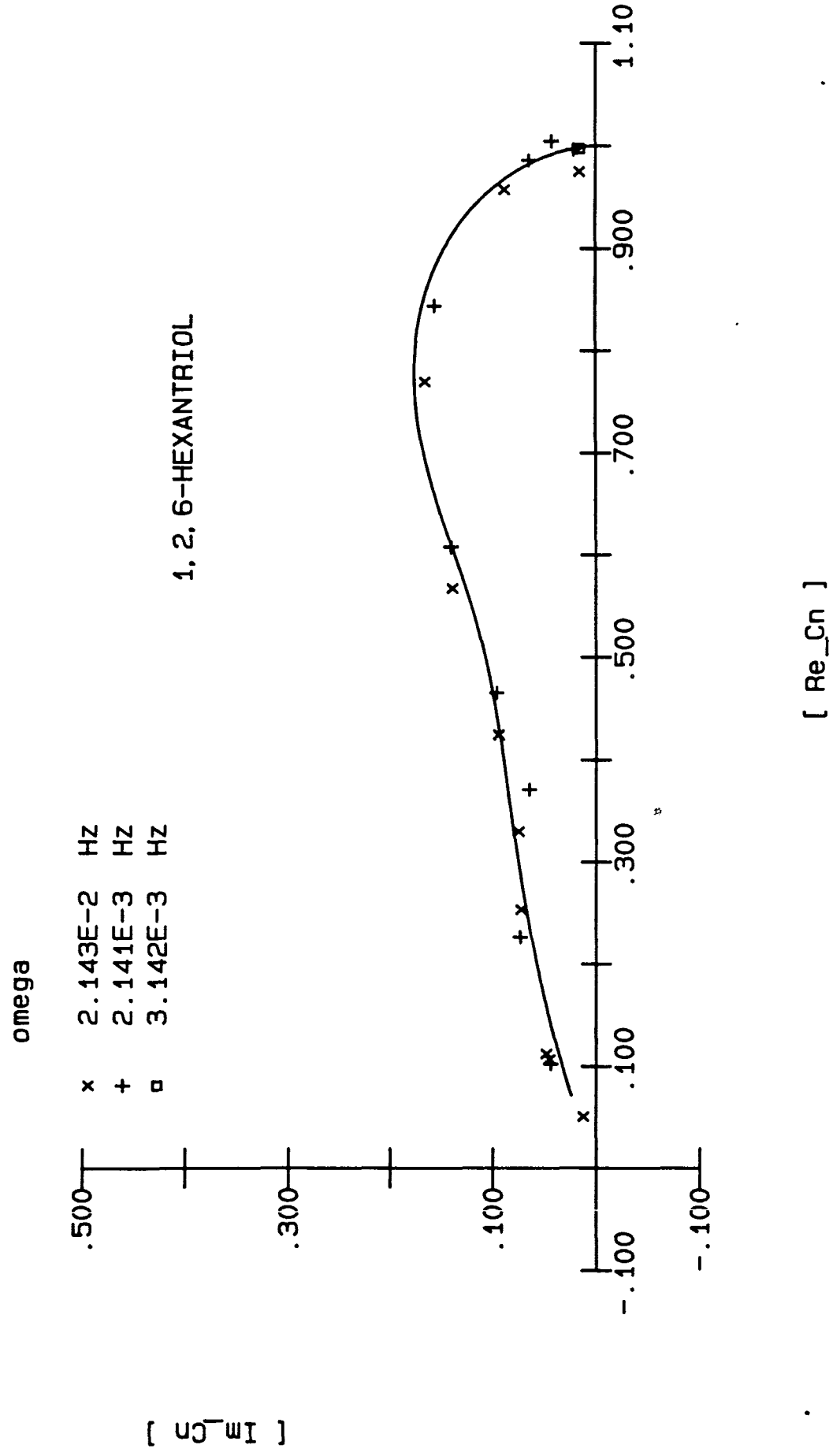
1, 2, 6-HEXANTRIOL
omega
x 2.143E-2 Hz
+ 2.141E-3 Hz
□ 3.142E-3 Hz
.500
.300
.100
-.100
-.100
.100
.300
.500
.700
.900
1.10
[Im_Cn]
[Re_Cn]

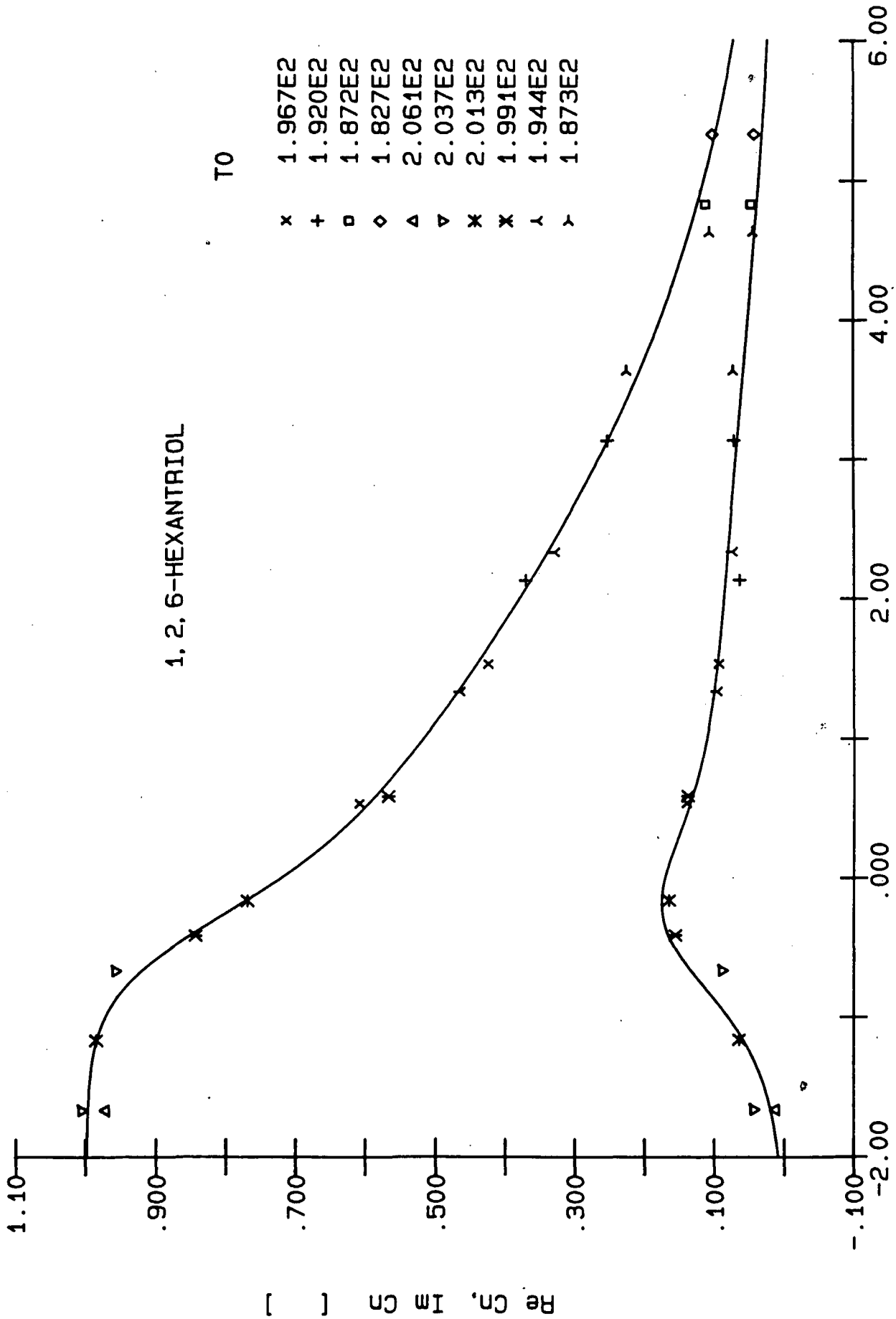
1,2,6-HEXANTRIOL
TO
1.967E2
1.920E2
1.872E2
1.827E2
2.061E2
2.037E2
2.013E2
1.991E2
1.944E2
1.873E2
Re Cn, Im Cn [ ]
LOG omega [ ]
1.10
.900
.700
.500
.300
.100
-.100
-2.00
.000
2.00
4.00
6.00

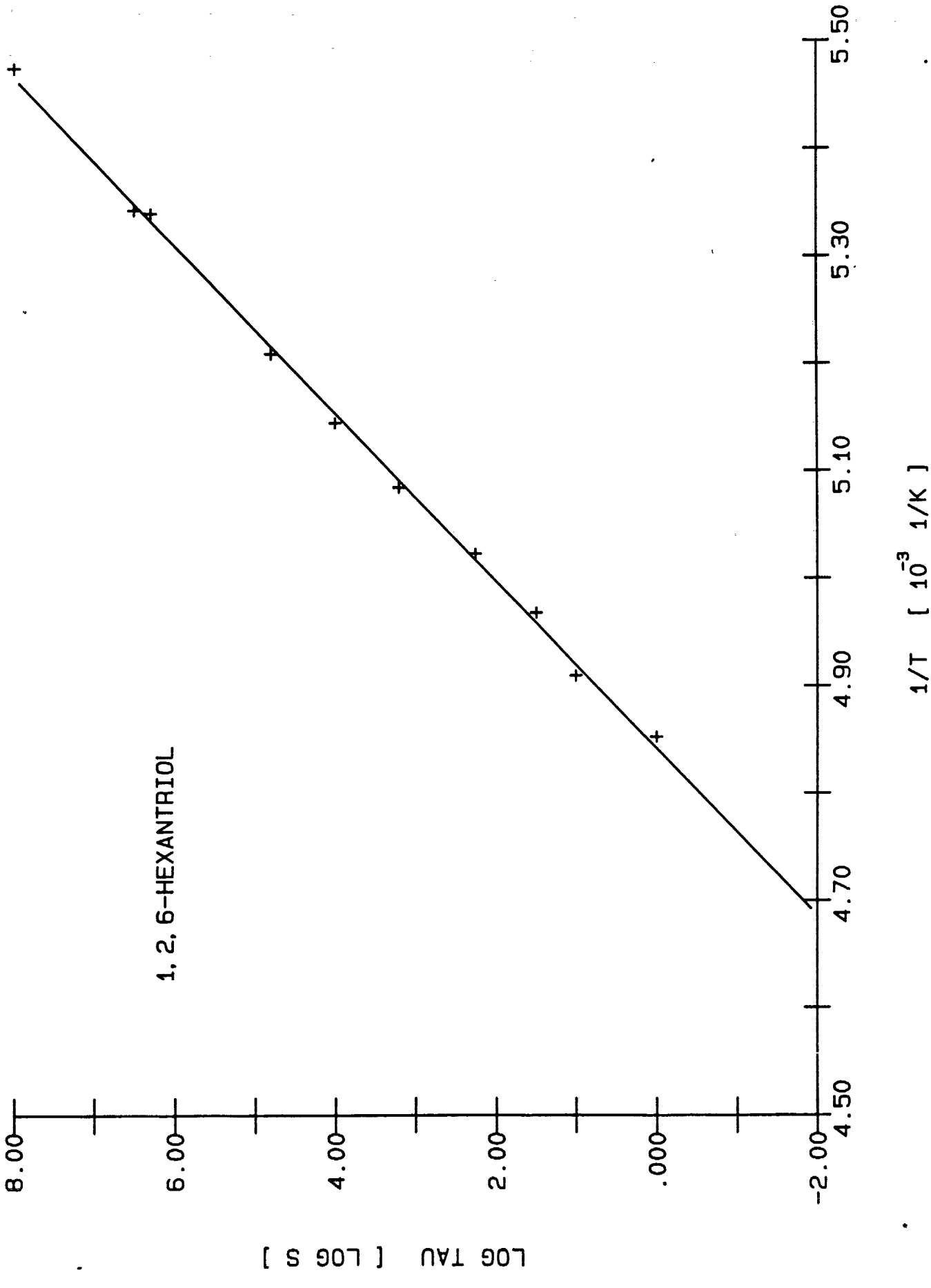
1, 2, 6-HEXANTRIOL
LOG TAU [LOG S]
8.00
6.00
4.00
2.00
.000
-2.00
4.50
4.70
4.90
5.10
5.30
5.50
1/T [10^-3 1/K]

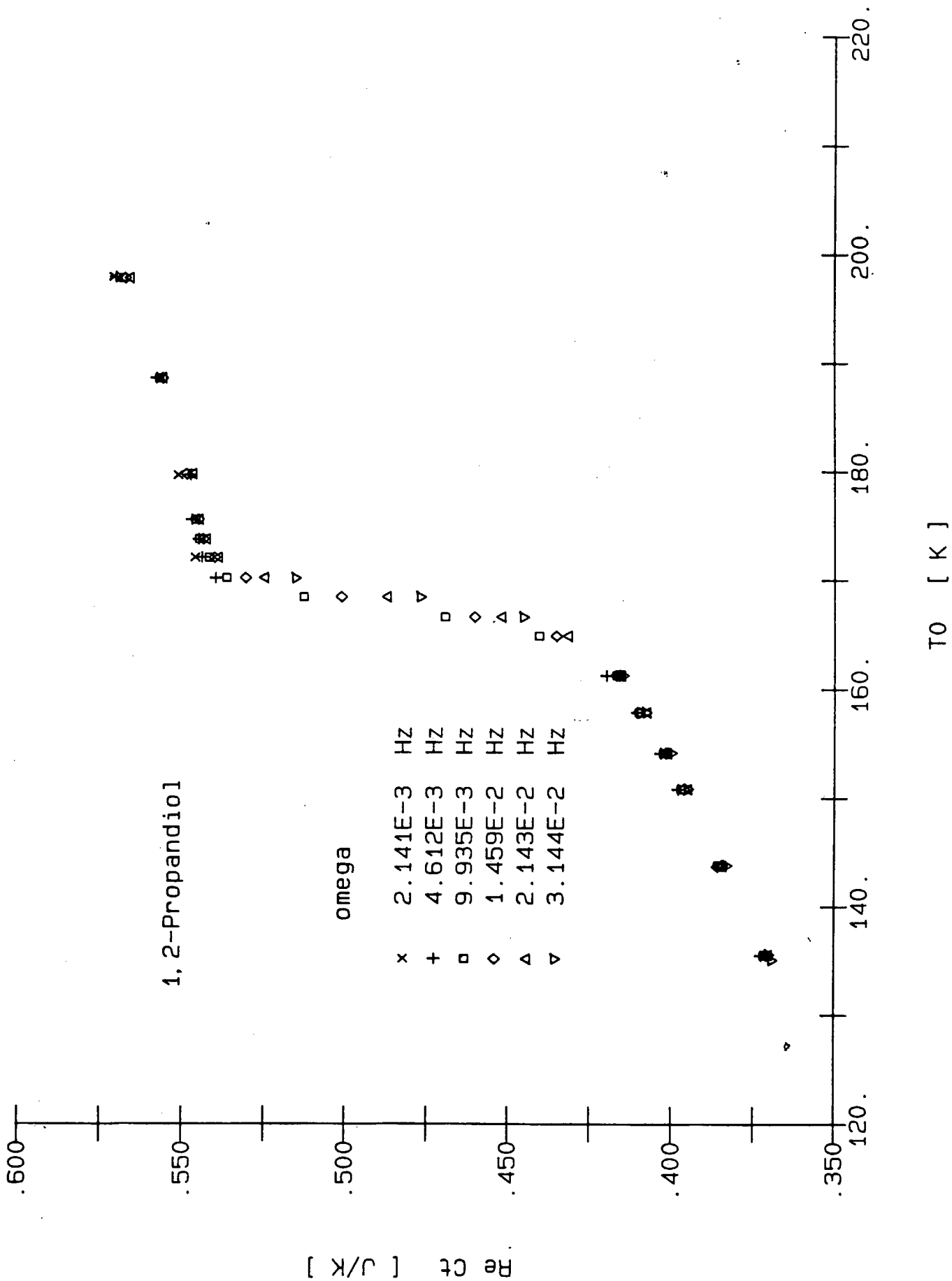
1,2-Propandiol
omega
x 2.141E-3 Hz
+ 4.612E-3 Hz
□ 9.935E-3 Hz
◇ 1.459E-2 Hz
△ 2.143E-2 Hz
▽ 3.144E-2 Hz
Re Ct [J/K]
.600
.550
.500
.450
.400
.350
120.
140.
160.
180.
200.
220.
TO [K]

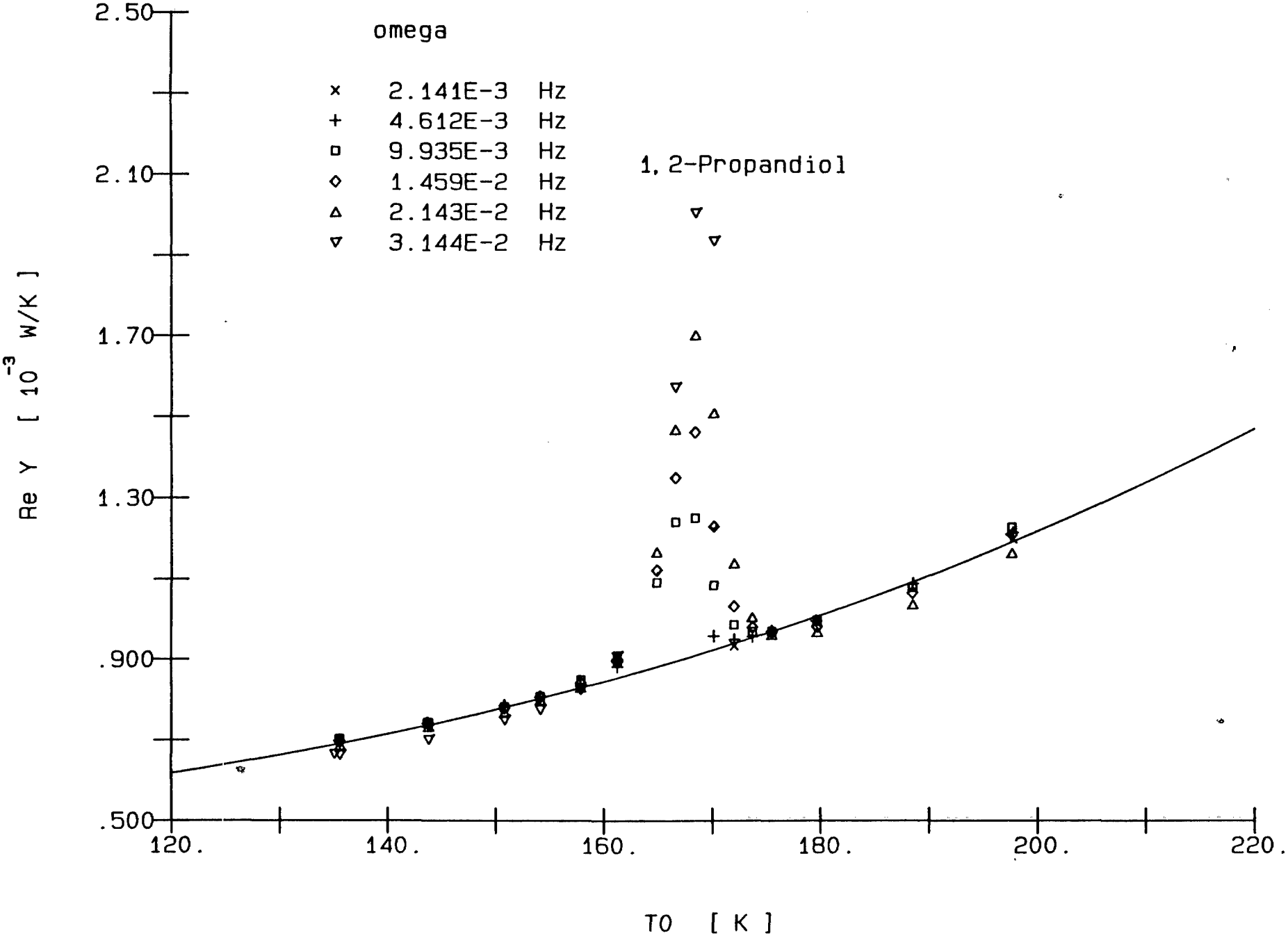
omega
× 2.141E-3 Hz
+ 4.612E-3 Hz
▫ 9.935E-3 Hz
◇ 1.459E-2 Hz
△ 2.143E-2 Hz
▽ 3.144E-2 Hz
1,2-Propandiol
2.50
2.10
1.70
1.30
.900
.500
Re Y [10^-3 W/K]
120.
140.
160.
180.
200.
220.
TO [K]

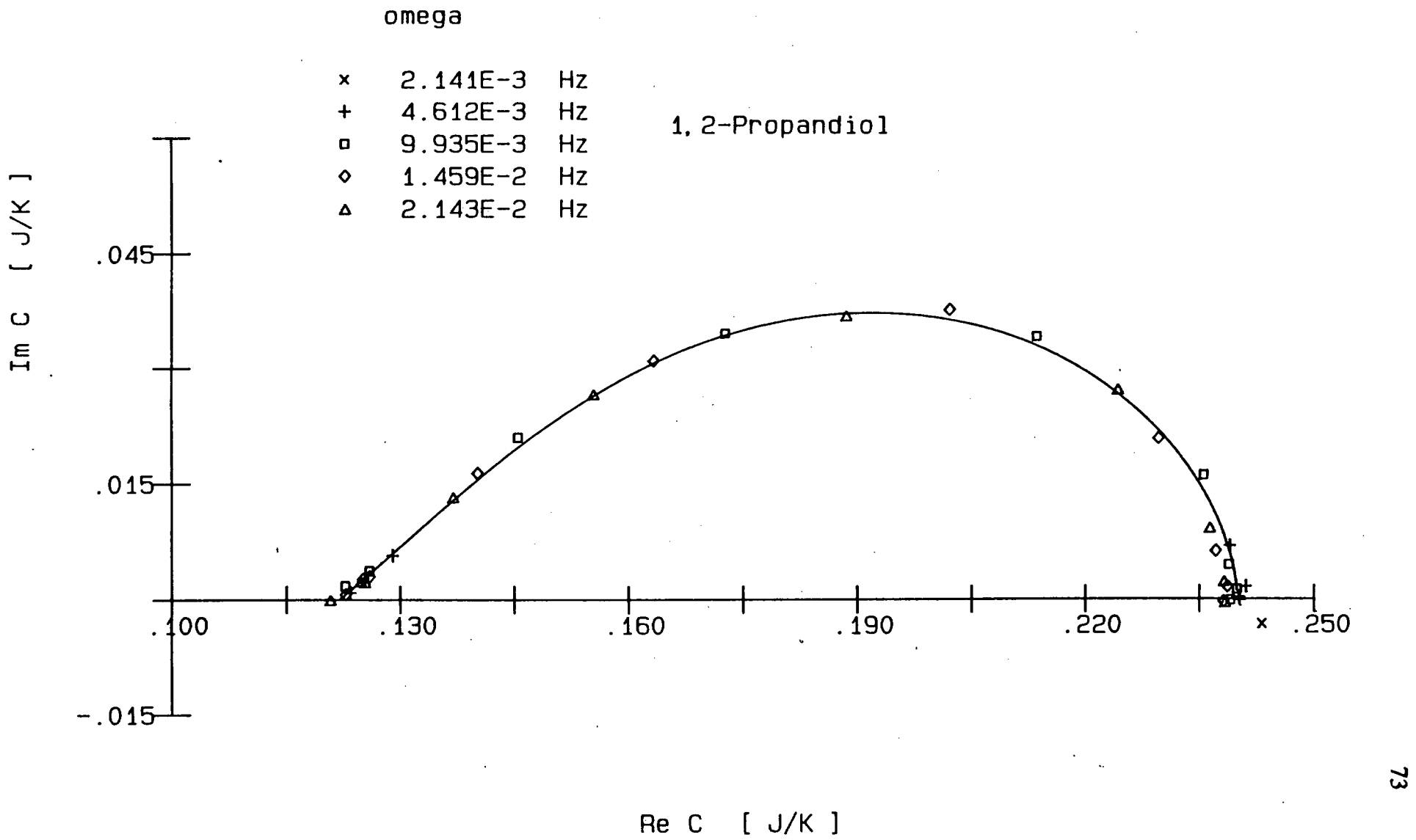
omega
× 2.141E-3 Hz
+ 4.612E-3 Hz
▫ 9.935E-3 Hz
◇ 1.459E-2 Hz
△ 2.143E-2 Hz
1,2-Propandiol
Im C [J/K]
.045
.015
-.015
.100
.130
.160
.190
.220
× .250
Re C [J/K]

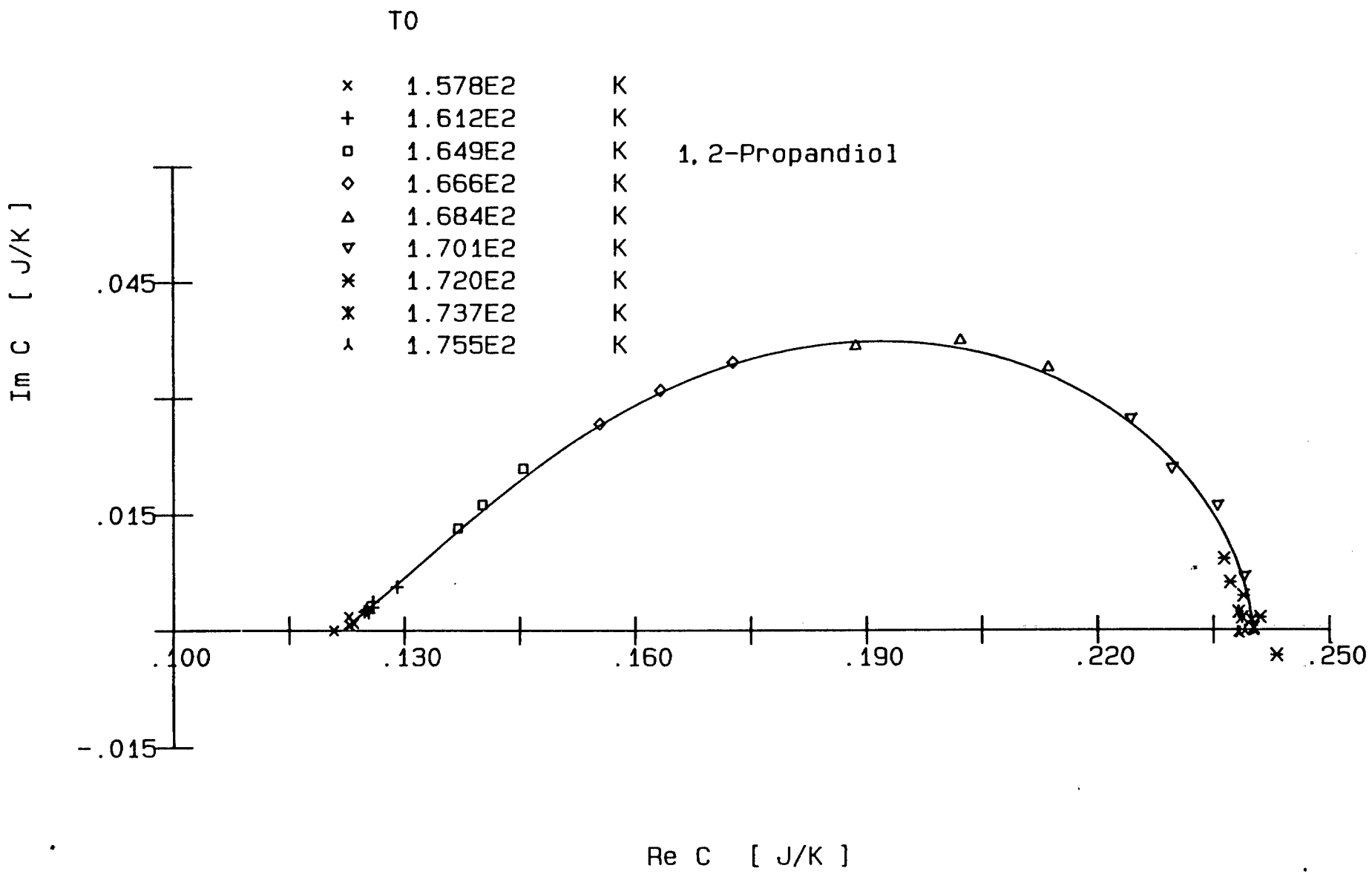
T0
× 1.578E2 K
+ 1.612E2 K
▫ 1.649E2 K
◇ 1.666E2 K
△ 1.684E2 K
▽ 1.701E2 K
✳ 1.720E2 K
✳ 1.737E2 K
✳ 1.755E2 K
1,2-Propandiol
Im C [J/K]
.045
.015
-.015
.100
.130
.160
.190
.220
.250
Re C [J/K]

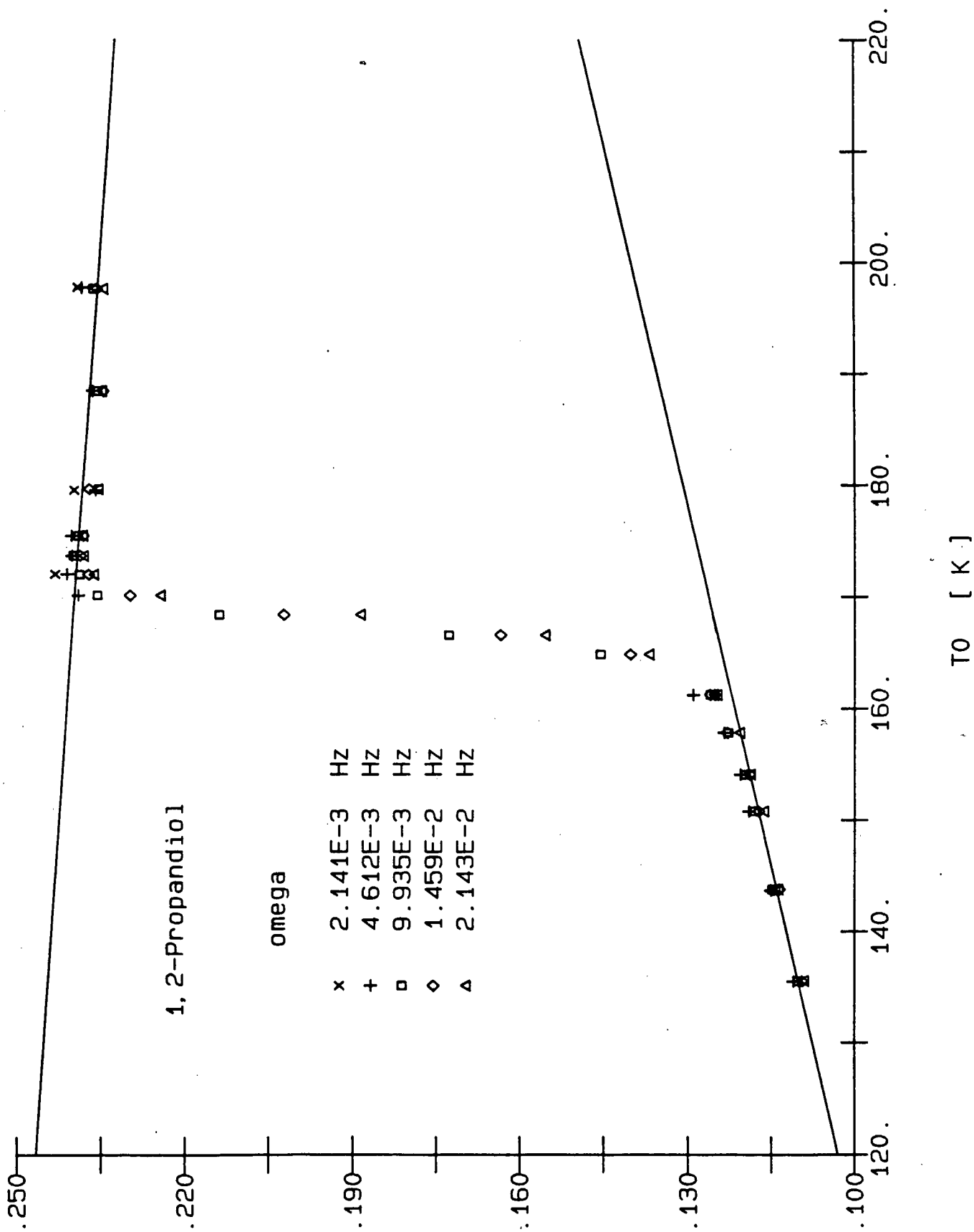
1,2-Propandiol
omega
2.141E-3 Hz
4.612E-3 Hz
9.935E-3 Hz
1.459E-2 Hz
2.143E-2 Hz
Re C [J/K]
TO [K]
.250
.220
.190
.160
.130
.100
120.
140.
160.
180.
200.
220.

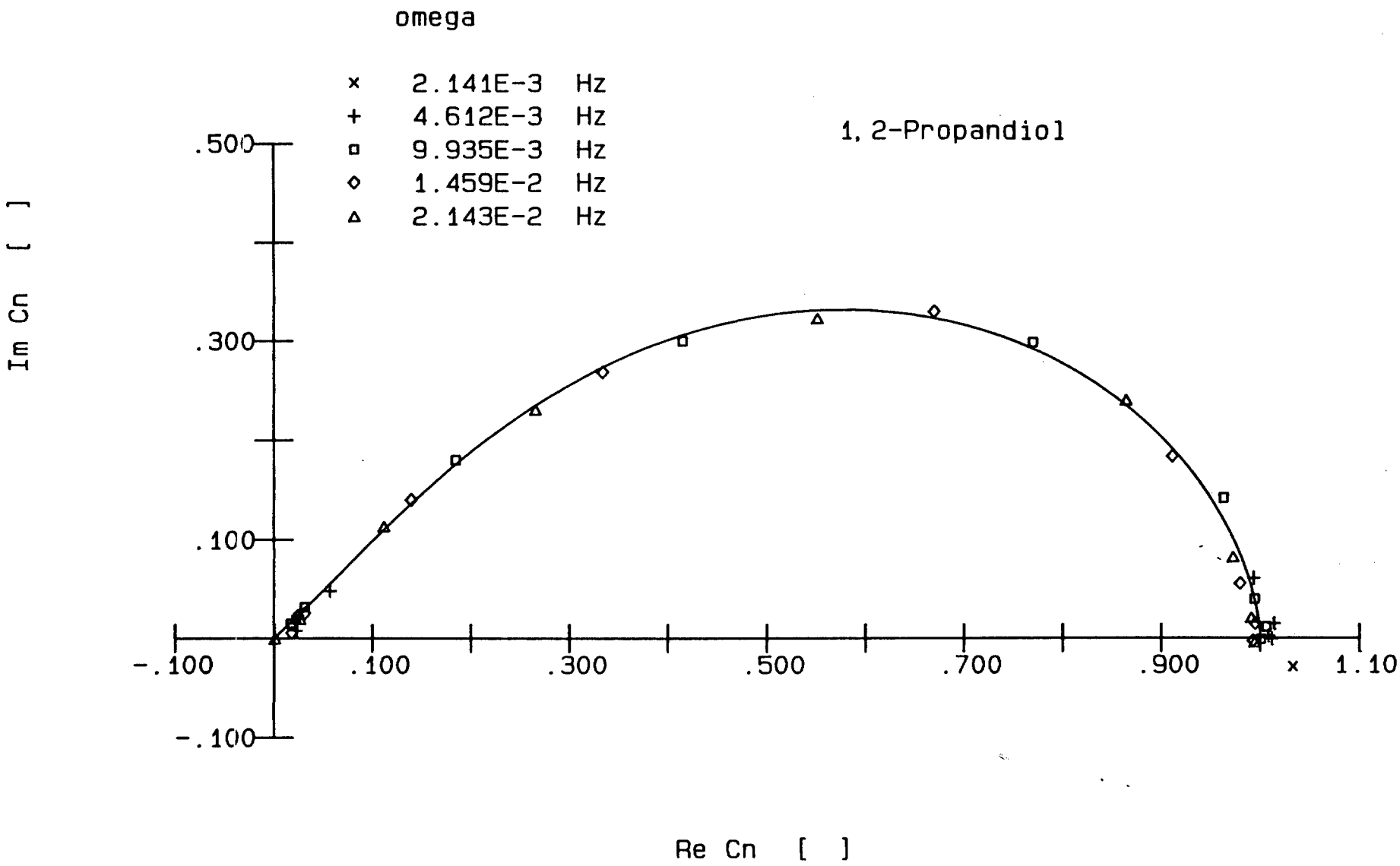
omega
× 2.141E-3 Hz
+ 4.612E-3 Hz
▫ 9.935E-3 Hz
◇ 1.459E-2 Hz
△ 2.143E-2 Hz
1,2-Propandiol
Im Cn [ ]
.500
.300
.100
-.100
-.100
.100
.300
.500
.700
.900
x 1.10
Re Cn [ ]

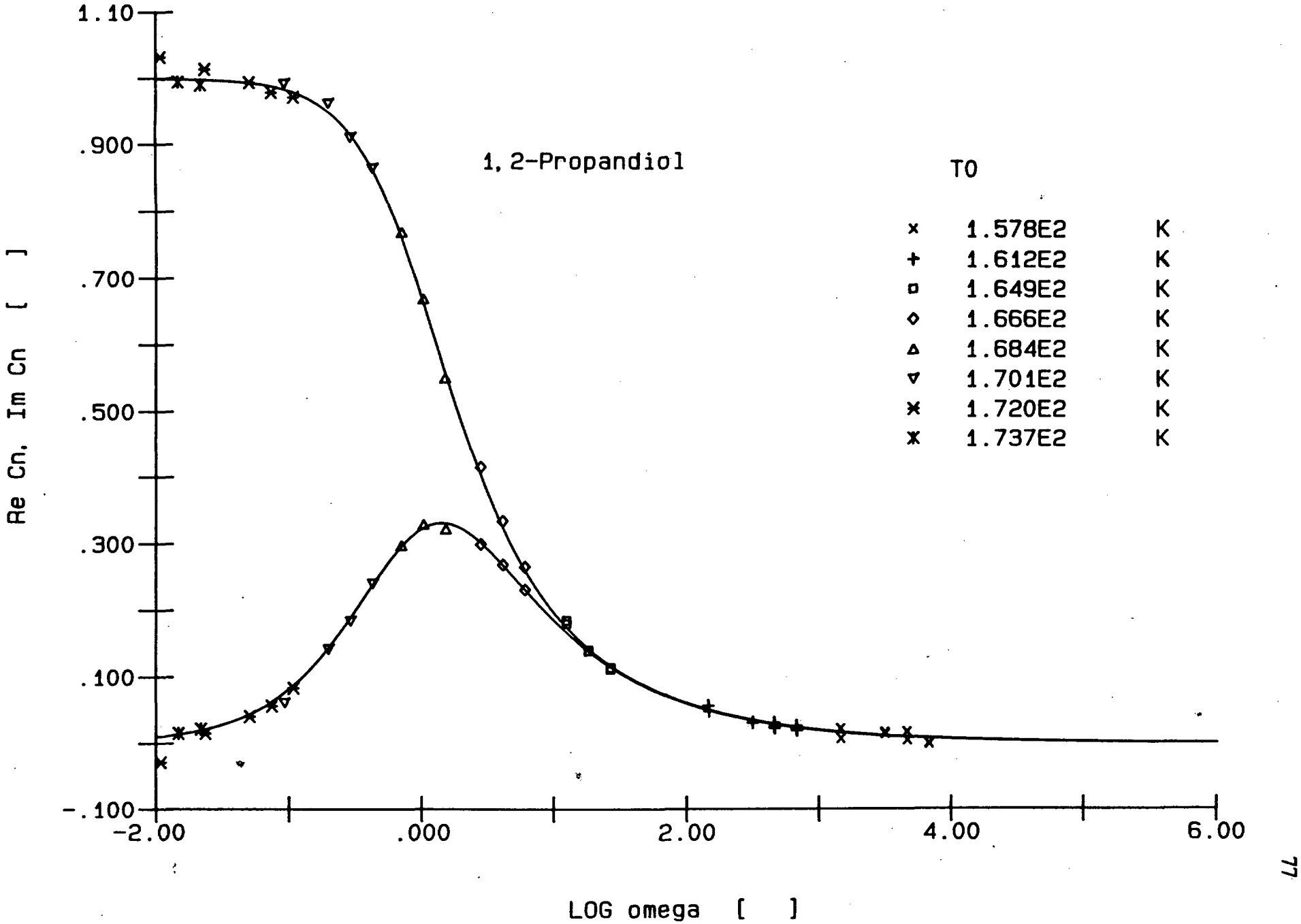
1.10
.900
.700
.500
.300
.100
-.100
-2.00
.000
2.00
4.00
6.00
Re Cn, Im Cn [ ]
LOG omega [ ]
1,2-Propandiol
T0
1.578E2 K
1.612E2 K
1.649E2 K
1.666E2 K
1.684E2 K
1.701E2 K
1.720E2 K
1.737E2 K

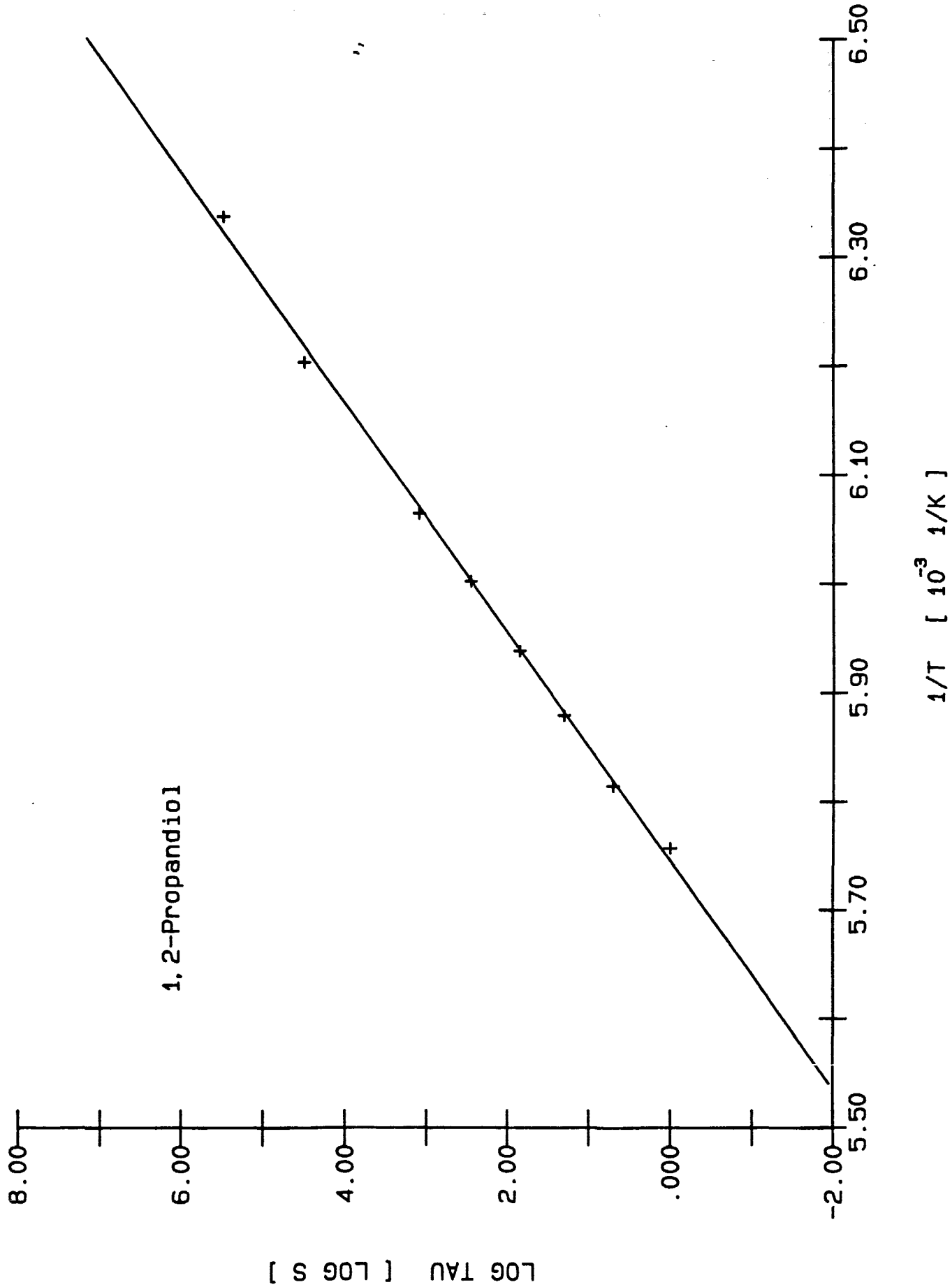
1, 2-Propandiol
LOG TAU [LOG S]
8.00
6.00
4.00
2.00
.000
-2.00
5.50
5.70
5.90
6.10
6.30
6.50
1/T [10^-3 1/K]

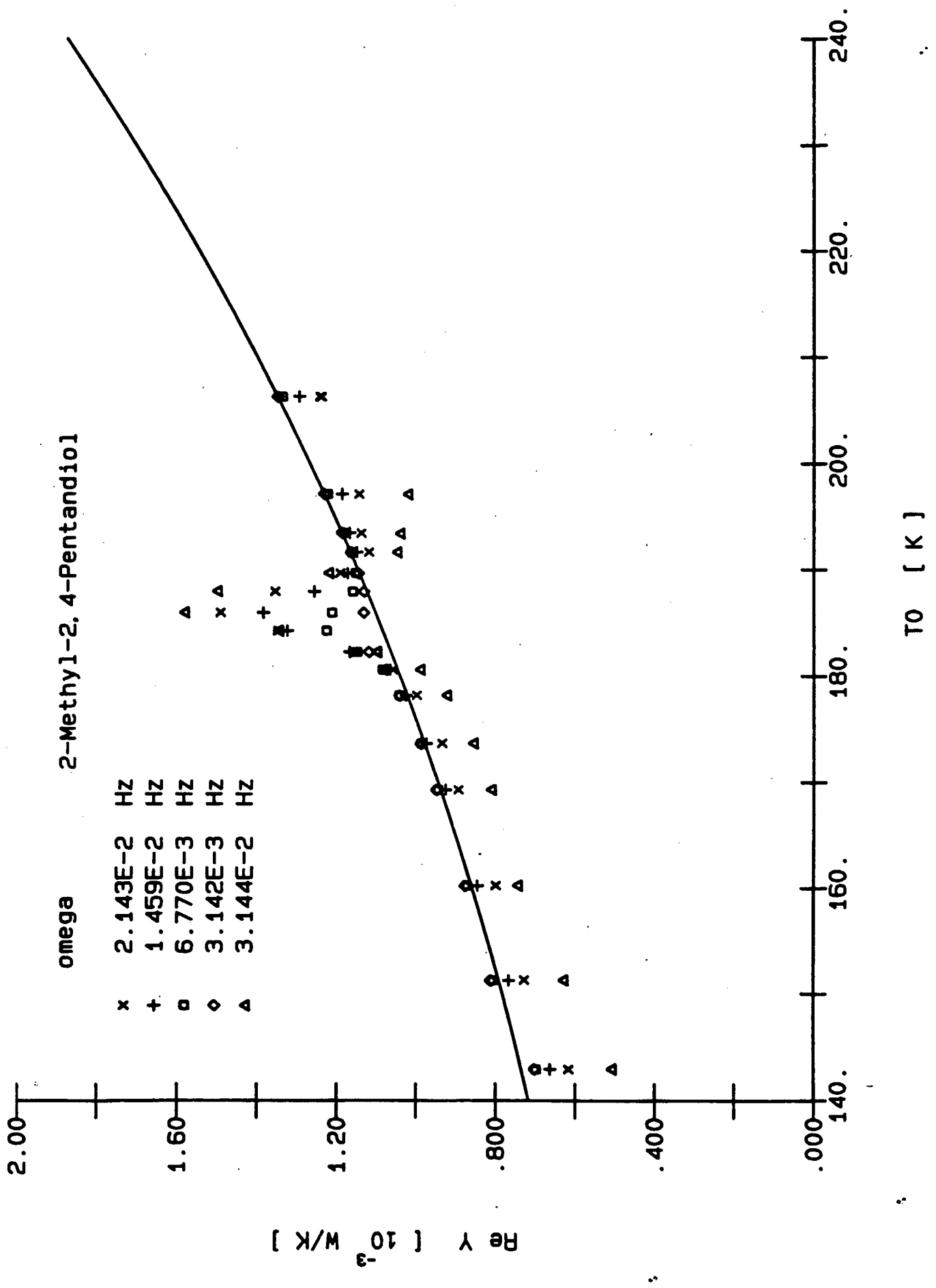
2-Methyl-2, 4-Pentandiol
omega
x 2.143E-2 Hz
+ 1.459E-2 Hz
□ 6.770E-3 Hz
◇ 3.142E-3 Hz
△ 3.144E-2 Hz
Re γ [10⁻³ W/K]
2.00
1.60
1.20
.800
.400
.000
140.
160.
180.
200.
220.
240.
TO [K]

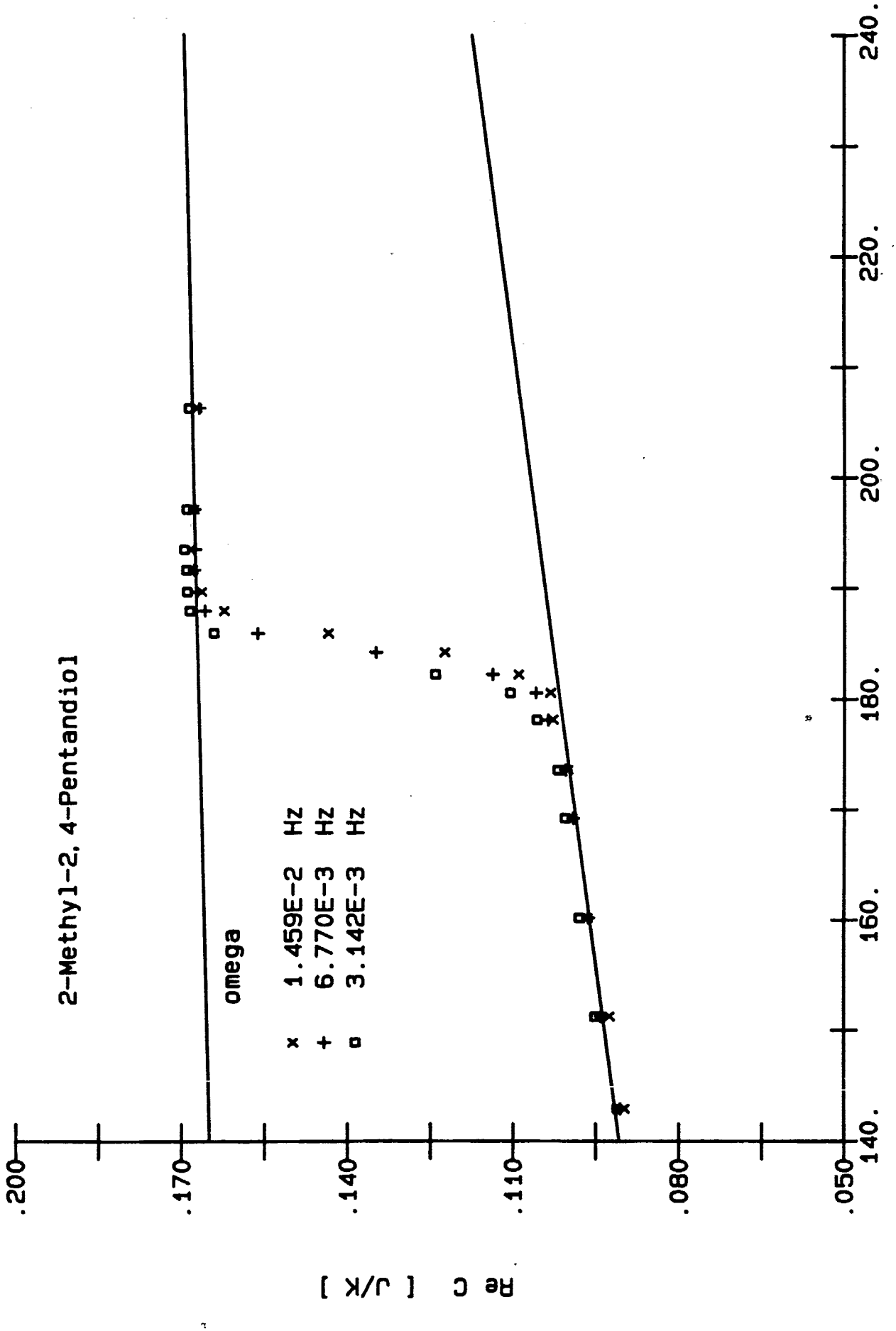
2-Methyl-2, 4-Pentandiol
omega
x 1.459E-2 Hz
+ 6.770E-3 Hz
□ 3.142E-3 Hz
Re C [J/K]
TO [K]
.200
.170
.140
.110
.080
.050
140.
160.
180.
200.
220.
240.

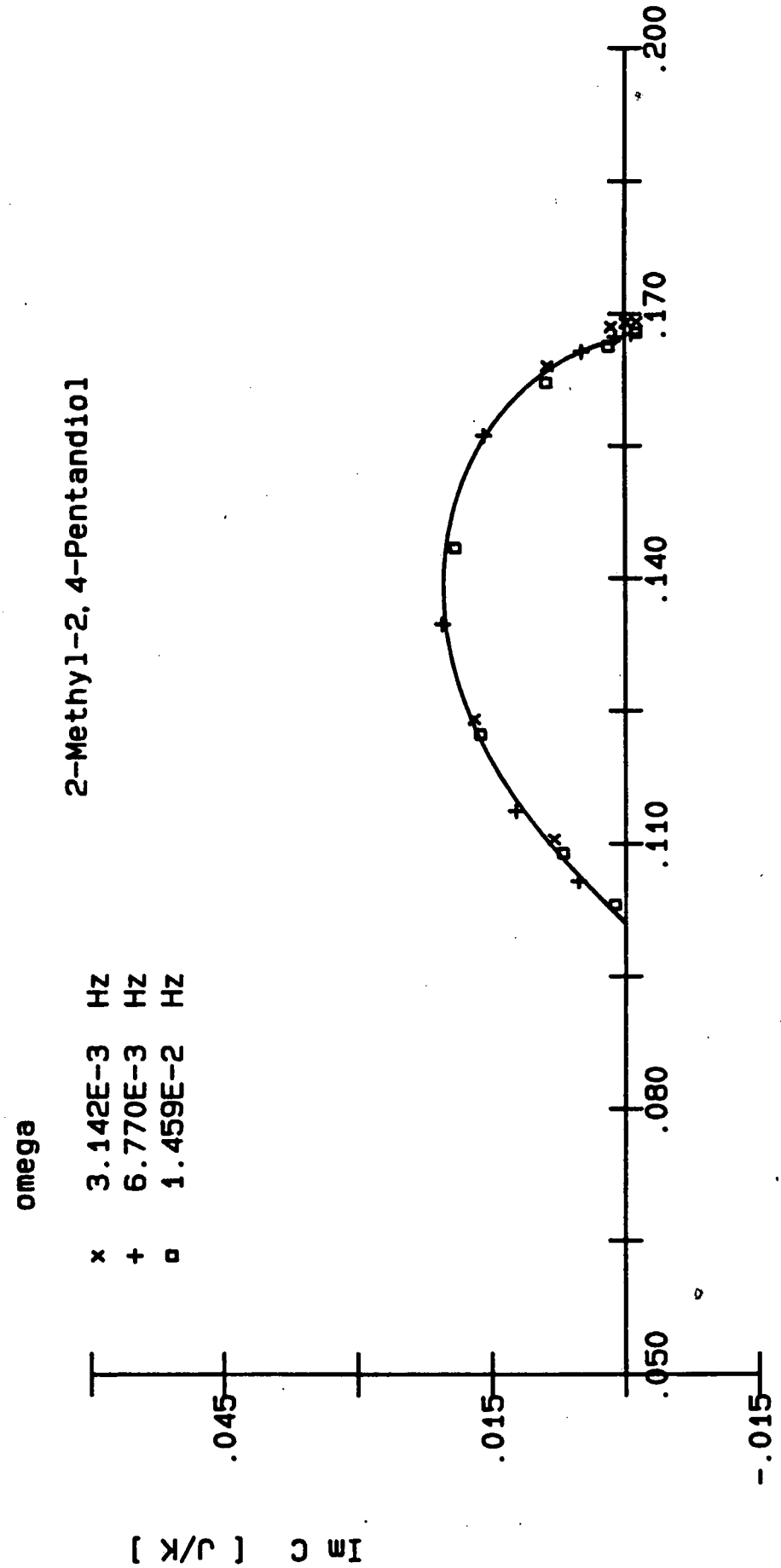
2-Methyl-2, 4-Pentandiol
omega
x 3.142E-3 Hz
+ 6.770E-3 Hz
□ 1.459E-2 Hz
Im C [J/K]
Re C [J/K]
.045
.015
-.015
.050
.080
.110
.140
.170
.200

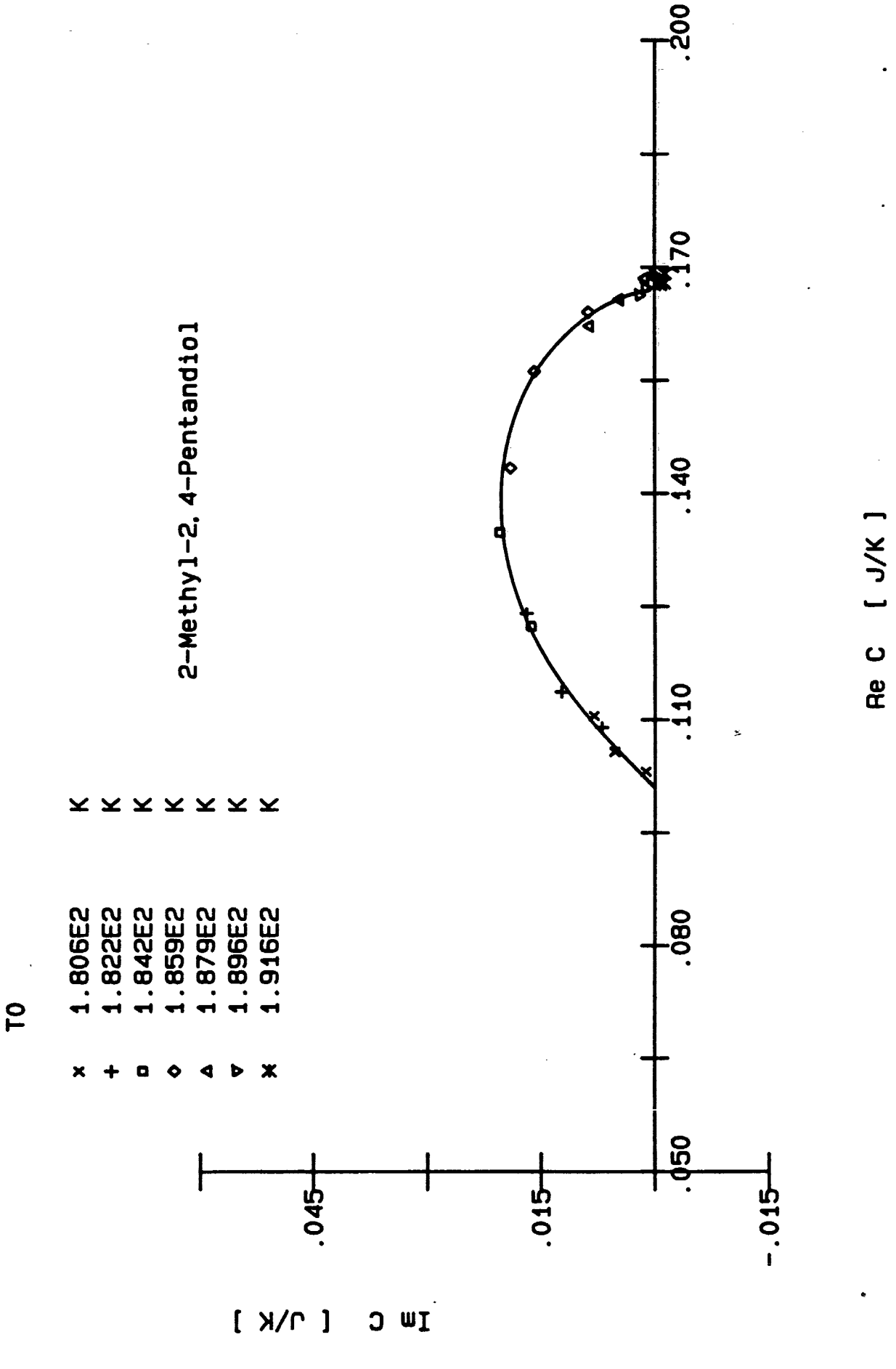
2-Methyl-2, 4-Pentandiol
TO
x 1.806E2 K
+ 1.822E2 K
□ 1.842E2 K
◇ 1.859E2 K
△ 1.879E2 K
▽ 1.896E2 K
✱ 1.916E2 K
.045
.015
-.015
.050
.080
.110
.140
.170
.200
Im C [J/K]
Re C [J/K]

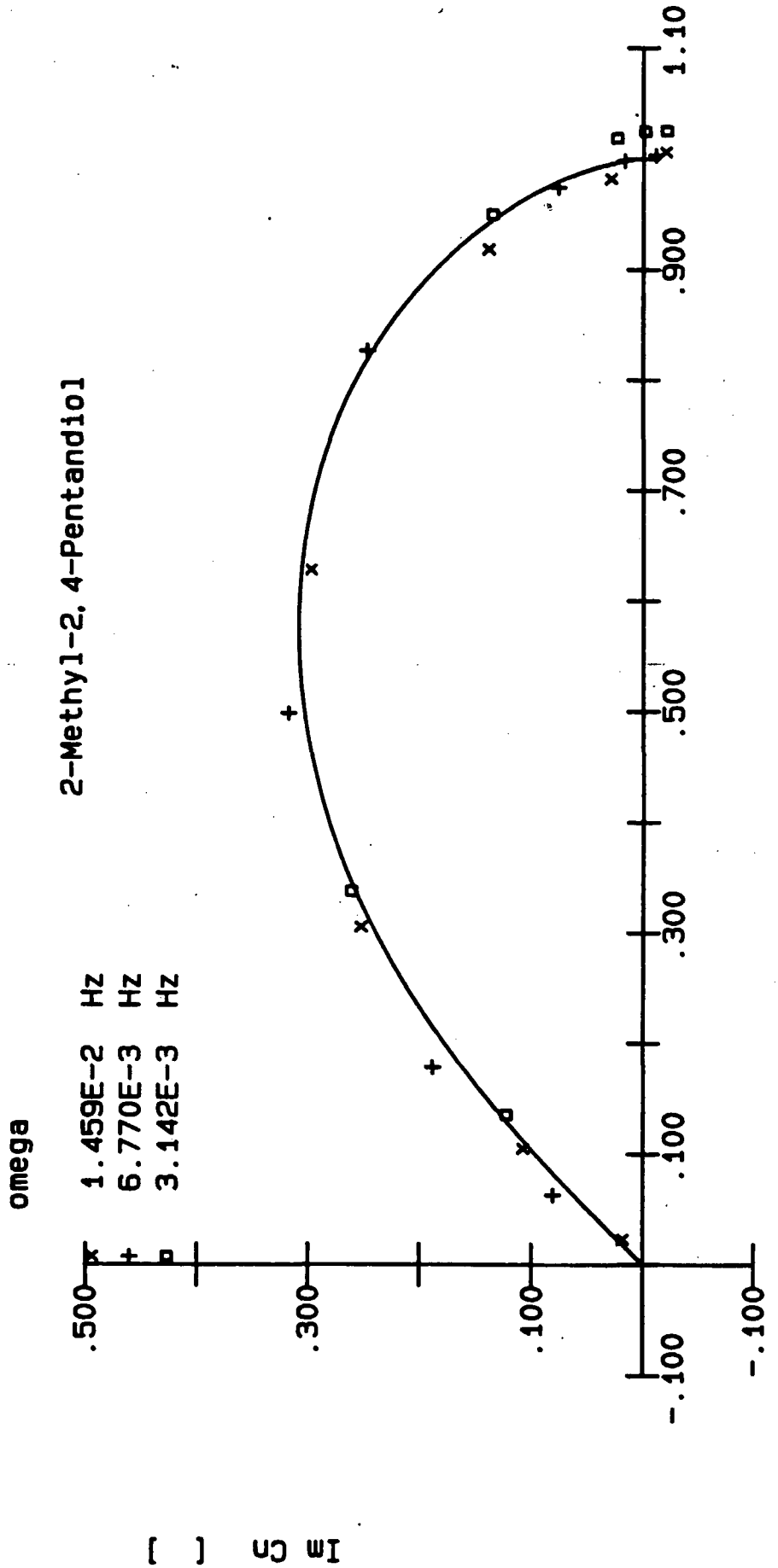
2-Methyl-2, 4-Pentandiol
omega
1.459E-2 Hz
6.770E-3 Hz
3.142E-3 Hz
.500
.300
.100
-.100
-.100
.100
.300
.500
.700
.900
1.10
Im Cn [ ]
Re Cn [ ]

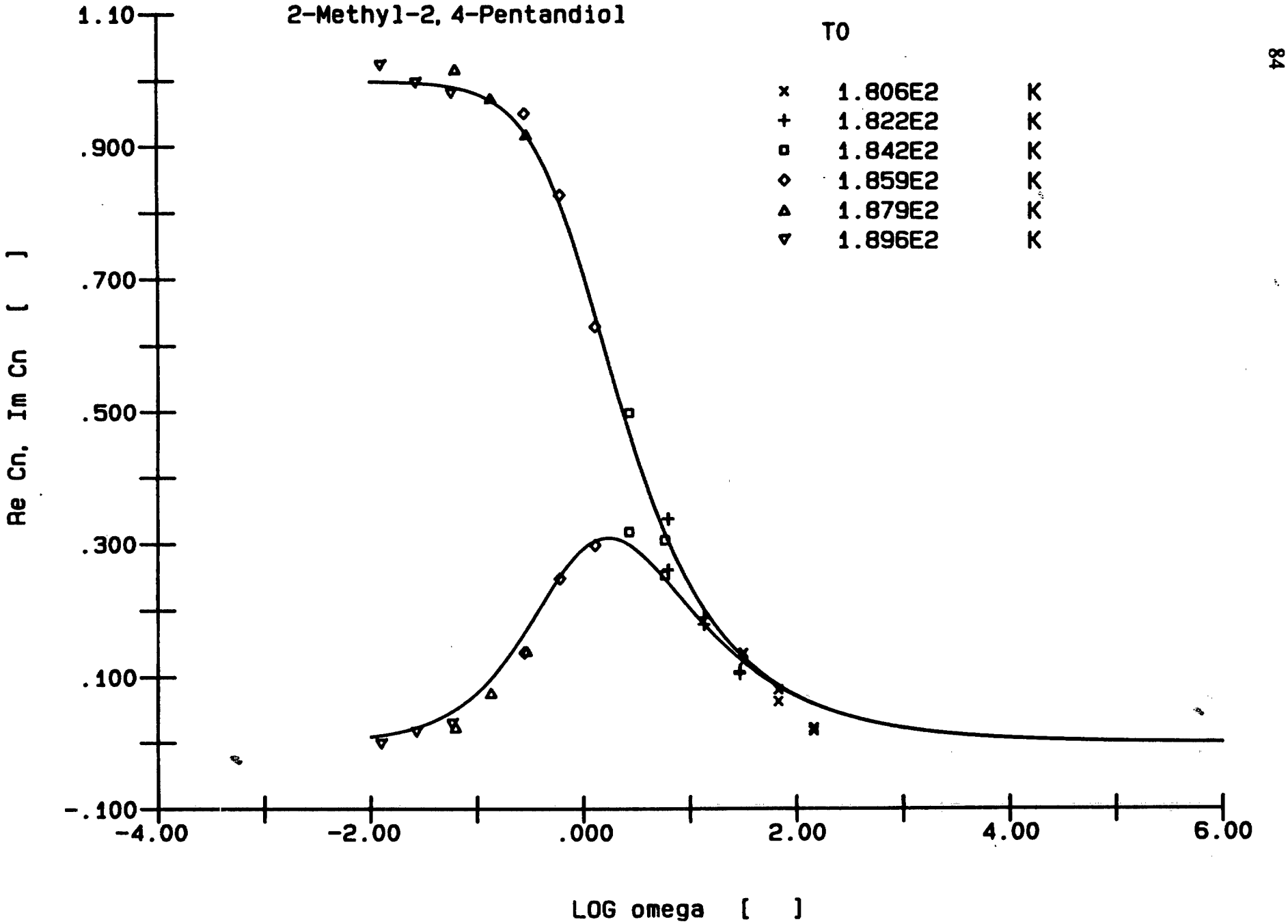
2-Methyl-2, 4-Pentandiol
TO
× 1.806E2 K
+ 1.822E2 K
▫ 1.842E2 K
◇ 1.859E2 K
△ 1.879E2 K
▽ 1.896E2 K
1.10
.900
.700
.500
.300
.100
-.100
-4.00
-2.00
.000
2.00
4.00
6.00
Re Cn, Im Cn [ ]
LOG omega [ ]

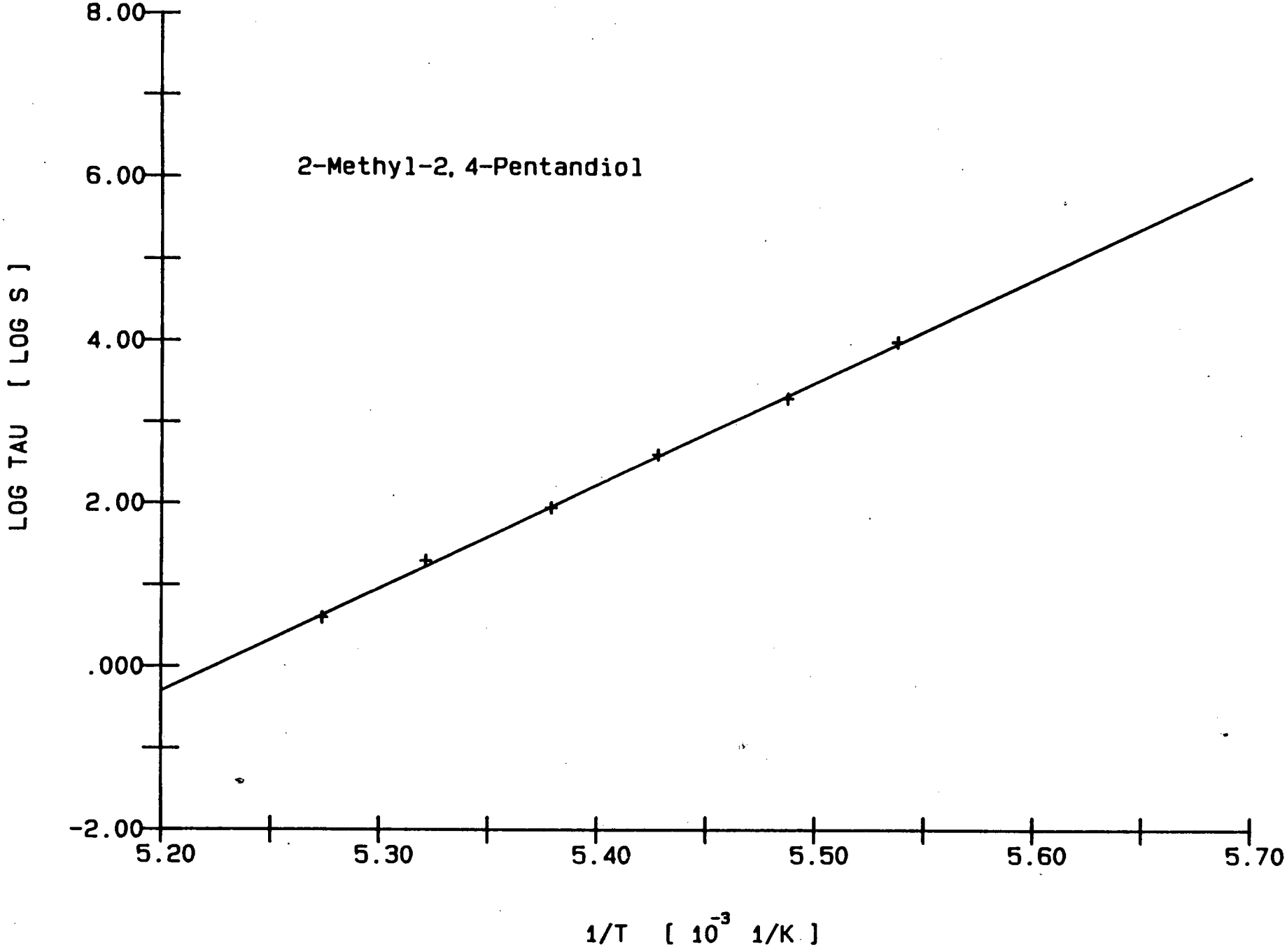
2-Methyl-2, 4-Pentandiol
LOG TAU [LOG S]
8.00
6.00
4.00
2.00
.000
-2.00
5.20
5.30
5.40
5.50
5.60
5.70
1/T [10^-3 1/K]

Liste over tidligere udkomne tekster tilsendes gerne. Henvendelse herom kan ske til IMFUFA's sekretariat tlf. 46 75 77 11 lokal 2263

217/92 "Two papers on APPLICATIONS AND MODELLING IN THE MATHEMATICS CURRICULUM"
by: Mogens Niss

218/92 "A Three-Square Theorem"
by: Lars Kadison

219/92 "RUPNOK - stationær strømning i elastiske rør"
af: Anja Boisen, Karen Birkelund, Mette Olufsen
Vejleder: Jesper Larsen

220/92 "Automatisk diagnosticering i digitale kredsløb"
af: Bjørn Christensen, Ole Møller Nielsen
Vejleder: Stig Andur Pedersen

221/92 "A BUNDLE VALUED RADON TRANSFORM, WITH APPLICATIONS TO INVARIANT WAVE EQUATIONS"
by: Thomas P. Branson, Gestur Olafsson and Henrik Schlichtkrull

222/92 On the Representations of some Infinite Dimensional Groups and Algebras Related to Quantum Physics
by: Johnny T. Ottesen

223/92 *THE FUNCTIONAL DETERMINANT*
by: Thomas P. Branson

224/92 *UNIVERSAL AC CONDUCTIVITY OF NON-METALLIC SOLIDS AT LOW TEMPERATURES*
by: Jeppe C. Dyre

225/92 *"HATMODELLEN" Impedansspektroskopi i ultrarent en-krystallinsk silicium*
af: Anja Boisen, Anders Gorm Larsen, Jesper Varmer, Johannes K. Nielsen, Kit R. Hansen, Peter Bøggild og Thomas Hougaard
Vejleder: Petr Viscor

226/92 *"METHODS AND MODELS FOR ESTIMATING THE GLOBAL CIRCULATION OF SELECTED EMISSIONS FROM ENERGY CONVERSION"*
by: Bent Sørensen

227/92 "Computersimulering og fysik"
af: Per M.Hansen, Steffen Holm, Peter Maibom, Mads K. Dall Petersen, Pernille Postgaard, Thomas B.Schrøder, Ivar P. Zeck
Vejleder: Peder Voetmann Christiansen

228/92 "Teknologi og historie"
Fire artikler af:
Mogens Niss, Jens Høyrup, Ib Thiersen, Hans Hedal

229/92 "Masser af information uden betydning"
En diskussion af informationsteorien i Tor Nørretranders' "Mærk Verden" og en skitse til et alternativ basseret på andenordens kybernetik og semiotik.
af: Søren Brier

230/92 "Vinklens tredeling - et klassisk problem"
et matematisk projekt af
Karen Birkelund, Bjørn Christensen
Vejleder: Johnny Ottesen

231A/92 "Elektrondiffusion i silicium - en matematisk model"
af: Jesper Voetmann, Karen Birkelund, Mette Olufsen, Ole Møller Nielsen
Vejledere: Johnny Ottesen, H.B.Hansen

231B/92 "Elektrondiffusion i silicium - en matematisk model" Kildetekster
af: Jesper Voetmann, Karen Birkelund, Mette Olufsen, Ole Møller Nielsen
Vejledere: Johnny Ottesen, H.B.Hansen

232/92 "Undersøgelse om den simultane opdagelse af energiens bevarelse og især̊eles om de af Mayer, Colding, Joule og Helmholtz udførte arbejder"
af: L.Arleth, G.I.Dybkjær, M.T.Østergård
Vejleder: Dorthe Posselt

233/92 "The effect of age-dependent host mortality on the dynamics of an endemic disease and
Instability in an SIR-model with age-dependent susceptibility
by: Viggo Andreasen

234/92 "THE FUNCTIONAL DETERMINANT OF A FOUR-DIMENSIONA BOUNDARY VALUE PROBLEM"
by: Thomas P. Branson and Peter B. Gilkey

235/92 OVERFLADESTRUKTUR OG POREUDVIKLING AF KOKS
- Modul 3 fysik projekt -
af: Thomas Jessen

236a/93 INTRODUKTION TIL KVANTE HALL EFFEKTEN

af: Anja Boisen, Peter Bøggild

Vejleder: Peder Voetmann Christiansen
Erland Brun Hansen

236b/93 STRØMSSAMMENBRUD AF KVANTE HALL EFFEKTEN

af: Anja Boisen, Peter Bøggild

Vejleder: Peder Voetmann Christiansen
Erland Brun Hansen

237/93 The Wedderburn principal theorem and Shukla cohomology

af: Lars Kadison

238/93 SEMIOTIK OG SYSTEMEGENSKABER (2)

Vektorbånd og tensorer

af: Peder Voetmann Christiansen

239/93 Valgsystemer - Modelbygning og analyse

Matematik 2. modul

af: Charlotte Gjerrild, Jane Hansen, Maria Hermannsson, Allan Jørgensen, Ragna Clauson-Kaas, Poul Lützen

Vejleder: Mogens Niss

240/93 Patologiske eksempler.
Om sære matematiske fisks betydning for den matematiske udvikling

af: Claus Dræby, Jørn Skov Hansen, Runa Ulsøe Johansen, Peter Meibom, Johannes Kristoffer Nielsen

Vejleder: Mogens Niss

241/93 FOTOVOLTAISK STATUSNOTAT 1

af: Bent Sørensen

242/93 Brovedligeholdelse - bevar mig vel

Analyse af Vejdirektoratets model for optimering af broreparationer

af: Linda Kyndlev, Kare Fundal, Kamma Tulinius, Ivar Zeck

Vejleder: Jesper Larsen

243/93 TANKEEKSPERIMENTER I FYSIKKEN

Et 1.modul fysikprojekt

af: Karen Birkelund, Stine Sofia Korremann

Vejleder: Dorthe Posselt

244/93 RADONTRANSFORMATIONEN og dens anvendelse i CT-scanning

Projektrapport

af: Trine Andreasen, Tine Guldager Christiansen, Nina Skov Hansen og Christine Iversen

Vejledere: Gestur Olafsson og Jesper Larsen

245a+b /93 Time-Of-Flight målinger på krystallinske halvledere
Specialerapport

af: Linda Szkotak Jensen og Lise Odgaard Gade

Vejledere: Petr Viscor og Niels Boye Olsen

246/93 HVERDAGSVIDEN OG MATEMATIK
- LÆREPROCESSER I SKOLEN

af: Lena Lindenskov, Statens Humanistiske Forskningsråd, RUC, IMFUFA

247/93 UNIVERSAL LOW TEMPERATURE AC CONDUCTIVITY OF MACROSCOPICALLY DISORDERED NON-METALS

by: Jeppe C. Dyre

248/93 DIRAC OPERATORS AND MANIFOLDS WITH BOUNDARY

by: B. Booss-Bavnbek, K.P.Wojciechowski

249/93 Perspectives on Teichmüller and the Jahresbericht Addendum to Schappacher, Scholz, et al.

by: B. Booss-Bavnbek

With comments by W.Abikoff, L.Ahlfors, J.Cerf, P.J.Davis, W.Fuchs, F.P.Gardiner, J.Jost, J.-P.Kahane, R.Lohan, L.Lorch, J.Radkau and T.Söderqvist

250/93 EULER OG BOLZANO - MATEMATISK ANALYSE SET I ET VIDENSKABSTEORETISK PERSPEKTIV

Projektrapport af: Anja Juul, Lone Michelsen, Tomas Højgård Jensen

Vejleder: Stig Andur Pedersen

251/93 Genotypic Proportions in Hybrid Zones

by: Freddy Bugge Christiansen, Viggo Andreasen and Ebbe Thue Poulsen

252/93 MODELLERING AF TILFÆLDIGE FÆNOMENER

Projektrapport af: Birthe Friis, Lisbeth Helmgaard Kristina Charlotte Jakobsen, Marina Mosbæk Johannessen, Lotte Ludvigsen, Mette Bass Nielsen

253/93 Kuglepakning

Teori og model

af: Lise Arleth, Kåre Fundal, Nils Kruse

Vejleder: Mogens Niss

254/93 Regressionsanalyse

Materiale til et statistikkursus

af: Jørgen Larsen

255/93 TID & BETINGET UAFHÆNGIGHED

af: Peter Harremoës

256/93 Determination of the Frequency Dependent Bulk Modulus of Liquids Using a Piezoelectric Spherical Shell (Preprint)

by: T. Christensen and N.B.Olsen

257/93 Modellering af dispersion i piezoelektriske keramikker

af: Pernille Postgaard, Jannik Rasmussen, Christina Specht, Mikko Østergård

Vejleder: Tage Christensen

258/93 Supplerende kursusmateriale til "Lineære strukturer fra algebra og analyse"

af: Mogens Brun Heefelt

259/93 STUDIES OF AC HOPPING CONDUCTION AT LOW TEMPERATURES

by: Jeppe C. Dyre

260/93 PARTITIONED MANIFOLDS AND INVARIANTS IN DIMENSIONS 2, 3, AND 4

by: B. Booss-Bavnbek, K.P.Wojciechowski

261/93 OPGAVESAMLING
Bredde-kursus i Fysik
Eksamensopgaver fra 1976-93

262/93 Separability and the Jones Polynomial
by: Lars Kadison

263/93 Supplerende kursusmateriale til "Lineære strukturer fra algebra og analyse" II
af: Mogens Brun Heefelt

264/93 FOTOVOLTAISK STATUSNOTAT 2
af: Bent Sørensen

265/94 SPHERICAL FUNCTIONS ON ORDERED SYMMETRIC SPACES
To Sigurdur Helgason on his sixtyfifth birthday
by: Jacques Faraut, Joachim Hilgert and Gestur Olafsson

266/94 Kommensurabilitets-oscillationer i laterale supergitre
Fysikspeciale af: Anja Boisen, Peter Bøggild, Karen Birkelund
Vejledere: Rafael Taboryski, Poul Erik Lindelof, Peder Voetmann Christiansen

267/94 Kom til kort med matematik på Eksperimentarium - Et forslag til en opstilling
af: Charlotte Gjerrild, Jane Hansen
Vejleder: Bernhelm Booss-Bavnbek

268/94 Life is like a sewer ...
Et projekt om modellering af aorta via en model for strømning i kloakrør
af: Anders Marcussen, Anne C. Nilsson, Lone Michelsen, Per M. Hansen
Vejleder: Jesper Larsen

269/94 Dimensionsanalyse en introduktion
metaprojekt, fysik
af: Tine Guldager Christiansen, Ken Andersen, Nikolaj Hermann, Jannik Rasmussen
Vejleder: Jens Højgaard Jensen

270/94 THE IMAGE OF THE ENVELOPING ALGEBRA AND IRREDUCIBILITY OF INDUCED REPRESENTATIONS OF EXPONENTIAL LIE GROUPS
by: Jacob Jacobsen

271/94 Matematikken i Fysikken.
Opdaget eller opfundet
NAT-BAS-projekt
vejleder: Jens Højgaard Jensen

272/94 Tradition og fornyelse
Det praktiske elevarbejde i gymnasiets fysikundervisning, 1907-1988
af: Kristian Hoppe og Jeppe Guldager
Vejledning: Karin Beyer og Nils Hybel

273/94 Model for kort- og mellemdistanceløb
Verifikation af model
af: Lise Fabricius Christensen, Helle Pilemann, Bettina Sørensen
Vejleder: Mette Olufsen

274/94 MODEL 10 - en matematisk model af intravenøse anæstetikas farmakokinetik
3. modul matematik, forår 1994
af: Trine Andreasen, Bjørn Christensen, Christine Green, Anja Skjoldborg Hansen. Lisbeth Helmgaard
Vejledere: Viggo Andreasen & Jesper Larsen

275/94 Perspectives on Teichmüller and the Jahresbericht
2nd Edition
by: Bernhelm Booss-Bavnbek

276/94 Dispersionsmodellering
Projektrapport 1. modul
af: Gitte Andersen, Rehannah Borup, Lisbeth Friis, Per Gregersen, Kristina Vejrø
Vejleder: Bernhelm Booss-Bavnbek

277/94 PROJEKTARBEJDSPÆDAGOGIK - Om tre tolkninger af problemorienteret projektarbejde
af: Claus Flensted Behrens, Frederik Voetmann Christiansen, Jørn Skov Hansen, Thomas Thingstrup
Vejleder: Jens Højgaard Jensen

278/94 The Models Underlying the Anaesthesia Simulator Sophus
by: Mette Olufsen(Math-Tech), Finn Nielsen (RISØ National Laboratory), Per Føge Jensen (Herlev University Hospital), Stig Andur Pedersen (Roskilde University)